Canadian Journal of
Earth Sciences

OPEN ACCESS | Review

Volcanogenic massive sulfide (VMS) deposits of the Dunnage Zone of the Newfoundland Appalachians: setting, styles, key advances, and future research

Stephen J. Piercey[a], **John G. Hinchey**[b], **and Gregory W. Sparkes**[b]

[a]Department of Earth Sciences, Memorial University of Newfoundland, 9 Arctic Ave, St. John's, NL A1B 1N3, Canada; [b]Mineral Deposits Section, Geological Survey of Newfoundland and Labrador, Department of Industry, Energy and Technology, Government of Newfoundland and Labrador, P.O. Box 8700, St. John's, NL A1B 4J6, Canada

Corresponding author: **Stephen J. Piercey** (email: spiercey@mun.ca)

Abstract

The Dunnage Zone of the Newfoundland Appalachians hosts diverse Cambrian–Ordovician volcanogenic massive sulfide (VMS) deposits. The peri-Laurentian Notre Dame Subzone contains Cu–Zn–Au mafic and bimodal mafic deposits in ∼501–485 Ma ophiolitic rocks and Zn–Pb–Cu–(Au–Ag) deposits in ∼471–465 Ma bimodal rifted continental arc sequences (e.g., Buchans). The peri-Gondwanan rocks of the Exploits Subzone host Zn–Pb–Cu–(Au–Ag) bimodal felsic, felsic siliciclastic, and Zn–Ag–Au hybrid bimodal felsic deposits in the ∼513–486 Ma Victoria Lake supergroup; Cu–Zn bimodal felsic to bimodal mafic deposits of the ∼486 Ma Wild Bight Group; and Cu–(Au) mafic siliciclastic deposits of the ∼466 Ma Great Burnt Lake/South Pond belt. Regardless of age or stratigraphic hosts, all VMS deposits are associated with specific magmatic assemblages and extensional tectonism (i.e., rifting). Gold-enriched deposits of the Rambler-Ming district are associated with felsic rocks that formed via slab melting and subsequent melt-mantle wedge interaction, which likely enhanced precious metal enrichment in these deposits. Whereas many deposits exhaled on the seafloor, some deposits formed via subseafloor replacement of host units or as re-sedimented sulfides generated in sediment-gravity flows. Metals in the deposits were derived from leaching of underlying footwall rocks; however, Au–Ag- and epithermal suite element-enriched deposits show evidence for metal contributions from magmatic hydrothermal fluids. Sulfur in deposits was derived predominantly from leaching of H_2S from underlying footwall rocks and from thermochemical sulfate reduction of seawater sulfate, with lesser input from bacteria-derived H_2S and magmatic-hydrothermal-derived H_2S. Despite recent research advances and historic mining, numerous questions remain unresolved and provide opportunities for future study.

Key words: volcanogenic massive sulfide, Newfoundland, Appalachians, metallogeny, sulfur isotopes, magmatism

Introduction

Volcanogenic massive sulfide (VMS) deposits are important sources of Cu, Zn, Pb, Au, Ag, and other metals for the Canadian and global economy (Franklin et al. 2005). They occur in extensional settings (e.g., mid-ocean ridges, back-arc basins, and rifted arcs) and have been forming from the Archean to present (Hannington et al. 2005; Piercey 2011; Ross and Mercier-Langevin 2014). Appalachian VMS deposits have been important contributors to the economy of much of eastern Canada, including the world class deposits of the Bathurst Mining District (Goodfellow 2007) and numerous districts in central Newfoundland (Swinden and Kean 1988). In the Dunnage Zone of central Newfoundland, VMS deposits were important sources of metal prior to Confederation with Canada (Martin 1983) and are still important contributors to the economy, as well as the foci of continued exploration and development.

In addition to economic significance, VMS deposits in the Newfoundland Dunnage Zone have contributed greatly to our global understanding of VMS deposits, including the roles of (1) footwall domains in influencing the metals present in VMS (e.g., Swinden and Thorpe 1984), (2) lithogeochemistry and applications in tectonostratigraphic research (e.g., Swinden 1991), (3) thrust imbrication and its importance in deposit reconstructions and exploration (e.g., Thurlow 2010), (4) the role of metamorphism in creating metamorphosed alteration assemblages (e.g., Upadhyay and Smitheringale 1972), (5) sulfur isotopes behaviour during sulfide metamorphism (e.g., Bachinski 1977; Cloutier et al. 2015), (6) exhalation and subseafloor replacement (e.g., Squires et al. 1991; Piercey et al. 2014), and (7) magmatic fluids/volatiles in promoting precious metal and epithermal suite (e.g., Au–Ag–Hg–As–Sb–Bi–Te–Se–Sn–W) element enrichments in VMS deposits (e.g., Santaguida and Hannington

1996; Brueckner et al. 2014*b*, 2016; Gill et al. 2016; Pilote et al. 2016).

In this paper, we review the geological setting and styles of VMS deposits in the Dunnage Zone of central Newfoundland and discuss recent key advances in our understanding of the genesis of these deposits and potential avenues for future research.

Classification and grade–tonnage data

Background

VMS deposits are the products of submarine hydrothermal systems that form in extensional (rifted) tectonic regimes via the circulation of seawater through crust driven by heat from underlying magmatic rocks (Fig. 1; Franklin et al. 1981, 2005; Lydon 1988). As seawater penetrates the underlying crust through the recharge zone, it heats up and reacts with host rocks, resulting in the leaching of metals (e.g., Zn, Pb, and Cu, among others) and reduced sulfur (H_2S) in the reaction zone; the metals then bond with Cl from seawater and are subsequently transported predominantly as metal chloride complexes (Lydon 1988; Galley 1993; Skirrow and Franklin 1994; Jowitt et al. 2012). If sulfate (SO_4^{2-}) is present in the downwelling seawater reaction zones and reductants are present in the wall rock (e.g., Fe and organic C), sulfate will undergo thermochemical sulfate reduction (TSR) to generate H_2S (Shanks et al. 1981; Shanks and Seyfried 1987). These hot, metal chloride- and H_2S-bearing fluids are generally buoyant and will move upwards from depth along synvolcanic (and synsedimentary) faults, will conductively cool, react with wall rock to form hydrothermal alteration zones (e.g., sericite–chlorite–quartz assemblages), and will mix with seawater at or near the seafloor, resulting in the precipitation of sulfides (Fig. 1; Lydon 1988; Large 1992). In some hydrothermal systems where magmatic fluids are important, precious metals and epithermal suite elements (e.g., Au–Ag–Hg–As–Sb–Bi–Te–Se–Sn–W) are discharged from underlying subvolcanic magma chambers into the overlying hydrothermal system, which upon cooling and mixing with seawater may result in precipitation of deposits enriched in these metals and having distinctive argillic/advanced argillic or adularia–sericite alteration assemblages (e.g., Sillitoe et al. 1996; Hannington et al. 1999).

Deposit classification

Although a generalized model for VMS deposits has been presented above, there are distinctive sub-types of VMS deposits and the most widely accepted classification of these sub-types is the tectonostratigraphic classification of Barrie and Hannington (1999) and subsequent revisions thereof (e.g., Franklin et al. 2005; Galley et al. 2007; Piercey et al. 2015). Minor variants on this classification have been proposed with expansions to deposits associated with specific rock types (e.g., ultramafic VMS classification of Patten et al. 2022), but these are not discussed herein as there are no bona fide examples of these in the Newfoundland Appalachians.

Deposits in the Newfoundland Appalachians are classified into the following groups (modified after Galley et al. 2007): (1) mafic, (2) bimodal mafic, (3) mafic siliciclastic, (4) bimodal felsic, (5) felsic siliciclastic, and (6) hybrid bimodal felsic (Fig. 2).

Mafic (also referred to as Cyprus-type) deposits are those hosted predominantly in mafic volcanic rocks and sheeted dikes within forearc or back-arc ophiolites (Fig. 2). These deposits are predominantly Cu-rich, but some have produced Zn and Au, whereas others contain enrichments in Co and Ni. In the Newfoundland Appalachians, deposits in the Lushs Bight, Betts Cove, and Bay of Islands ophiolites are examples of this deposit type (Fig. 3; Hibbard 1983; Swinden and Kean 1988; Kean et al. 1995).

Bimodal mafic (also referred to as Noranda-type) deposits are hosted in primitive arc belts dominated by mafic volcanic and intrusive rocks but where the deposits are specifically hosted by felsic volcanic rocks (Fig. 2). They typically occur in rifted primitive arcs and, in some cases, forearcs and are polymetallic with a Zn–Cu–(Au–Ag) metal signature. In the Newfoundland Appalachians, the Cu–Au-bearing Rambler and Ming deposits in the Baie Verte belt are examples of this VMS deposit type (Fig. 3; Brueckner et al. 2014*b*, 2016).

Mafic siliciclastic (also referred to as Besshi-type) deposits are hosted in belts that contain mafic volcanic rocks, volcaniclastic and intrusive rocks, and abundant sedimentary rocks, including argillite, siltstone, and sandstone (Fig. 2). Felsic volcanic rocks, if present, only comprise a minor component of the stratigraphy. These deposits are typically associated with back-arc (and forearc) environments and are Cu–Zn-rich. In the Newfoundland Appalachians, the Great Burnt Lake and South Pond deposits are examples of this VMS deposit type (Fig. 3; Swinden 1988*a*; Barry et al. 2022).

Bimodal felsic (also referred to as Kuroko-type) deposits are hosted in belts of predominantly felsic volcanic and volcaniclastic rocks with lesser mafic rocks and are interpreted to have formed in mature rifted continental arcs and back-arc basins (Fig. 2). These deposits are polymetallic with Zn–Pb–Cu–(Au–Ag), and in the Newfoundland Dunnage Zone, deposits of the Buchans district (Thurlow 2010), and some within the Tally Pond and Tulks belts of the Victoria Lake supergroup (Squires and Moore 2004; Hinchey 2011), are examples of this VMS deposit type (Fig. 3).

Felsic siliciclastic (also referred to as Bathurst-type) deposits are those hosted in siliciclastic sedimentary and felsic volcaniclastic-rich belts that contain abundant felsic volcaniclastic rocks, felsic intrusive and volcanic rocks, black shales and other siliciclastic sedimentary rocks, iron formations, and local mafic volcanic and intrusive rocks (Fig. 2). These deposits are interpreted to have formed in rifted continental margin arcs with high rates of sedimentation and are polymetallic with Zn–Pb–Cu–(Au–Ag) metal signatures. In the Newfoundland Appalachians, deposits in the southern part of the Tulks belt of the Victoria Lake supergroup, including the Boomerang and Tulks East deposits (Hinchey 2011), are examples of this VMS deposit type (Fig. 3).

Hybrid bimodal felsic deposits were defined by Galley et al. (2007) as those with geological features like bimodal felsic deposits but also with features similar to epithermal Au deposits, including argillic to advanced argillic alteration (±adularia–sericite alteration), epithermal suite el-

Can. J. Earth Sci. **00:** 1–39 (2023) | dx.doi.org/10.1139/cjes-2022-0148

Fig. 1. Model for the genesis of volcanogenic massive sulfide (VMS) deposits. While based on mafic VMS deposits in ophiolites and on modern systems, generalizations shown here are applicable to most VMS deposits. Solid red lines represent deep hydrothermal fluid recharge (downwelling), dashed red lines represent shallow hydrothermal fluid recharge (downwelling), solid black arrows represent focused hydrothermal fluid discharge (upwelling), and grey solid arrows represent diffuse hydrothermal fluid discharge (upwelling). Dark blue area area represents the top of the subvolcanic magma chamber (partly crystallized?). Modified from Alt (1995) and Hannington (2014).

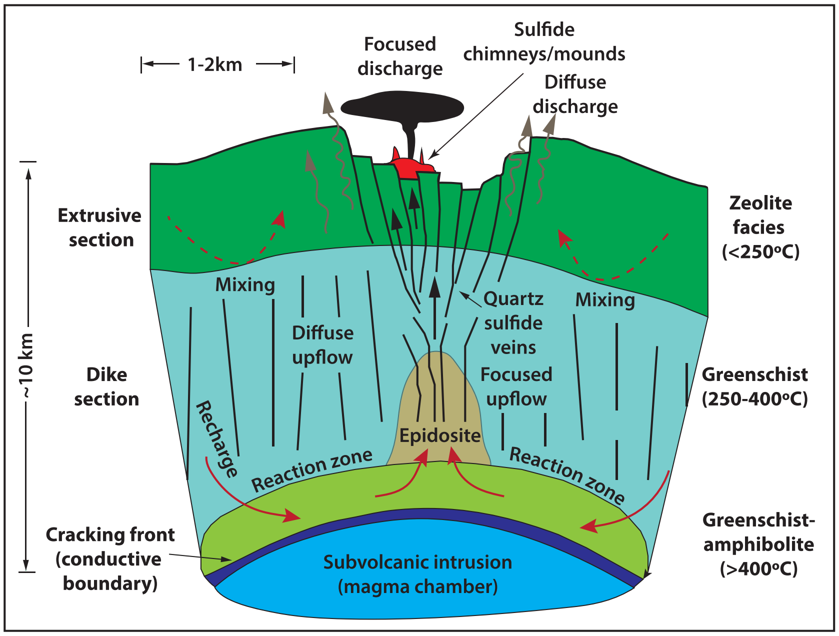

ement enrichments (e.g., Au–Ag–Hg–As–Sb–Bi–Te–Se–Sn–W), and complex sulfide and sulfosalt ore mineral assemblages (Fig. 2). These deposits are interpreted to have formed in relatively shallow water (<1500 m below sea level) within rifted arc settings like those deposits actively forming in the Manus Basin or Kermadec arc and have evidence for both VMS and magmatic-hydrothermal (epithermal) fluid inputs (e.g., Binns and Scott 1993; Sillitoe et al. 1996; de Ronde et al. 2005). In the Newfoundland Appalachians, the Bobby's Pond and Daniels Pond deposits in the northern part of the Tulks belt in the Victoria Lake supergroup (Hinchey 2011; Sparkes and Hinchey 2023) show some characteristics of this VMS deposit type (Fig. 3). Although a hybrid bimodal mafic classification was not advanced by Galley et al. (2007), the Au–Ag-sulfosalt-rich deposits of the Rambler-Ming district are potential examples of a hybrid bimodal-mafic deposit (i.e., bimodal mafic—Au-rich) having features like bimodal mafic VMS deposits but also displaying geological and mineralogical features of intermediate sulfidation epithermal Au–Ag deposits (Fig. 3; Brueckner et al. 2014*b*, 2016).

Grade–tonnage data

Grade–tonnage data for VMS deposits from central Newfoundland are presented in Figs. 4 and 5 and Table S1 in the Data Repository. These data are compiled from previous studies, including Franklin et al. (2005), Galley et al. (2007), Huston et al. (2015), and Piercey et al. (2015). Further updates include recent National Instrument (NI)-43-101 resource data obtained from company technical reports. Grade–tonnage data without recent NI-43-101 resources are considered historic resources and reserves. All data are presented as geological (total) resources, are in metric tonnes, and include both resources and reserves where relevant.

Base metal abundances in the deposits are shown in grade–tonnage space in Fig. 4. The highest-grade deposits are predominantly bimodal felsic and felsic-siliciclastic deposits; however, this result is partly influenced by deposits from the Buchans mining district, which are some of the highest-grade VMS deposits on the planet (e.g., Piercey et al. 2015). The highest tonnage deposits include those from every type of VMS deposit (Fig. 4A). In general, the mafic deposits are Cu- and Cu–Zn-dominated, whereas all other deposit types associated with felsic rocks are polymetallic with Zn–Cu–Pb, albeit those of the bimodal felsic, felsic siliciclastic, and hybrid bimodal felsic types contain greater Zn and Pb enrichment relative to Cu (Fig. 5A).

Gold and Ag are generally not enriched in most VMS deposits in central Newfoundland (Figs. 4B, 5B–5C). The deposits in the Rambler-Ming district in Baie Verte, specifically the Rambler Main deposit and ancillary lenses, are auriferous, whereas the Rendell-Jackman prospect has high Au grades but is low tonnage (Figs. 4B, 5B–5C). Other deposits do have precious metal-enriched zones and Au–Ag as ancillary metals, including Ming (e.g., 1806 zone; Brueckner et al. 2014*b*), Lemarchant (e.g., Gill et al. 2016), and Boomerang and Daniels Pond (e.g., Hinchey 2011); however, the geological resources are not considered Au-rich or auriferous (see Mercier-Langevin et al. 2011).

Fig. 2. Sub-classes of volcanogenic massive sulfide deposits showing lithostratigraphic and grade–tonnage information for Canadian VMS deposits. Modified from Galley et al. (2007).

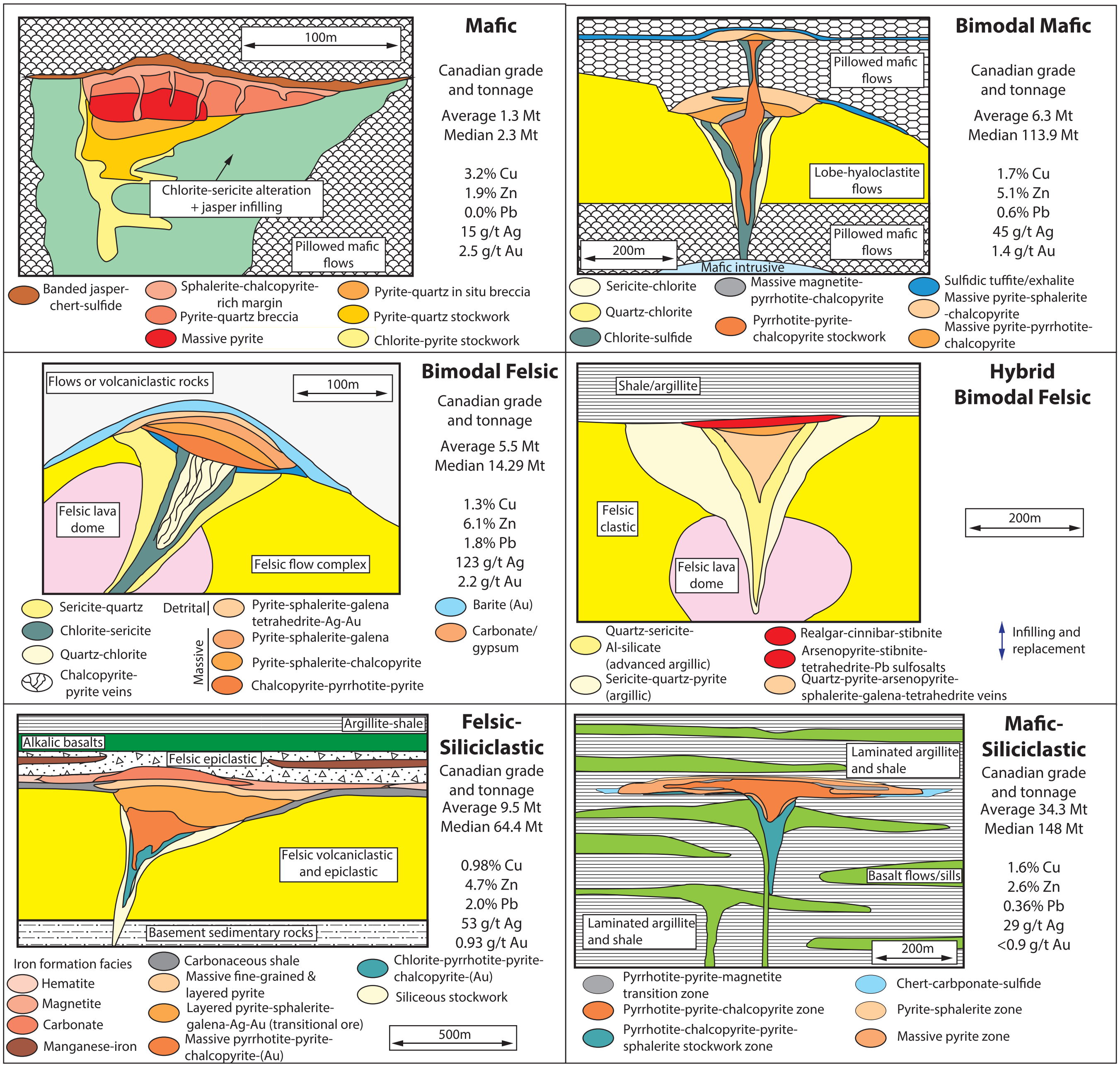

Descriptions of deposits in this paper refer primarily to those that have published resources and we will not focus here on small showings or occurrences, unless they provide critical insight into processes or the VMS metallogeny of the central Newfoundland Appalachians.

Geological setting and VMS belts

Regional geological setting

The Newfoundland Appalachians are divided into four tectonostratigraphic zones (Williams 1979), from west to east: Humber, Dunnage, Gander, and Avalon (Fig. 3). The Dunnage Zone hosts most VMS deposits in central Newfoundland and separates rocks of the Humber Zone from those zones of Gondwanan affinity—Gander, Avalon, and Meguma (van Staal and Barr 2012). The Dunnage Zone is subsequently subdivided into the peri-Laurentian Notre Dame Subzone and the peri-Gondwanan Exploits Subzone, which are juxtaposed along the Beothuk Lake Line (=Red Indian Line; Williams et al. 1988; Fig. 3). The Dunnage Zone comprises arc, back-arc, and ophiolitic rocks built on variable basements and contains vestiges of the Iapetus Ocean. The peri-Laurentian portion of the Dunnage Zone, west of the Beothuk Lake Line, consists of ophiolitic sequences in the Lushs Bight (∼505 Ma) and Baie Verte (∼489–485 Ma) oceanic tracts and

Can. J. Earth Sci. 00: 1–39 (2023) | dx.doi.org/10.1139/cjes-2022-0148

Fig. 3. Geological setting of the Newfoundland Appalachians showing tectonostratigraphic zones and VMS deposits (modified after van Staal 2007; van Staal and Barr 2012; Piercey et al. 2018). Abbreviations: BBL, Baie Verte-Brompton Line; BLL, Beothuk Lake Line (=Red Indian Line); BOI, Bay of Islands; BVOT, Baie Verte oceanic tract; CF, Cabot fault; CP, Coy Pond complex, DBL, Dog Bay Line; GBF, Green Bay fault; GRUB, Gander River ultramafic belt; LBOT, Lushs Bight oceanic tract; LCF, Lobster Cove fault; LR, Long Range; LRF, Lloyds River fault; PP, Pipestone Pond complex; SA, St. Anthony; TP, Tally Pond belt; TU, Tulks volcanic belt; VA, Victoria arc; WB, Wild Bight Group.

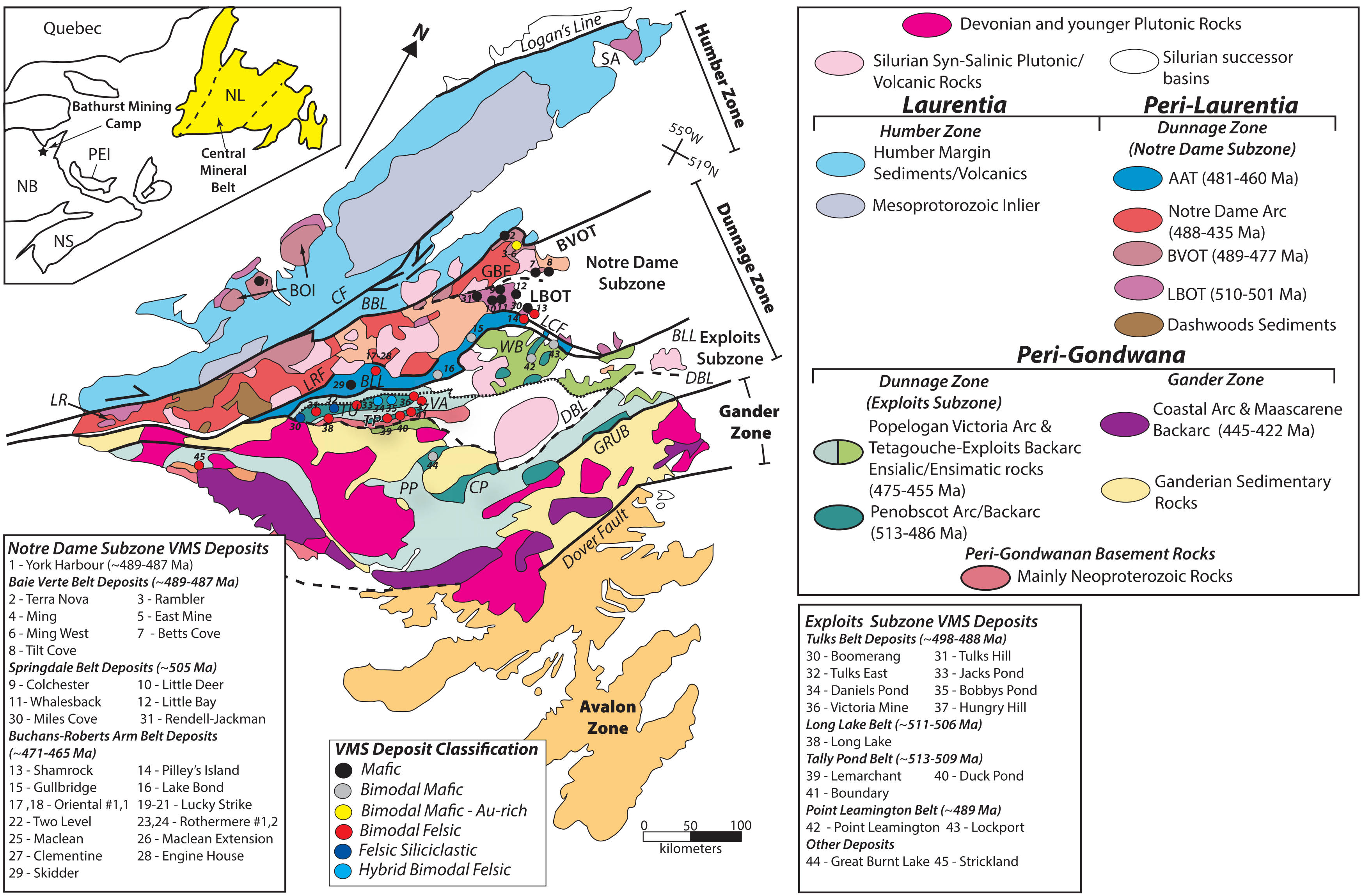

Fig. 4. Grade–tonnage data for VMS deposits of the Newfoundland Dunnage Zone: (A) Cu–Zn–Pb (%) vs. tonnage (Mt) and (B) Au (g/t) vs. tonnage (Mt).

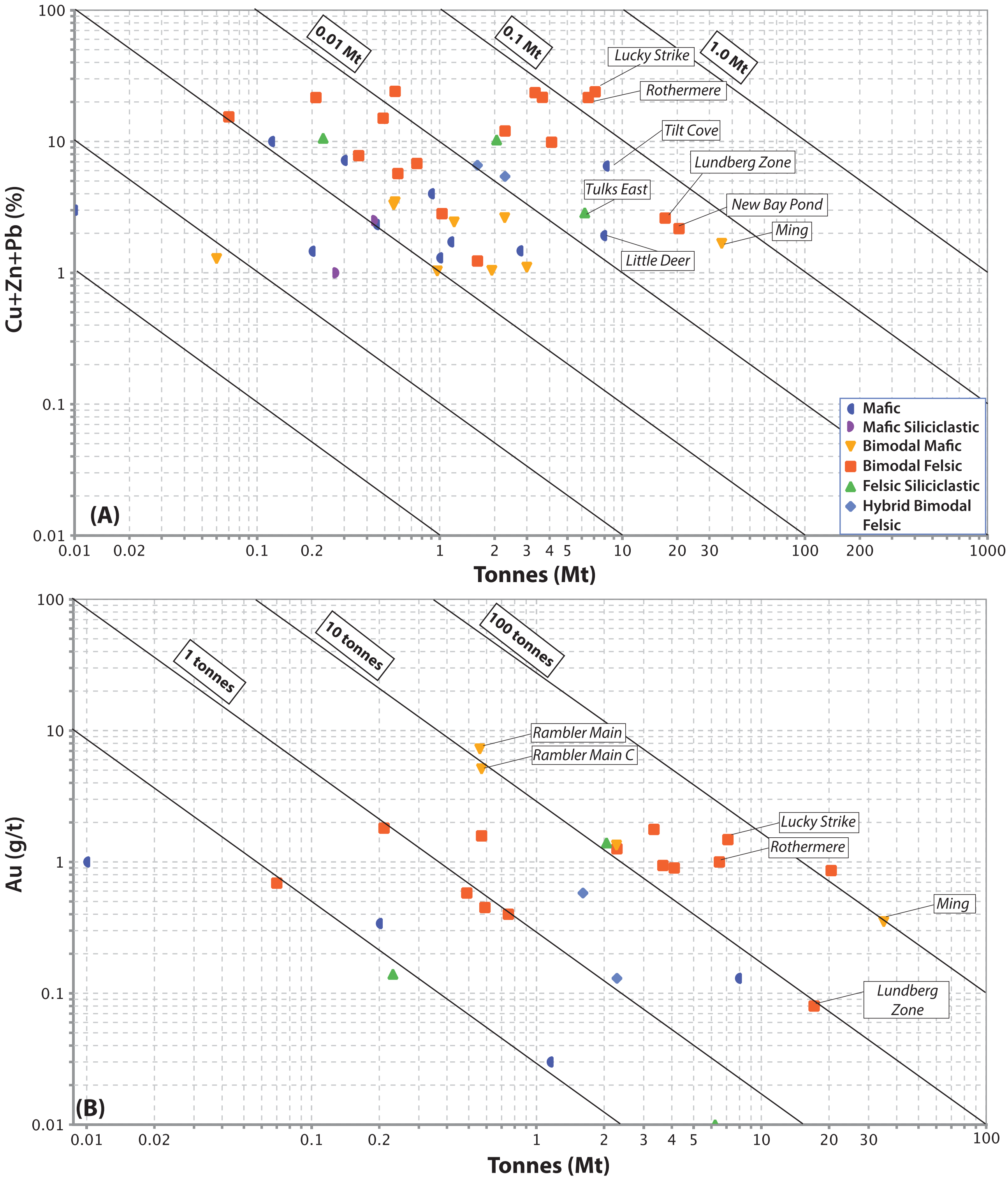

rocks of the Annieopsquotch accretionary tract and Buchans-Roberts Arm belt (~480–460 Ma; Fig. 3; Dunning and Krogh 1985; Swinden et al. 1997; Zagorevski et al. 2006; Skulski et al. 2010). The peri-Gondwanan portion of the Dunnage Zone east of the Beothuk Lake Line consists of remnants of the Penobscot (~515–485 Ma) and Popelogan-Victoria (~475–455 Ma) arc and back-arc systems that formed proximal to Ganderia (Fig. 3; MacLachlan and Dunning 1998; van Staal et al. 1998; Rogers et al. 2006; Zagorevski et al. 2007). These terranes were built atop Neoproterozoic to Early Cambrian (~620–530 Ma) basement rocks that have subduction-related affinities (Barr et al. 2003; Rogers et al. 2006; Zagorevski et

Can. J. Earth Sci. **00:** 1–39 (2023) | dx.doi.org/10.1139/cjes-2022-0148

Fig. 5. Metal contents and relationships for VMS deposits of the Newfoundland Dunnage Zone: (A) Pb–Cu–Zn ternary diagram, (B) Cu + Zn + Pb (%)–Au–Ag ternary diagram (from Hannington et al. 1999), and (C) Cu + Zn + Pb (%) vs. Au (g/t) (from Mercier-Langevin et al. 2011).

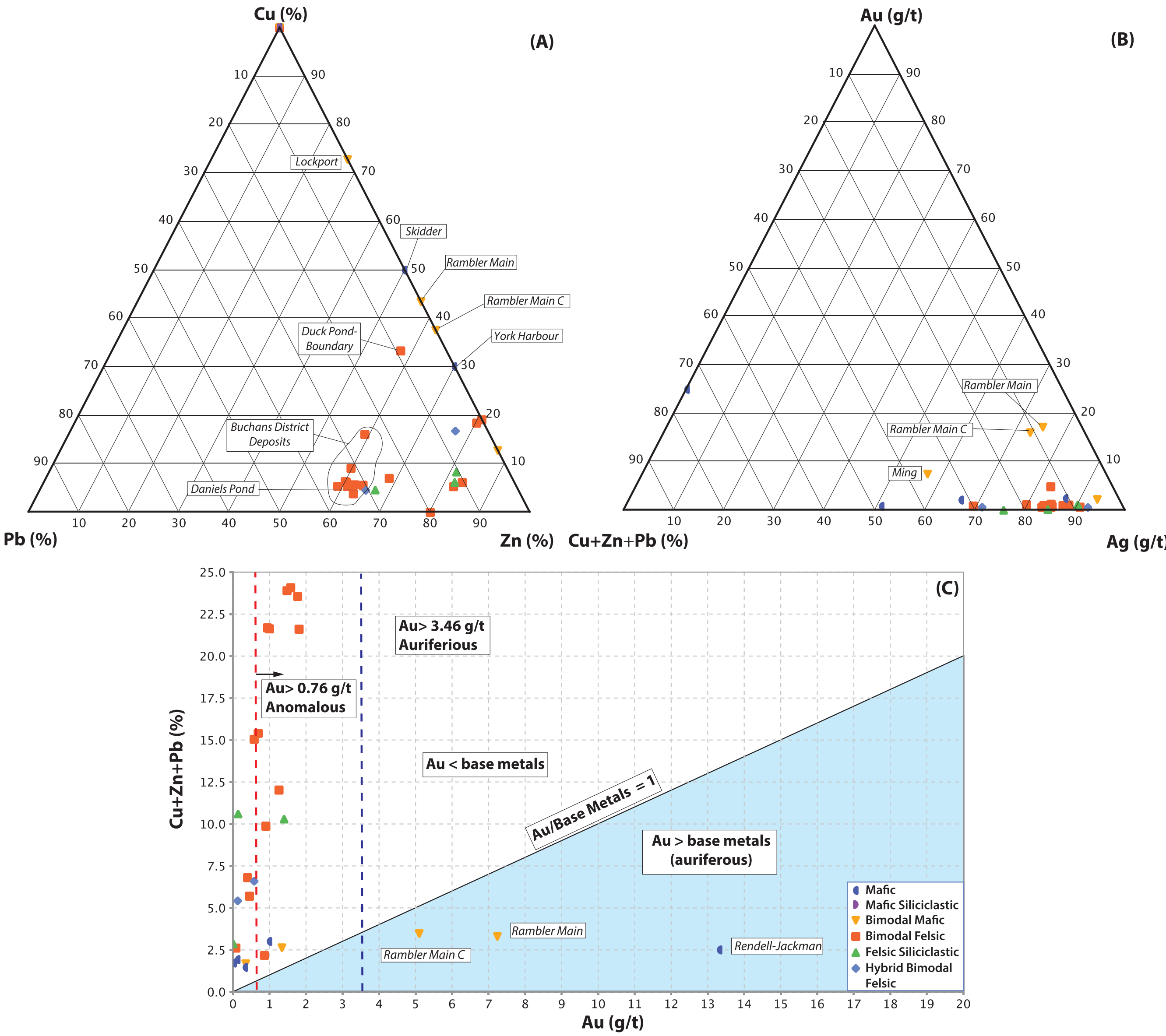

al. 2007, 2010). Peri-Laurentian rocks of the Dunnage Zone were obducted during the Taconic orogeny when rocks of the Lushs Bight Group were emplaced onto the Dashwoods microcontinent, a rifted fragment of Laurentian basement, during Taconic 1 obduction (∼500–493 Ma). Then, these rocks and the ophiolitic rocks of the Baie Verte oceanic tract were emplaced onto the Humber margin during Taconic 2 obduction at ∼475–460 Ma (e.g., Bedard 1999; Waldron and van Staal 2001; van Staal 2007; Staal and Barr 2012; Castonguay et al. 2014). Rocks of the peri-Gondwanan Exploits Subzone were emplaced upon the Gander margin during the Penobscot orogeny (∼486–475 Ma; e.g., Colman-Sadd et al. 1992; van Staal 2007; Zagorevski et al. 2009; Fyffe et al. 2012; Johnson et al. 2012; van Staal and Barr 2012). The Notre Dame and Exploits subzone rocks were accreted to each another along the Beothuk Lake line in the last stages of the Taconic orogeny during Taconic 3 (∼455–450 Ma) arc–arc collision (van Staal and Barr 2012).

Rocks and VMS deposits of the Dunnage Zone were also influenced by younger tectonothermal events related to (1) protracted magmatism within the Notre Dame arc (∼488–435 Ma), (2) syn- to post-Taconic deformation (Whalen et al. 1997; van Staal et al. 2007; van Staal and Barr 2012), (3) ∼453–430 Ma Salinic (Dunning et al. 1990; van Staal 1994; van Staal et al. 1998; van Staal et al. 2003), (4) ∼420–400 Ma Acadian (e.g., Robinson et al. 1998; Bradley et al. 2000; Castonguay and Tremblay 2003; van Staal 2007; van Staal et al. 2009, 2014), and (5) ∼400–350 Ma Neoacadian orogenesis (Murphy et al. 1999; van Staal 2007; van Staal and Barr 2012).

Outlined below are the main VMS belts within the central Newfoundland Appalachians, subdivided into peri-Laurentian/Notre Dame Subzone-hosted VMS belts and the peri-Gondwanan Exploits Subzone-hosted VMS belts (Fig. 3).

Peri-Laurentian VMS belts

Springdale belt

The Springdale belt contains VMS deposits hosted in ∼510–501 Ma ophiolitic rocks of the Lushs Bight Group (Kean et al. 1995) that form part of the broader Lushs Bight oceanic tract (Fig. S1; van Staal 2007). The Lushs Bight Group contains pillow lavas, sheeted dikes and mafic intrusive rocks, ultramafic rocks, red cherts, and rarer felsic volcaniclastic rocks (Kean et al. 1995). The main deposits within the belt include the mafic-type Little Deer, Whalesback, and Little Bay deposits (all past producers), which are hosted within arc tholeiitic and boninitic pillow lavas and are interpreted to have formed within forearc assemblages associated with subduction zone initiation (Fig. S1; Kean et al. 1995; Swinden et al. 1997; van Staal 2007). The Miles Cove mine, Rendell-Jackman, Whalesback, and Little Bay deposits are dominated by stringer vein, breccia, and locally massive to semi-massive pyrite–chalcopyrite–pyrrhotite assemblages with lesser sphalerite, cobaltite, and secondary, deformation-related Ag–Bi–Hg tellurides and arsenides (Figs. S1 and S6; Kean et al. 1995; Toman 2013; Cloutier et al. 2015). Kanehira and Baschinski (1968) also noted in the Whalesback deposit the occurrence of pentlandite, mackinawite, magnetite, cubanite, galena, and ilmenite, with minor supergene marcasite, covellite, and goethite. In the above deposits, mineralization is hosted in variably chlorite altered basalts and is commonly deformed into sulfide-bearing chlorite-(sericite) schists and locally quartz-chlorite-(carbonate) schists (Fig. 6; Kean et al. 1995; Toman 2013; Cloutier et al. 2015). The main Cu-rich assemblages in the deposits are interpreted to have formed from high temperature ($T > 300\,^{\circ}\mathrm{C}$), reduced, acidic fluids, typical of ophiolite-hosted mineralization globally (Toman 2013; Cloutier et al. 2015).

Baie Verte belt

The Baie Verte belt contains VMS deposits within the ∼489–487 Ma ophiolitic rocks of the Betts Cove Complex and correlative rocks across the peninsula (e.g., Hibbard 1983). The rocks of the Baie Verte oceanic tract are interpreted to have formed within a forearc setting during subduction zone initiation within the Humber seaway (Bedard 1999; van Staal 2007). The two main types of deposits in the belt are mafic deposits hosted within the Betts Cove Complex and Au-enriched bimodal mafic deposits hosted within the Pacquet Complex in the Rambler-Ming district (Figs. S2 and S7). In the Betts Cove Complex, VMS deposits are hosted by boninitic to island arc tholeiitic rocks of the Betts Head Formation and occur at two stratigraphic positions: within mafic volcanic/pillow lavas just above the sheeted dike complex (Betts Cove) or higher in the stratigraphy within mafic volcanic/pillow lavas (Tilt Cove; Fig. 7; Strong and Saunders 1988; Sangster et al. 2007). These are overlain by the Nugget Pond horizon, which includes red chert with hematite and magnetite that is interpreted to be an exhalative iron formation (e.g., Mueller et al. 2021*b*); locally, this unit also hosts Silurian–Devonian orogenic Au mineralization. In the past-producing Betts Cove and Tilt Cove deposits, mineralization is dominated by Cu–Zn–Au with lesser Ag and Pb and comprised predominantly pyrite and chalcopyrite with lesser sphalerite, and trace galena, gold, and Ag- and Pb-tellurides (Fig. 7; Upadhyay and Strong 1973; Strong and Saunders 1988; Sangster et al. 2007). Deposits vary from semi-massive to disseminated sulfides and are locally deformed resulting in chlorite–sulfide-rich shear zones (Sangster et al. 2007). In some locales, the disseminated sulfides and chlorite-altered rocks form pipe-like bodies interpreted to be VMS-related feeder/stringer vein upflow zones (Sangster et al. 2007). In some areas proximal to the VMS deposits, shear zones cut underlying ultramafic rocks and host Ni–As-rich sulfides; however, these are interpreted to be unrelated to (and postdate) the VMS mineralization (Papezik 1964; Sangster et al. 2007).

The Cu–Au deposits of the Rambler-Ming district are within a bimodal mafic sequence composed of boninitic to arc tholeiitic rocks of the Mount Misery Formation, which are overlain by dacitic to rhyolitic rocks of the Rambler Rhyolite formation that hosts the Ming, Rambler, and Rambler East deposits (Figs. S2 and S7). These bimodal-mafic deposits occur within a package of coherent and volcaniclastic dacitic rocks with the sulfide lenses overlain by lapilli tuffs and tuff breccias that contain fragments of the underlying host rocks and massive sulfides (Coates 1990; Pilote et al. 2017); the latter sulfide fragments are locally Au-rich (Pilote et al. 2016). The Rambler Rhyolite formation and VMS deposits are regionally overlain by the Goldenville horizon (Fig. 7), an iron formation interpreted to be equivalent to the Nugget Pond horizon in the Betts Cove region (Skulski et al. 2009) and to represent low-temperature hydrothermal discharge related to the Rambler-Ming deposits (Mueller et al. 2021*a*). The Rambler-Ming deposits contain both massive sulfide and stringer sulfides (Fig. 7). In the past-producing Rambler Main mine, the deposit consists of banded to massive pyrite–chalcopyrite–sphalerite with rarer galena and Au–Ag–Te-bearing phases, which are underlain by stringer pyrite–chalcopyrite–(sphalerite) in green mica (fuchsite)-sericite schists (Coates 1990; Weick 1993). The producing Ming mine contains numerous massive sulfide zones with variable grades and metal assemblages, which are underlain by an intensely chlorite-altered footwall zone with a stringer-type chalcopyrite–pyrite–pyrrhotite assemblage (Fig. 7; Brueckner et al. 2016). Significant mineralogical and metal diversity exists in the massive sulfide zones, which are dominated by pyrite–chalcopyrite with lesser sphalerite and galena. These zones also contain a plethora of sulfosalts, tellurides, Ag–Au–Hg–Bi phases, and Fe- and Sn-oxides; these complex assemblages are interpreted to be reflective of normal VMS metal leaching processes and magmatic-hydrothermal input into the Ming hydrothermal system (Fig. 7; Brueckner et al. 2014*b*, 2016). The Ming deposit also displays typical VMS-related hydrothermal alteration, includ-

 Can. J. Earth Sci. **00:** 1–39 (2023) | dx.doi.org/10.1139/cjes-2022-0148

Fig. 6. (A) Block model of Cu grades within the Whalesback deposit (from Cloutier et al. 2015). (B) Semi-massive to stringer pyrrhotite-rich sulfide mineralization from the Little Deer deposit with minor pyrite and strongly deformed chlorite-quartz-altered wall rock. Note rounded chlorite- and quartz-rich fragments in ore—this texture is typical of deformed massive sulfide and durchbewegung textures (e.g., Lafrance et al. 2020). (C) Chalcopyrite-(pyrrhotite)-rich stringer sulfides hosted within chlorite-altered basalts from the Little Deer deposit. (D) Banded, pyritic sulfides with chlorite stringers and porphyroblastic pyrite layers from the Whalesback deposit. (E) Stringer of pyrite and pyrrhotite among chlorite altered basalt fragments from the Little Bay deposit.

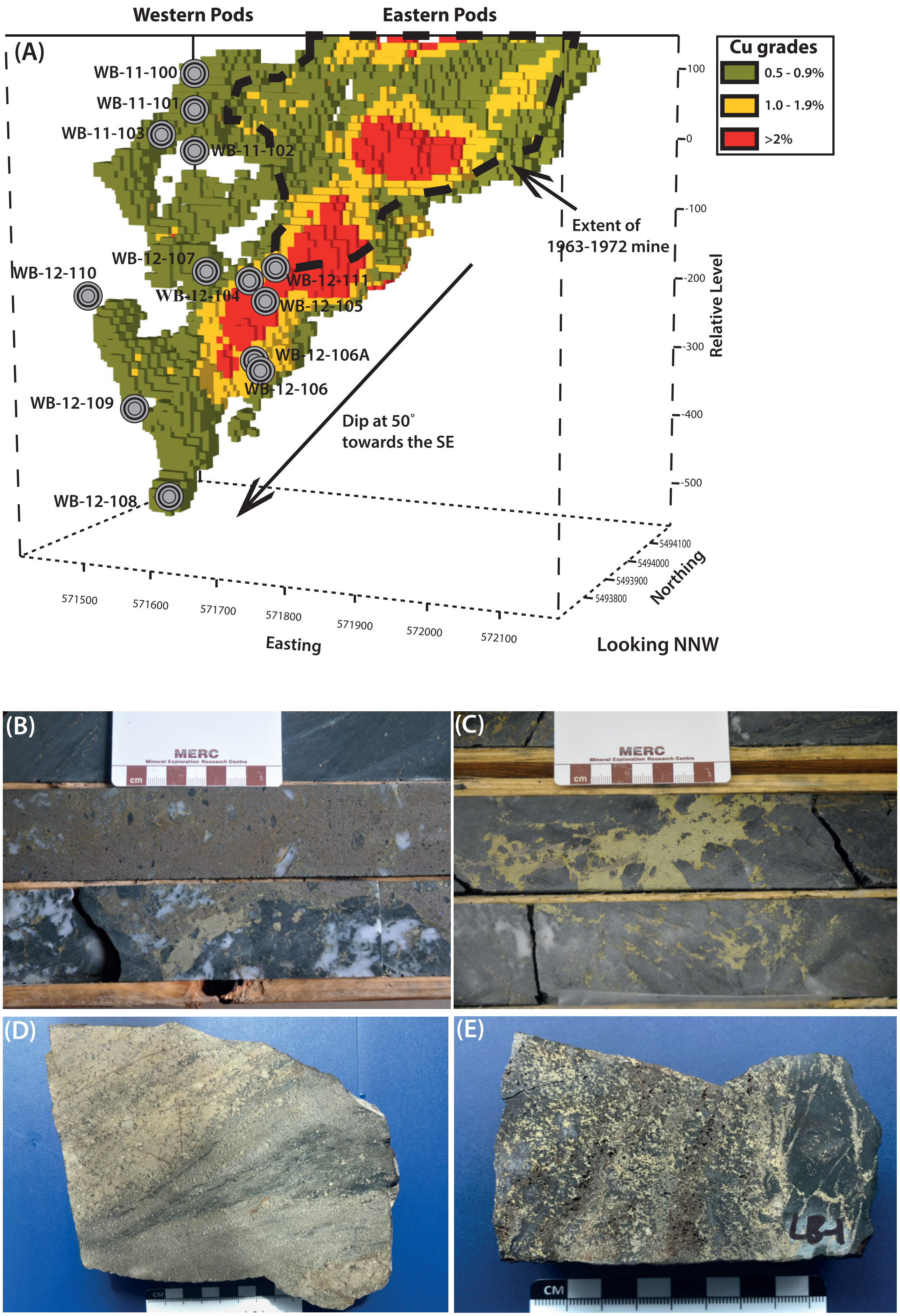

Fig. 7. (A) Stratigraphy of ophiolitic and cover rocks of the Baie Verte Peninsula and stratigraphic position of various VMS (red ovals) and orogenic Au deposits (yellow ovals). VMS deposits—BC, Betts Cove; TC, Tilt Cove; M, Ming; R, Rambler. Orogenic Au deposits—DC, Deer Cove; GV, Goldenville; NP, Nugget Pond; A, Argyle; ST, Stog'er Tight; PC, Pine Cove (modified after Bedard et al. 2000 and Skulski et al. 2009, 2010). (B) Deformation-related banded pyrite–sphalerite-bearing massive sulfides from the Betts Cove VMS deposit. (C) Pyrite-dominated sulfides with quartz-green mica altered dacite fragments from the Ming deposit; this style of mineralization is typically Au-rich. (D) Photo from underground in the Ming mine showing a stringer of chalcopyrite–pyrite–pyrrhotite in chlorite-altered footwall dacite. (E) Relict colloform and euhedral pyrite with interstitial chalcopyrite from the Ming deposit. (F) Polymetallic assemblages of pyrite–chalcopyrite–sphalerite–galena–tetrahedrite from the Ming deposit. (G) Gold/electrum with arsenopyrite in a pyrite–chalcopyrite–tetrahedrite–sphalerite assemblage from the Ming deposit.

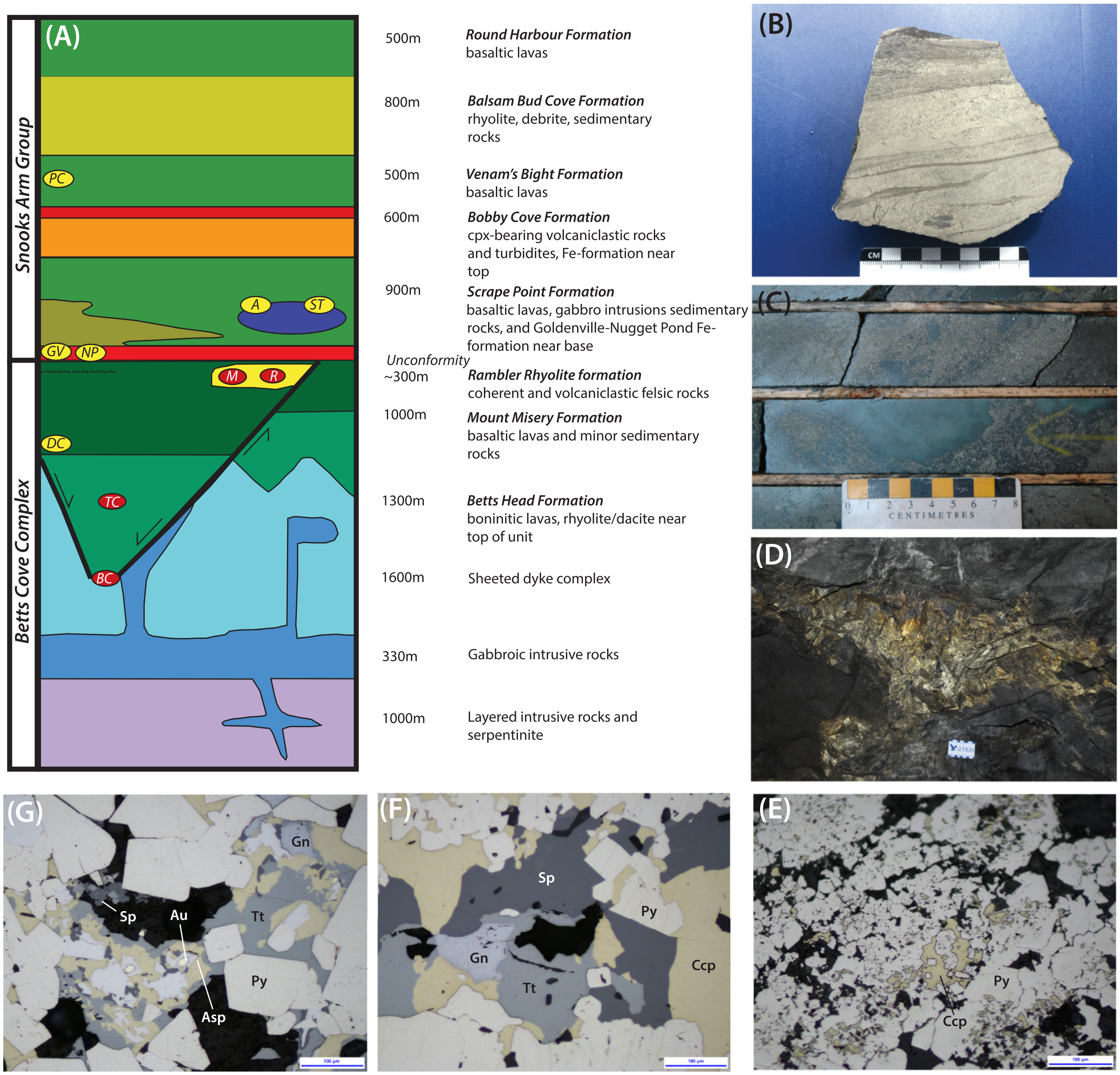

ing sericite proximal to the massive sulfide mineralization and intense chlorite–(quartz) alteration in the footwall zones; however, this deposit also contains distinctive green mica (fuchsite?) like that present at the Rambler Main deposit (Fig. 7; Pilote et al. 2020).

Buchans-Roberts Arm belt

The Buchans-Roberts Arm belt extends from Buchans in the south to Pilleys Island in the north and contains past-producing VMS deposits in the Buchans, Gullbridge-Lake Bond, and Pilley's Island regions (Fig. S3).

 Can. J. Earth Sci. 00: 1–39 (2023) | dx.doi.org/10.1139/cjes-2022-0148

The Buchans district is host to numerous VMS deposits that have some of the highest grades globally with exceptional Zn–Pb grades (Figs. 4–5 and Table S1; e.g., Piercey et al. 2015). The district produced from 1928 to 1984 (Thurlow 2010) and has been the subject of numerous comprehensive studies (e.g., Swanson et al. 1981, and references therein; Kirkham 1987, and references therein), recent research (e.g., van Hees et al. 2012), and more recent exploration, discovery, and deposit expansion (e.g., Lundberg Zone deposit of Buchans Resources Ltd.). The deposits are bimodal-felsic and hosted in calc-alkalic sequences, with most mineralization occurring in the felsic-dominated Buchans River Formation and less in the underlying basalts of the Ski Hill Formation (Fig. 8). Rocks of the district are pervasively imbricated by thrust faults (Fig. 8) with most VMS deposits having at least one faulted contact; these thrust faults are interpreted to be reactivated synvolcanic faults that nucleated on phyllosilicate-rich alteration zones during basin inversion associated with Taconic thrusting (Thurlow and Swanson 1987; Thurlow 2010).

Past-producing deposits of the district are of three main types: in situ (e.g., Lucky Strike), stringer/stockwork deposits (e.g., Lundberg zone), and transported (e.g., MacLean; Fig. 8). The in situ deposits (i.e., formed within and proximal to volcanic hosts in interpreted exhalative chimneys/mounds) are the least well-understood deposits because most were mined out by the 1960s and before comprehensive research was undertaken in the district (Thurlow 2010). These deposits contain massive sulfides of varying textures that are underlain by stockwork mineralization with associated chlorite–sericite alteration zones and are variably deformed due to thrust faults (Thurlow 2010).

Transported ore deposits consist of unsorted, matrix-supported conglomeratic ores that contain clasts of both volcanic rocks, as well as sphalerite–galena (black ore), chalcopyrite (yellow ore), and barite within a matrix of ash and fine-grained barite (Fig. 8). These ores are interpreted to have been sulfide–volcaniclastic debris flows that were channelized within extensional basins during rifting (Thurlow and Swanson 1981; Binney 1987).

Stockwork mineralization is hosted predominantly in basalts of the Ski Hill Formation and partly in felsic rocks of part of the Buchans River Formation and consists of stringer-style base metal sulfides, barite, and locally quartz, commonly exhibiting zonation in alteration from chlorite and quartz proximal to the stockwork and sericite distal from the stockwork (Thurlow 2010; van Hees et al. 2012). Locally, there is evidence of bladed barite (Fig. 8) and quartz and illite alteration that has been interpreted to reflect magmatic-hydrothermal fluid input in these stringer systems (Thurlow 2010), which has also been observed elsewhere in the Buchans-Roberts Arm belt (Sparkes 2022; Sparkes and Hinchey 2023).

The mineralization in the Buchans district has remarkably low pyrite contents and is dominated by sphalerite, galena, chalcopyrite, and barite with lesser tetrahedrite–tennantite that display excellent textural preservation and have features like those found on the modern seafloor, including relict framboids and chimney structures, atoll textures, and evidence for zone refining and dissolution–reprecipitation processes (Fig. 8).

The Gullbridge-Lake Bond district is hosted within a structurally imbricated, ∼470 Ma bimodal volcanic sequence that contains arc tholeiitic to back-arc basin basalts and lesser calc-alkalic felsic to intermediate composition tuffaceous volcanic rocks (Sparkes et al. 2021). The two main deposits are the bimodal-mafic Gullbridge and Lake Bond deposits (O'Brien 2007; Fig. 9A). The Gullbridge deposit contains Cu-rich stockwork vein and disseminated mineralization that contains pyrite, pyrrhotite, chalcopyrite, and magnetite within a metamorphosed VMS alteration zone dominated by cordierite−andalusite−anthophyllite−iron chlorite (Upadhyay and Smitheringale 1972; Sparkes 2020; Fig. 9B). The Lake Bond deposit consists of a Zn-rich zone of stockwork-style mineralization dominated by pyrite, sphalerite, lesser chalcopyrite, and trace galena, hosted by ∼470 Ma chlorite–epidote-altered island arc tholeiitic mafic rocks (Fig. 9C; Swinden 1988*b*).

The Pilley's Island district is within the northern extremity of the Buchans-Roberts Arm belt in Notre Dame Bay (Fig. S3). Like elsewhere in this belt, the Roberts Arm Group in this region is thrust imbricated and comprises panels of felsic volcanic and volcaniclastic rocks intercalated with panels of basaltic rocks (Thurlow 1996; McKinley 2013). All VMS deposits in the region are hosted within the Spencer's Dock, Old Mine, and Bull Road thrust panels (Fig. 10). Only the Old Mine deposit has a historic resource; other deposits (Jane's Cove, Rowsell's Cove, and Spencer's Dock) within the Spencer's Dock panel are pyrite-dominated and lack formally reported resources (Thurlow 1996). The Old Mine and 3B panels contain showings, some of which have high grades but are of limited areal extent. The historic, past-producing Old Mine is found within the Old Mine panel and is hosted by multiple rhyolite/dacite flow units and volcaniclastic rocks. It contains chalcopyrite–pyrite lenses underlain by stockwork mineralization associated with sericite (and lesser chlorite) alteration (Tuach 1988, 1990; Santaguida et al. 1992; McKinley 2013). The mineralization is interpreted to have formed from exhalative processes with deposition of the sulfide on the seafloor and having been fed by an underlying stockwork feeder system; these deposits have numerous textures similar to sulfides that have formed on the modern seafloor (Fig. 10; Tuach 1988, 1990; Santaguida et al. 1992; McKinley 2013). The Old Mine panel also hosts the 3B and Bumblebee Bight showings. The 3B showing consists of lenses of pyrite and chalcopyrite with underlying stringer mineralization hosted in rocks like the Old Mine stratigraphy (Santaguida et al. 1992), whereas the Bumblebee Bight showing comprises pyrite–chalcopyrite stringers within pillow lavas and felsic volcaniclastic rocks (Fig. 10). The Bull Road showing is hosted in the Bull Road panel and consists of massive sulfide clasts within a polylithic breccia containing both sulfide clasts and volcanic fragments; locally, clasts can be traced over 200 m and some have Zn–Pb–Cu grades and sulfide textures (Fig. 10) like the transported ores in the Buchans district (Tuach 1988, 1990).

Fig. 8. (A) Geological map and distribution of VMS deposit types in the Buchans district (modified after Thurlow et al. 1992 and van Hees et al. 2012). (B) Transported clastic ore from the Maclean Extension deposit showing clasts of host rocks (e.g., basalt and rhyolite) but also sulfides within a matrix of barite- and sulfide-bearing sand. (C) Polymetallic massive sulfide from the Maclean deposit with pyrite, chalcopyrite, and barite. (D) Pyrite framboids (PyF) and pyrite atolls infilled with galena (Gn) and chalcopyrite (Ccp) within a chalcopyrite–galena–sphalerite-rich assemblage, Maclean Extension deposit (photomicrograph, reflected light). (E) Sphalerite–galena-rich ore with lesser tetrahedrite and chalcopyrite from the Maclean Extension deposit (photomicrograph, reflected light). (F) Zoned euhedral pyrite (Py) grains with interstitial colloform pyrite (PyC) inclusions and interstitial chalcopyrite (Ccp) with sphalerite (Sp) inclusions, typical of zone-refined massive sulfide mineralization (photomicrograph, reflected light). (G) Detailed photomicrograph of (F) using a differential interference contrast image. Note the fine-scale growth zoning and texture preserved in the pyrite grains (pyrite was etched in 8 N nitric acid for 30 s prior to image capture in (F) and (G)). (H) Scanning electron microscope (SEM)–back scatter electron (BSE) image of relict pyrite framboids partly replaced by galena (Py-Gn) intergrown with galena and barite, Maclean Extension deposit. (I) SEM–BSE image of colloform pyrite (Py) grains completely surrounded by galena (Gn) with barite, oriental deposit. (J) SEM–BSE image of zoned colloform pyrite (Py) grain partially replaced by intergrown chalcopyrite–sphalerite and surrounded by assemblages of galena–chalcopyrite–sphalerite, oriental deposit. (K) SEM–BSE image of bladed barite (Brt) grains with sphalerite (Sp) and galena (Gn) from the oriental deposit. These textures are like bladed barite found in some low- to intermediate-sulfidation Au deposits.

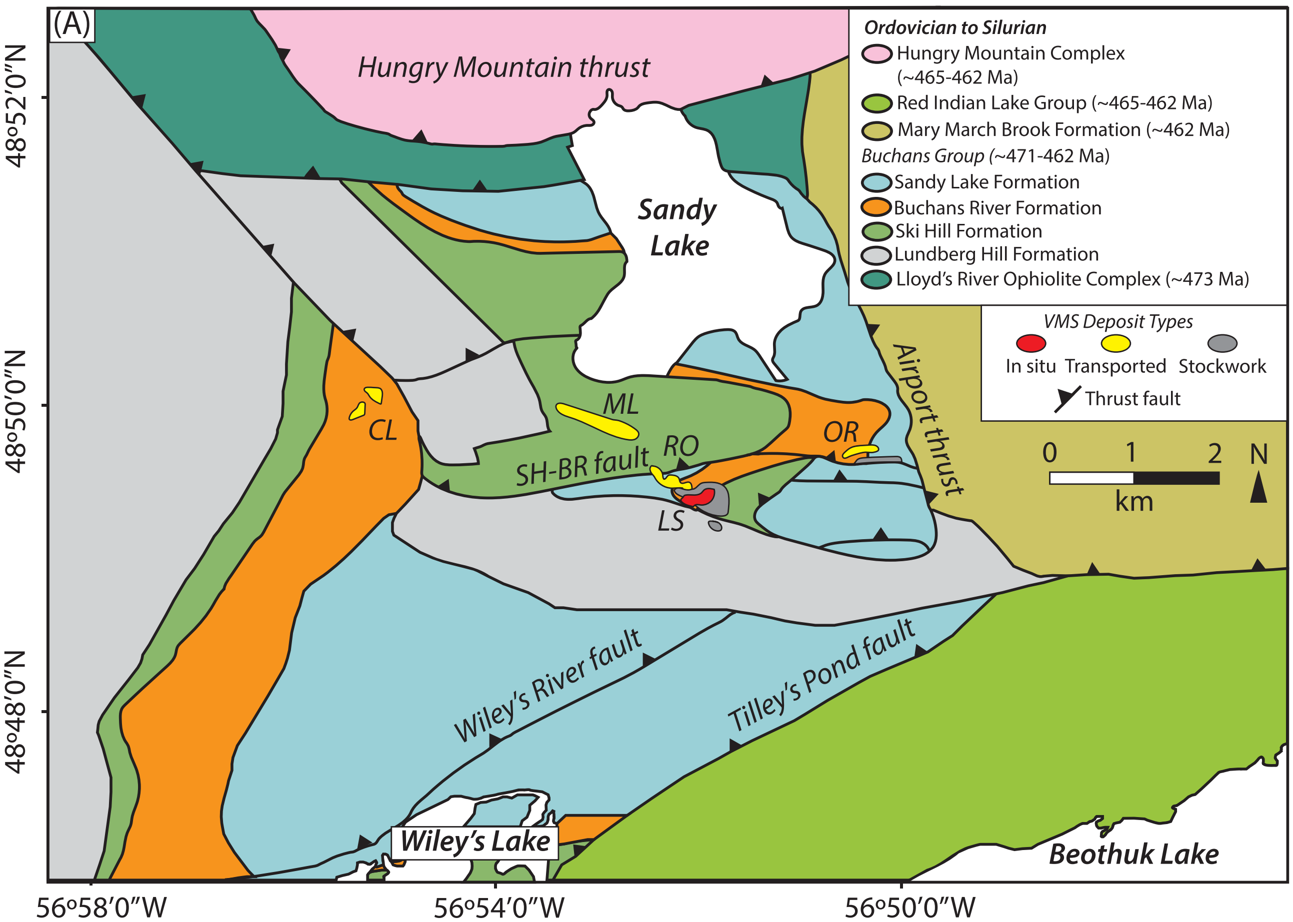

In the Spencer's Dock panel, three pyrite-dominated deposits are hosted by dacitic rocks in three sub-panels (Thurlow 1996). Volcanic rocks in this panel are remarkably well preserved and dominated by flow-banded dacite and rhyolite that contain vesicles, amygdules, and perlitic cracks (Fig. 10; Thurlow 1996). Deposits in the Spencer's Dock panel are associated with extensive sericite alteration and show evidence for formation via subseafloor replacement of the felsic flows (Thurlow 1996).

Peri-Gondwanan VMS belts

Tally Pond belt

The Tally Pond belt contains VMS deposits hosted by the bimodal ∼513–509 Ma Tally Pond group (Table S1; Fig. 14). The Tally Pond group has been subdivided into the felsic-dominated Bindons Pond formation and the mafic-dominated Lake Ambrose formation, which collectively are interpreted to represent a rifted arc that was built on

Fig. 8. (*concluded*).

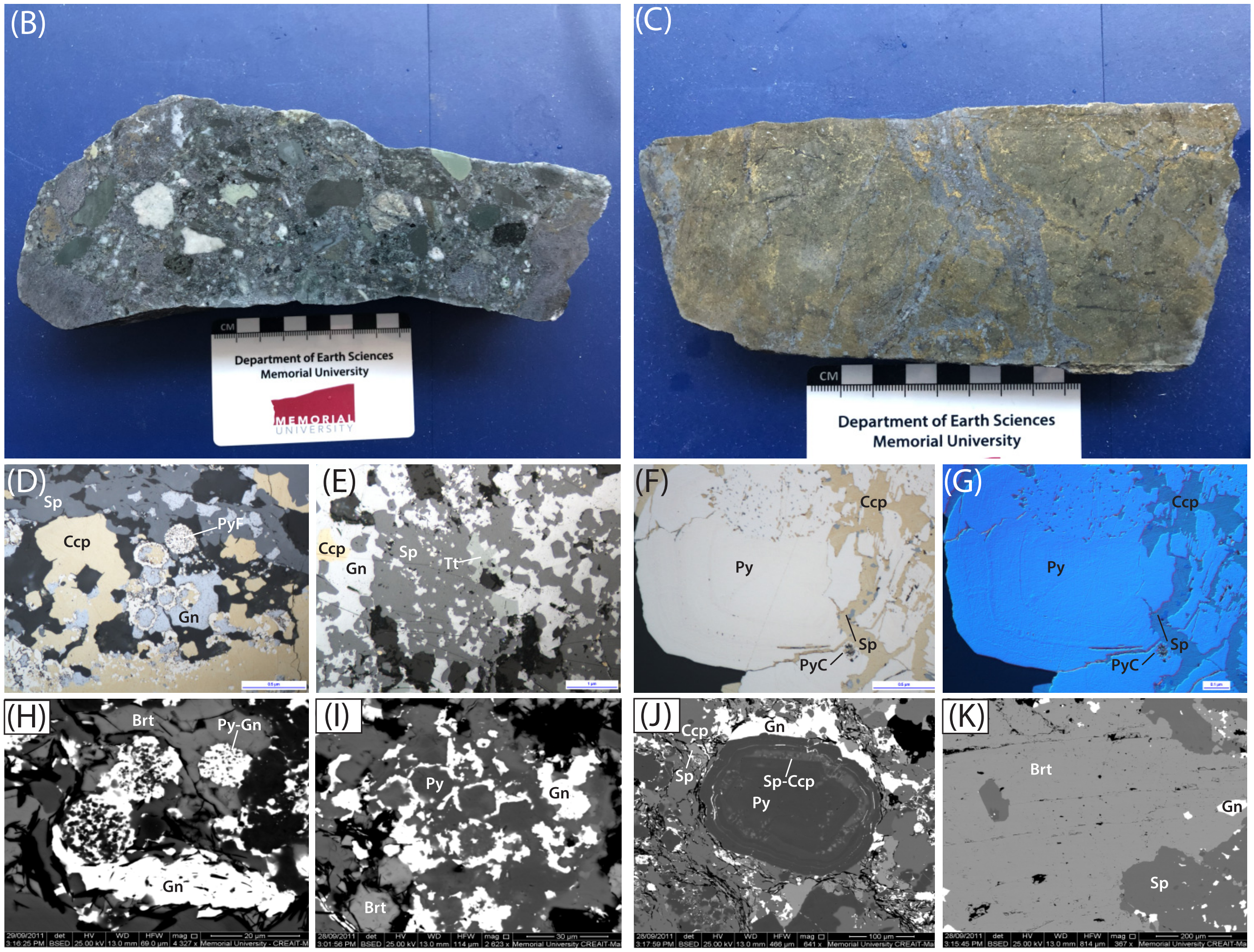

~565 Ma juvenile arc crust of Ganderian affinity (Dunning et al. 1991; Rogers et al. 2006).

The deposits are subdivided into the past-producing Cu–Zn Duck Pond and Boundary deposits (Table S1) and the Zn–Pb–(Ag–Au–Cu) Lemarchant deposit (Squires et al. 2001; McNicoll et al. 2010; Piercey et al. 2014; Gill et al. 2016; Cloutier et al. 2017). The Duck Pond deposit is hosted by ~509 Ma felsic rocks of the Bindons Pond formation within a mineralized block that is overthrust by a bimodal sequence of basalts and rhyolitic rocks that host minor hydrothermal mudstones but lack significant mineralization (Fig. S4). The Duck Pond deposit consists of numerous lenses of pyrite, chalcopyrite, sphalerite, and lesser galena and sulfosalts, with the bulk of all mined mineralization coming from the Upper Duck lens. The lenses are hosted within jigsaw-fit rhyolite breccias and to a lesser extent massive, blocky rhyolite (Figs. 11 and 12). Individual sub-lenses within the Upper Duck lens show zone refining with earlier pyrite–sphalerite assemblages overprinted and recrystallized by chalcopyrite-rich assemblages, which are associated with sericite and chlorite-(dolomite) alteration, respectively (Fig. 13).

The Boundary deposit is located ~5 km north of the Duck Pond deposit and consists of two mineralized zones, the North and South zones, offset by the Wagner fault. The deposit is hosted by a footwall lapilli tuff and lapillistone and a hanging wall of flow-banded rhyolite (Figs. 11 and 12; Squires et al. 2001; Piercey et al. 2014). The mineralized zones consist of pyrite, sphalerite, chalcopyrite, and lesser galena and exhibits features indicative of zone refining. The mineralized zones are also spatially associated with both pipe-like and laterally extensive blankets of footwall chlorite–(dolomite) and sericite–quartz alteration and a hanging wall dominated by quartz–sericite alteration (Fig. 12). The ores at both Duck Pond and Boundary display features that indicate formation occurred predominantly by subseafloor replacement of volcaniclastic and volcanic rocks, with much lesser exhalative mineralization (Squires et al. 2001; Piercey et al. 2014).

The Lemarchant deposit is located south of the Duck Pond deposit and is hosted in a thrust-imbricated package of bimodal volcanic rocks (Gill et al. 2016; Cloutier et al. 2017). The deposit contains two zones, the Main Zone and Northwest Zone, with most sulfide mineralization found in the Main Zone. The deposit consists of stratiform sulfide–barite that is at the boundary between footwall blocky rhyolite, rhyolite breccias, and hanging wall basaltic rocks (Figs. 11 and 12; Gill et al. 2016; Cloutier et al. 2017). The mineralization is min-

Fig. 9. (A) Regional geology of the central portion of the Buchans-Roberts Arm belt (from Sparkes et al. 2021), (B) Representative sample from the Gullbridge deposit containing pyrrhotite–chalcopyrite within cordierite–chlorite-rich groundmass, and (C) sphalerite-dominated stockwork-style mineralization from the Lake Bond deposit.

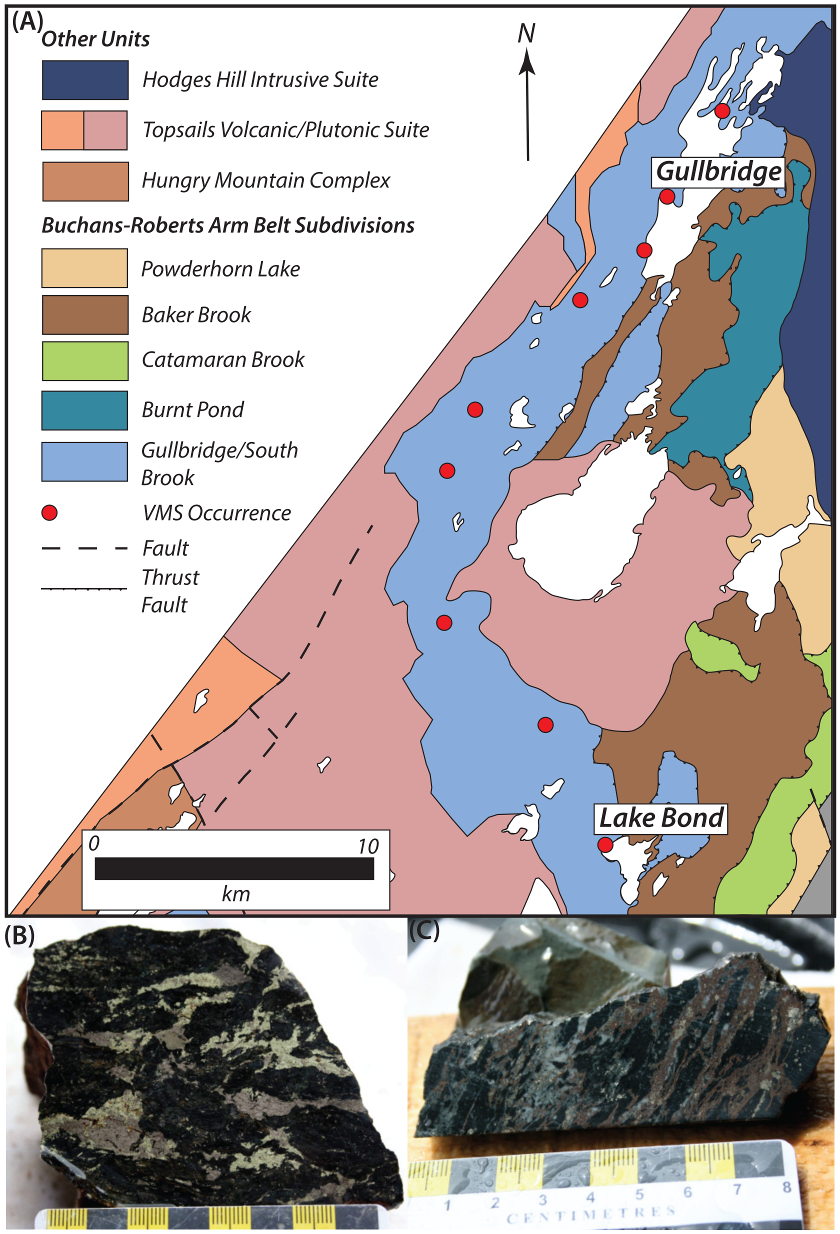

eralogically complex, consisting of massive sulfide, barite, and stringer sulfides that contain abundant sulfides, oxides, precious metal phases, and sulfosalts that show evidence of formation from both exhalative processes, as well as potential fluid boiling and input from magmatic-hydrothermal fluids and deposition in relatively shallow water (~1500 mbsl; Fig. 12; Gill et al. 2016).

Long Lake belt

The Long Lake belt contains the Long Lake VMS deposit and several other occurrences within the ~514–506 Ma volcanic and volcaniclastic rocks of the Long Lake Group of the Victoria Lake supergroup (Fig. 13; Evans and Kean 2002; Hinchey and McNicoll 2016). The basalt, andesite, and rhyolite host rocks have partially overlapping U–Pb ages with the Tally Pond group. Near the Long Lake deposit, the rocks are bimodal with felsic-(to intermediate) compositions predominating over mafic rocks. Felsic rocks within the group can be broadly divided into two packages: (1) ~506 Ma quartz ± feldspar phyric, felsic to intermediate rocks and medium- to coarse-grained volcaniclastic rocks—the upper stratigraphy and (2) ~514 Ma white to pink, aphyric to quartz ± feldspar porphyritic, magnetite bearing, massive rhyolite, and fine-grained magnetite-bearing felsic tuff—the lower stratigraphy (Fig. 13; Hinchey and McNicoll 2016). Both packages contain fine-grained tuff, volcanogenic siltstone, and graphitic shale and are associated with hydrothermal

Fig. 10. (A) Geological map and thrust panels for the Pilley's Island VMS district showing deposits projected to surface (modified from Thurlow 1996; McKinley 2013). (B) Pillow lavas with pyrite staining from the Bumblebee Bight deposit. (C) Spherulitic dacite flows from the Spencer's Dock panel—these rocks host mineralization in the Spencer's Dock and Rowsell's/Jane's Cove deposit. (D) Dacite breccia with sericite altered fragments from the Old Mine panel. (E) Relict colloform pyrite and euhedral pyrite associated with chalcopyrite from massive sulfides from the Old Mine (photomicrograph, reflected light). (F) Sphalerite with partial replacement by chalcopyrite forming chalcopyrite disease (Barton and Bethke 1987) and surrounded by euhedral pyrite and chalcopyrite from the Bull Road occurrence (photomicrograph, reflected light). Mineral and mineral textural abbreviations as in Fig. 11.

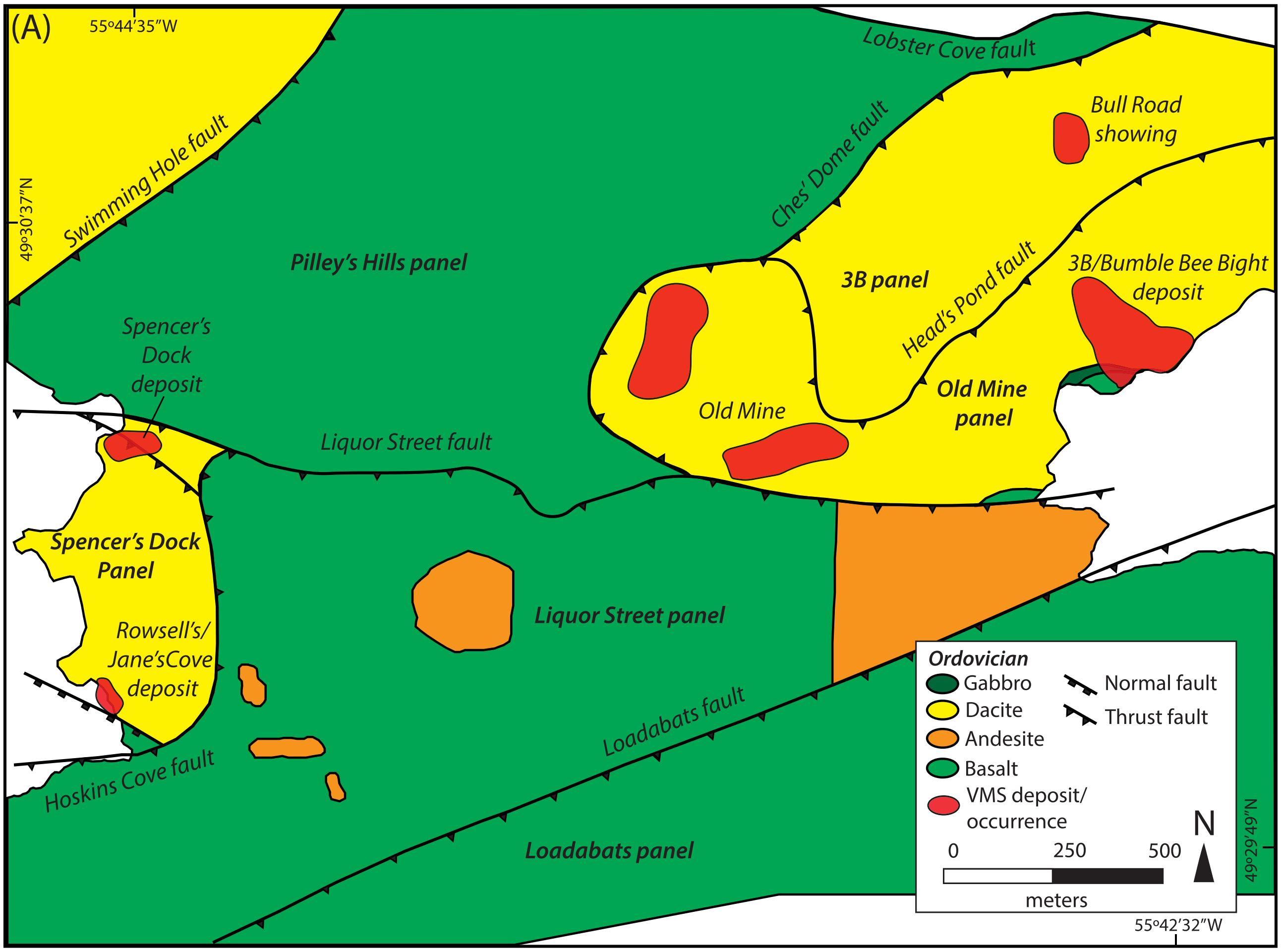

alteration associated and disseminated to massive sulfides. Mafic rocks in the group are dominated by mafic tuff, pillow basalt, and breccia. The bimodal felsic Long Lake deposit is hosted within the lower stratigraphic units. The group has been subjected to polyphase deformation resulting in fold-thrusted structures that have overprinted and modified stratigraphy and mineralized horizons (Hinchey 2014). The Long Lake group is interpreted to have formed within a continental arc environment with the lower VMS package having geochemical signatures indicative of formation in a rifted continental arc (Hinchey and McNicoll 2016), like other parts of the Penobscot–Victoria arc, including the Tally Pond group to the east (Rogers et al. 2006; Zagorevski et al. 2010; Piercey et al. 2014).

The Long Lake deposit is hosted by a sequence of felsic and mafic volcanic rocks with minor cherty sedimentary rocks that contain narrow (cm to m scale) intervals of barite-rich massive sulfide composed of sphalerite, chalcopyrite, galena, and pyrite (Fig. 14). The host rocks have experienced pervasive and intense sericite, pyrite, chlorite, carbonate, and quartz alteration. Both the host rocks as well as the massive sulfides display evidence of recrystallization related to post-VMS structural overprinting (Hinchey 2014).

Tulks belt

The ~498–491 Ma Tulks volcanic belt outcrops as a 65 km long by 8 km wide belt of rocks trending from the northeast to southwest parallel to the Beothuk Lake Line (Fig. 15). This volcano-sedimentary belt is dominated by felsic compositions with lesser mafic volcanic/volcaniclastic and sedimentary rocks. The predominant lithologies are quartz–feldspar porphyritic felsic to intermediate composition volcaniclastic rocks, massive rhyolite, and felsic to intermedi-

Fig. 10. (*concluded*).

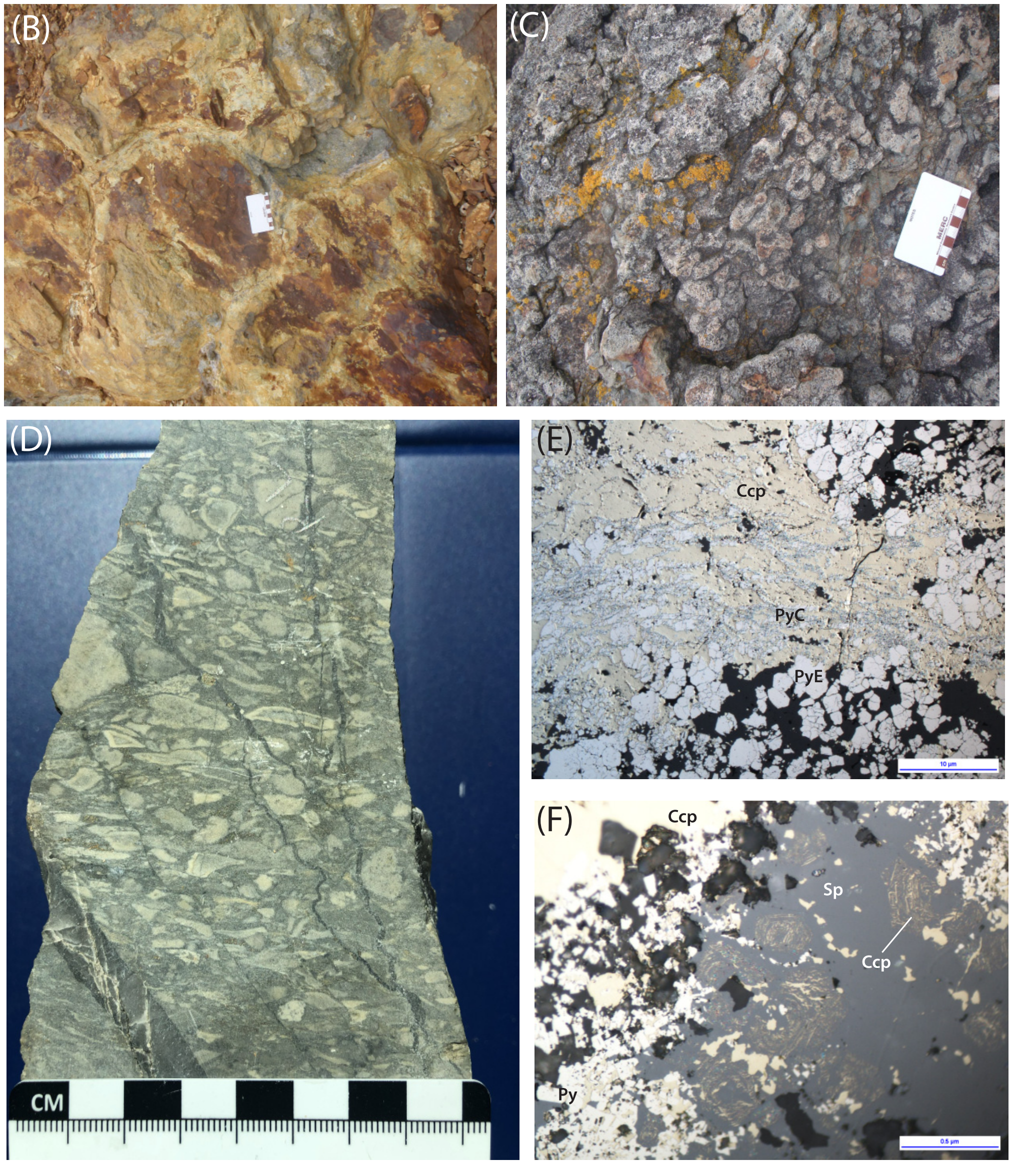

ate tuffs (with variable crystals and lapilli) and minor subvolcanic porphyritic intrusions. Mafic volcanic rocks are subordinate and consist of fine tuff, lapilli tuff, breccia, local pillow basalt, massive flows, and hypabyssal intrusions. Black shale, argillite, and greywacke are also locally abundant, especially in the southern portion of the belt (Hinchey 2011).

The Tulks volcanic belt hosts five VMS deposits, from south to north: Boomerang/Domino, Tulks Hill, Tulks East, Daniels Pond, and Bobby's Pond (Fig. 15). The deposits are hosted by felsic volcanic and volcaniclastic rocks and sedimentary rocks. They are interpreted to have had varying emplacement styles of formation, including exhalative deposition (e.g., Daniels Pond) and subseafloor replacement (e.g., Boomerang, Tulks East, Tulks Hill; Kean and Evans 1986; Hinchey 2011, and references therein). The deposits are interpreted to have formed within a continental back-arc or arc rift environment as it transitioned from normal continental arc magmatism (Hinchey 2011).

The deposits in the belt include felsic–siliciclastic, bimodal-felsic, and hybrid bimodal-felsic deposit types. There is a regional shift in volcanic environment and interpreted tectonic setting from the southern to northern part of the belt. Deposits in the southern part of the belt (Boomerang/Domino, Tulks Hill, and Tulks East) are bimodal-felsic to felsic–siliciclastic deposits that are Zn-rich and polymetallic (Zn–Pb–Cu–Ag–Au) and have variable sericite–chlorite–quartz–pyrite alteration. In some deposits, siliciclastic sedimentary rocks are more abundant, particularly proximal to the mineralized zones (e.g., Boomerang deposit; Fig. 14). Of these deposits, Boomerang deposit displays textural evidence for subseafloor replacement-style mineralization whereby sulfides contain relict textures and crystals of the original host, which is interpreted to reflect replacement of permeable volcanic and sedimentary facies by sulfide during ore formation (Hinchey 2011, and references therein; English 2019).

 Can. J. Earth Sci. 00: 1–39 (2023) | dx.doi.org/10.1139/cjes-2022-0148

Fig. 11. (A) Cross-section 9200 N through the Duck Pond VMS deposit (modified after Squires et al. 1991, 2001). (B) Cross-section 225 W and (C) cross-section 050 W from the North Zone of the Boundary VMS deposit (modified after Squires et al. 1991, 2001 and Piercey et al. 2014). (D) Long section through the Lemarchant deposit, including both the main zone and Northwest zone (modified after Gill et al. 2016).

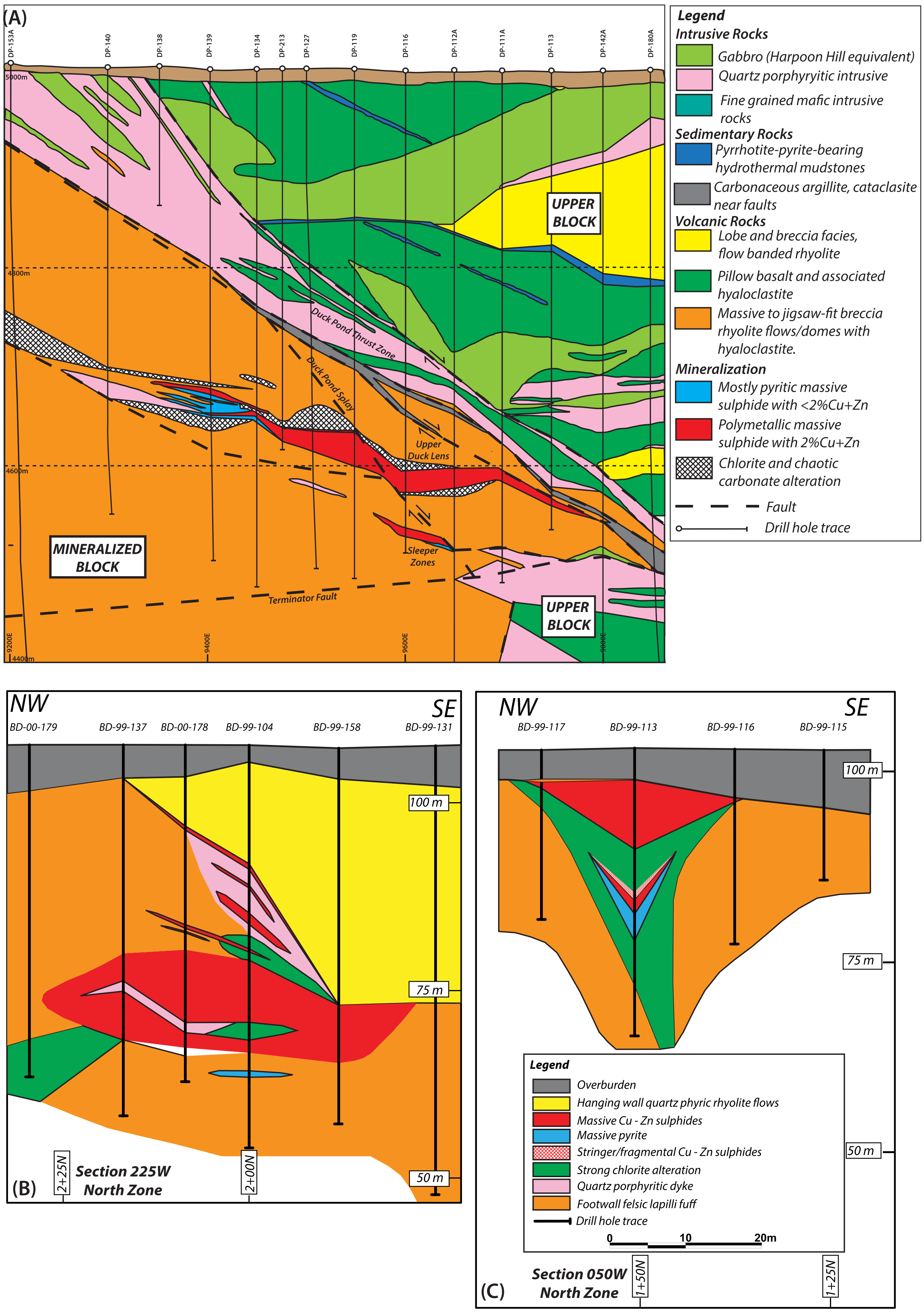

Fig. 11. (*concluded*).

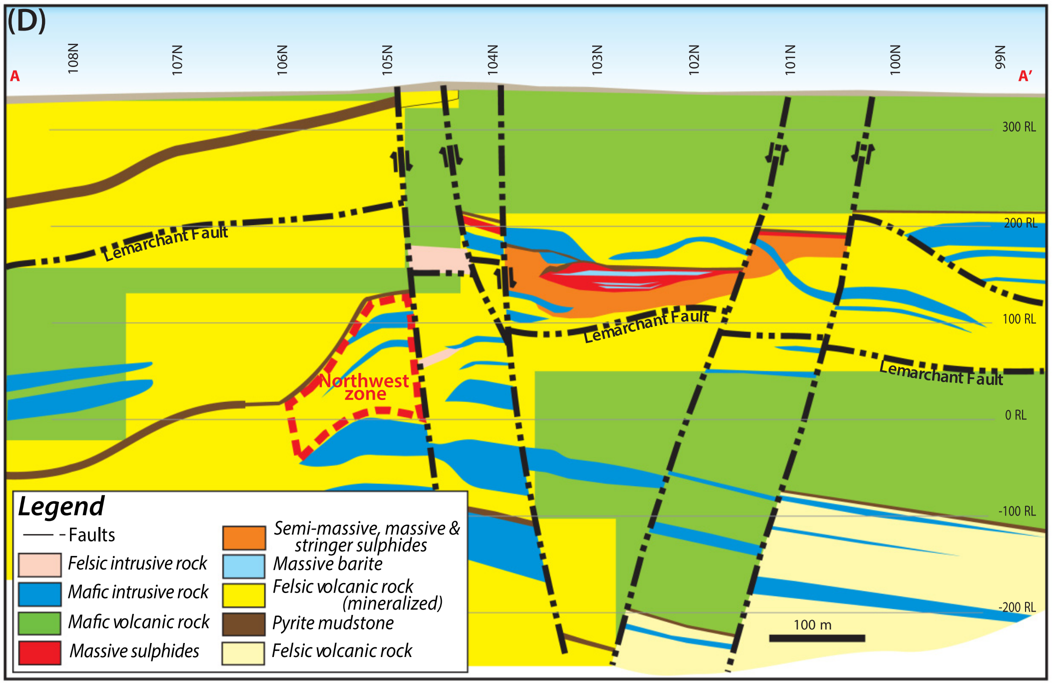

In the northern part of the Tulks belt, the VMS deposits are bimodal felsic to hybrid bimodal felsic, polymetallic and hosted by felsic to intermediate volcanic successions. The host rocks commonly display jigsaw-fit breccia textures and vent-proximal rhyolite facies (Fig. 14; Gibson et al. 1999). In addition to sericite, quartz, chlorite and pyrite alteration zones, the Bobby's Pond and Daniels Pond deposits also have minor aluminous argillic alteration with paragonite, montmorillonite ± kaolinite (Fig. 14), assemblages that are common of VMS deposits that have been influenced from low-pH magmatic-hydrothermal fluids (Sillitoe et al. 1996; Huston and Kamprad 2001; Dubé et al. 2007). Situated geographically between the Daniels Pond and the Bobby's Pond VMS deposits are the Bobby's Pond native sulfur occurrence (Fig. 14) and the North Pond VMS occurrence. These occurrences contain massive to laminated sulfide (predominantly pyrite) hosted within felsic volcanic rocks with zones of advanced argillic, aluminous alteration (e.g., pyrophyllite, dickite, and alunite), native sulfur, topaz, orpiment, and possible stibnite (Fig. 14), which are flanked by paragonite- and kaolinite-bearing zones. The Bobby's Pond native sulfur occurrence also displays vuggy textures, in addition to having laminated exhalative massive sulfide horizons. When considered together, the local examples of acidic aluminous argillic alteration at the Bobby's Pond and Daniels Pond VMS deposits, this hybrid epithermal-VMS environment occurs over a strike length of 8 km (Fig. 15). The deposits in the northern Tulks belt are interpreted to have formed in relatively shallow water (<1500 mbsl) relative to the deep water, sediment-rich distal environment suggested for the southern Tulks belt (Hinchey 2011; Sparkes and Hinchey 2023).

Great Burnt Lake/South Pond belt

The Great Burnt Lake volcanic belt contains VMS deposits within the Ordovician (~466 Ma) Cold Spring Pond Formation (Fig. 16) (Swinden 1988*a*). The Cold Spring Pond Formation is composed of volcano-sedimentary rocks dominated by siliciclastic sedimentary rocks (volcaniclastic arkose, argillite, and greywacke) with subordinate (~30%) mafic volcanic rocks, including pillow lavas and massive basalt and felsic volcanic rocks (Swinden 1988*a*). The formation is in fault contact on all sides with rocks of the Baie D'Espoir Group of the Exploits Subgroup and the Pipestone Pond ophiolite complex to the east and rocks of the Meelpaeg Subzone of the Gander Zone to the west (Fig. 17).

Mafic–siliciclastic-type VMS deposits in the belt occur within sequences of interlayered chlorite quartz ± carbonate-altered basalt flows and mafic tuffs and fine-grained, finely laminated biotite-rich argillite to siltstone (Fig. 16) inferred to have formed in a back-arc basin environment (Swinden 1988*a*; Barry et al. 2022). Sulfide zones are close to lithological contacts. Four main zones of mineralization are recognized, including the Great Burnt copper deposit, the South Pond copper deposit, the South Pond copper–gold zone and the End Zone copper prospect (Fig. 16); the first two have formal calculated resources (Barry et al. 2022). The Great Burnt copper deposit comprises stratabound zones of pyrrhotite–chalcopyrite ± sphalerite, galena, and pyrite as stringers, blebs, and massive sulfide (Fig. 17); more recent drilling has also documented Au-enriched (over 1 g/t over 4 m; Putrich and Barry 2015) pyrrhotite–chalcopyrite zones down dip from the main deposit. The South Pond copper deposit occurs approximately 10 km to the north of the Great Burnt deposit and is hosted within chlorite–quartz-altered mafic

Can. J. Earth Sci. **00:** 1–39 (2023) | dx.doi.org/10.1139/cjes-2022-0148

Fig. 12. (A) Rhyolite with hexagonal jointing and interstitial sulfide replacement from the mineralized block of the Duck Pond deposit. (B) Jigsaw-fit rhyolite breccia with rhyolite fragments that have sericite-altered cores and chlorite-altered rims and replacement-style mineralization among fragments of pyrite and sphalerite from the mineralized block of the Duck Pond deposit. (C) Granular massive pyritic sulfides with chlorite-altered fragments within the sulfides from the mineralized block of the Duck Pond deposit. (D) Sphalerite–(chalcopyrite)-rich ore from the Upper Duck lens of the Duck Pond deposit. Note chorite-altered fragments included in the ore. (E) Chalcopyrite-rich ore from the Upper Duck lens of the Duck Pond deposit with lesser pyrite. (F) Photomicrograph of atoll textures preserved in pyrite with rounded relict colloform pyrite (Py) preserved in the centre of the grain surrounded by zoned euhedral pyrite partially resorbed by chalcopyrite (Ccp). Sample was etched in 8 N nitric acid prior to image capture (photomicrograph, reflected light). (G) Flow-banded rhyolite (top) and underlying glassy (black) flow lobe from the upper block of the Duck Pond deposit. (H) Lapilli tuff from the Boundary deposit that contains fragments that are partially replaced by sericite (grey) and chlorite (black) and containing interstitial pyrite. (I) Lapilli tuff from the Boundary Deposit in which chlorite has completely replaced rhyolitic fragments and the fragments are surrounded by replacement-type pyritic sulfides. (J) Semi-massive sulfides from the Boundary deposit with chlorite-altered fragments and interstitial pyrite–sphalerite–chalcopyrite. (K) Massive pyrite–sphalerite–chalcopyrite sulfides form the Boundary deposit with chlorite-altered fragments. Note the wispy shapes of the included fragments—these are interpreted to be relict volcanic glass or pumice (e.g., Piercey et al. 2014). (L) Replacement-type sulfides from the Boundary deposit with framboidal pyrite that form the nucleus upon which other sulfides grow, including euhedral pyrite or infill as interstitial sphalerite and chalcopyrite. (M) Jigsaw-fit rhyolite breccia from the Lemarchant deposit with concentric sericite–(illite) alteration assemblage and interstitial sulfides. (N) Massive barite with stringers of chalcopyrite and bornite from the Lemarchant deposit. (O) Low-Fe sphalerite and galena with black chlorite-altered felsic material from the Lemarchant deposit. (P) Bornite-rich sulfides with pyrite, sphalerite, galena, and tetrahedrite from the Lemarchant deposit. (Q) SEM–BSE image of barite with pyrite, sphalerite, and stroemeryite from the Lemarchant deposit. (R) SEM–BSE image of bladed barite from the Lemarchant deposit showing textures that are similar to bladed barite found in some low–intermediate sulfidation Au deposits. Mineral and mineral textural abbreviations as in Fig. 11.

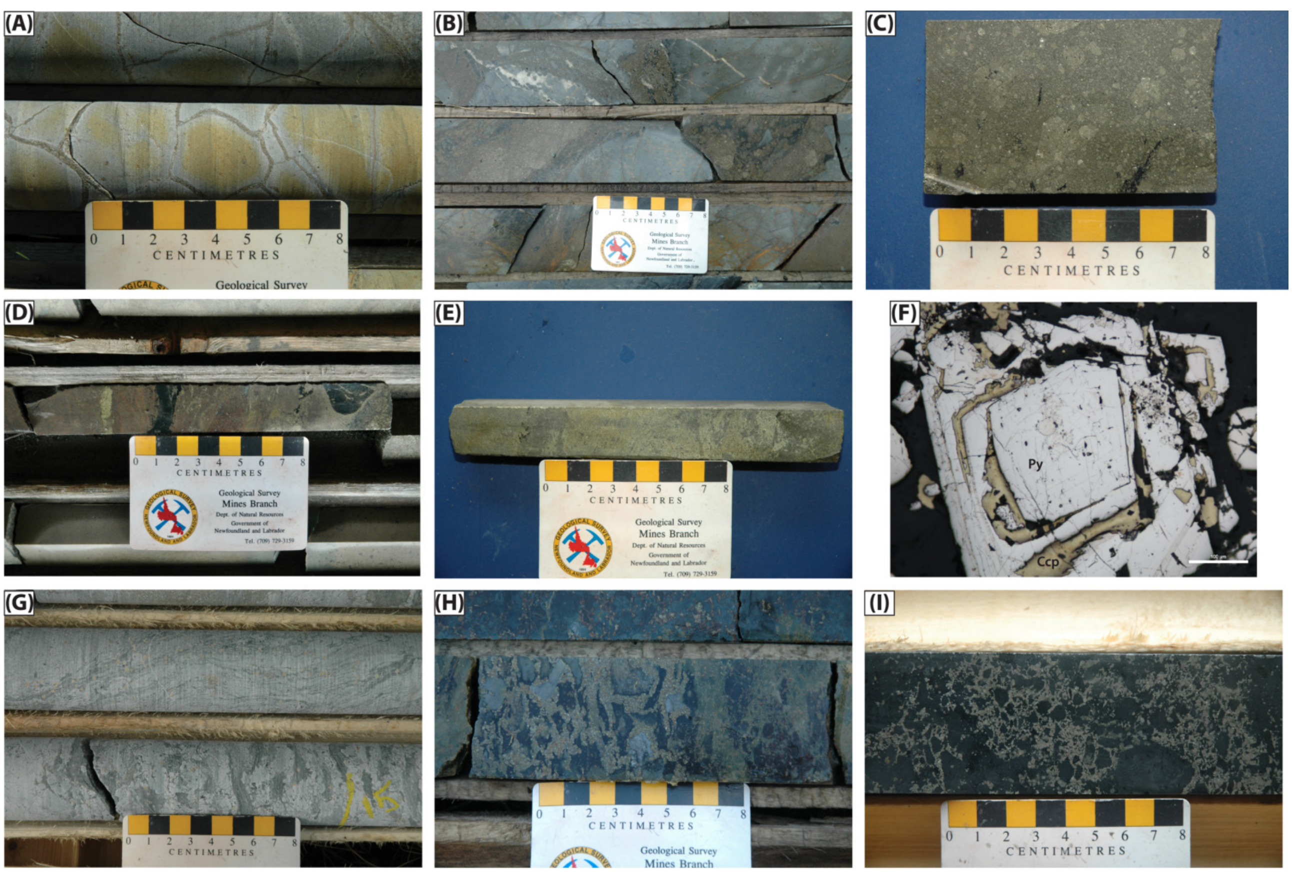

tuffaceous rocks interbedded with fine-grained volcaniclastic rocks (Figs. 16 and 18).

Although very similar to the Great Burnt and South Pond copper deposits, the South Pond Cu–Au zone has predominant gold-bearing sulfides disseminated to semi-massive pyrrhotite, chalcopyrite, and pyrite hosted within quartz-altered and sheared mafic tuffaceous rocks interbedded with fine-grained metasedimentary rocks (Figs. 17 and 18). Gold

Fig. 12. (*concluded*).

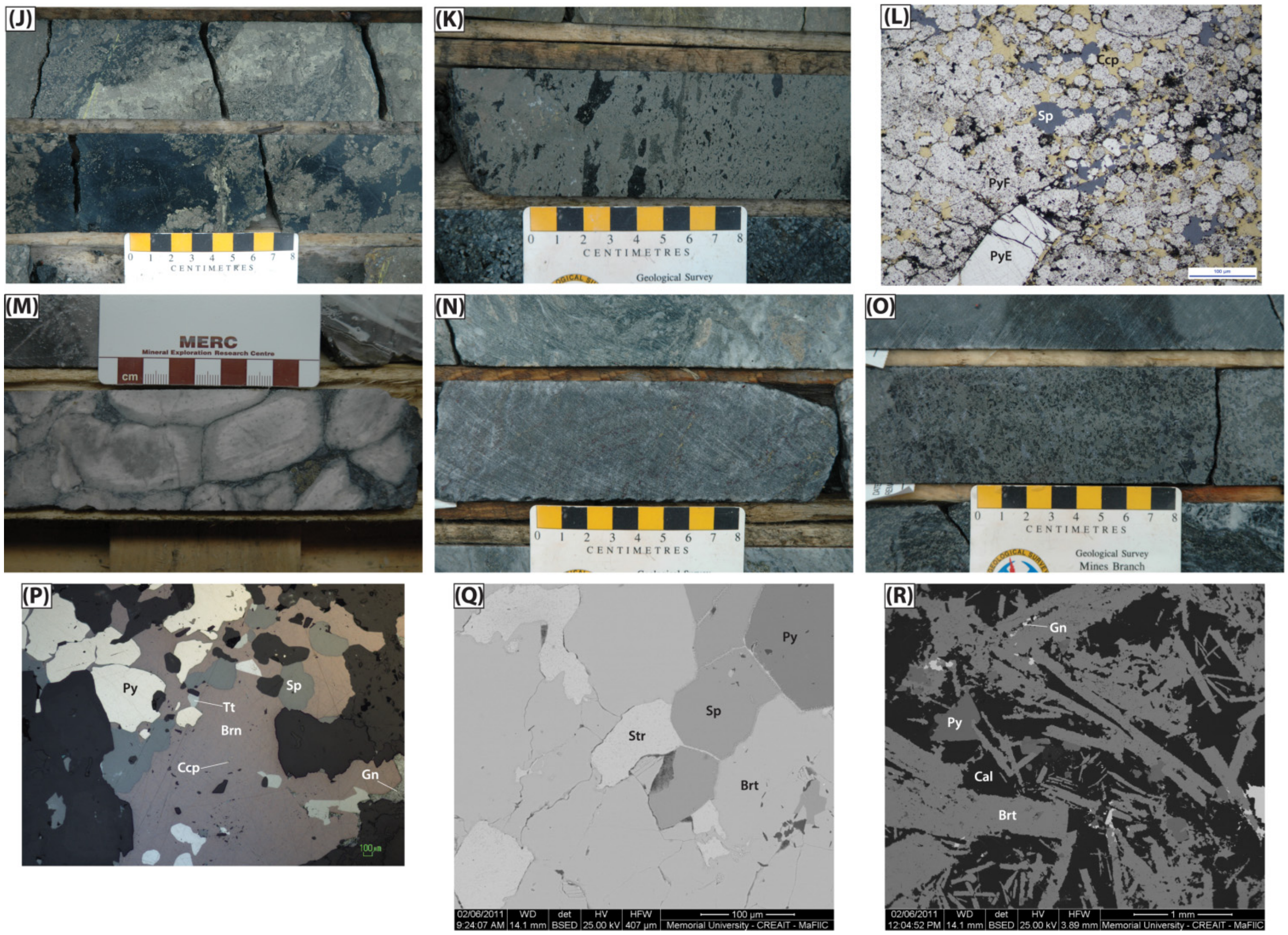

grades range from 100 to 3000 ppb; values up to 13.37 g/t gold over 1.17 m have been drilled (Denoyers 1991; Barry et al. 2022) with higher gold grades correlating with increased sulfide content. However, it is uncertain whether the gold enrichment is syngenetic or epigenetic, given the intense foliation and shearing, local brecciation, and increased quartz alteration (Fig. 17; e.g., Desnoyers 1991).

Point Leamington belt

The Point Leamington belt is within Cambrian volcanic and volcaniclastic rocks of the Wild Bight Group (Fig. S5; Swinden 1988*b*; MacLachlan and Dunning 1998; MacLachlan et al. 2001). Sulfide deposits are hosted predominantly in the Glover's Harbour Formation, which is composed of a >486 Ma sequence of pillowed and brecciated mafic rocks, lesser quartz–feldspar phyric felsic flows and domes, interbedded breccias, lapilli tuffs, green and red chert, and argillite (MacLachlan and Dunning 1998; MacLachlan et al. 2001). Compositionally, mafic and felsic rocks of this formation have island arc tholeiitic and low-K, high-silica rhyolite affinities, respectively, and are interpreted to record formation within a peri-Gondwanan rifted primitive arc (MacLachlan and Dunning 1998; MacLachlan et al. 2001).

The Point Leamington VMS deposit is contained in the southwestern part of the Wild Bight Group within a variably thrust-imbricated and folded package of volcanic and volcaniclastic rocks (Fig. S5; Swinden 1988*b*; Walker and Collins 1988; Stone et al. 2021). The deposit has a deep mafic footwall that is overlain by felsic volcanic and volcaniclastic rocks that form the immediate stratigraphic footwall to the sulfide zone (Walker and Collins 1988; Stone et al. 2021). These shallow footwall felsic rocks are variably quartz- and feldspar-bearing and altered to a chlorite–sericite–pyrite alteration assemblage proximal to mineralization (Fig. 18). Overlying the sulfide zone is a marker unit of chert–argillite that occurs in most locales at the contact between hanging wall and footwall rocks and is overlain by a hanging wall of mafic to intermediate volcanic and volcaniclastic rocks (Stone et al. 2021). Mineralized zones consist of pyrite-dominated massive sulfide and fine-grained, pyrite-clast bearing sulfides that contain much lesser sphalerite, chalcopyrite, galena, and other trace sulfide/sulfosalt phases (Fig. 18; Walker and Collins 1988; Stone et al. 2021). The mineralized lenses are typically lower grade along their upper contacts but increase in grade both inwards and down dip, with higher Zn–Au-enrichments occurring at the base of the lenses (Stone et al. 2021). There are also possibly multiple lenses, as some sulfide lenses are intercalated with altered felsic volcaniclastic rocks (Stone et

Fig. 13. General geology of the southwestern portion of the Long Lake group from van Staal et al. (2005) and Lissenberg et al. (2005). Also shown are locations of the Long Lake main deposit and other areas of exploration focus and of dated samples. Dot plots represent various concentrations of high-field strength elements (Zr + Hf + Nb + Y) for outcrop samples collected by Hinchey and McNicoll (2016); breaks are Jenks natural breaks in the dataset. The dashed red line trending from southwest to northeast represents the approximate location proposed for the division of the upper and lower stratigraphy (after Hinchey and McNicoll 2016).

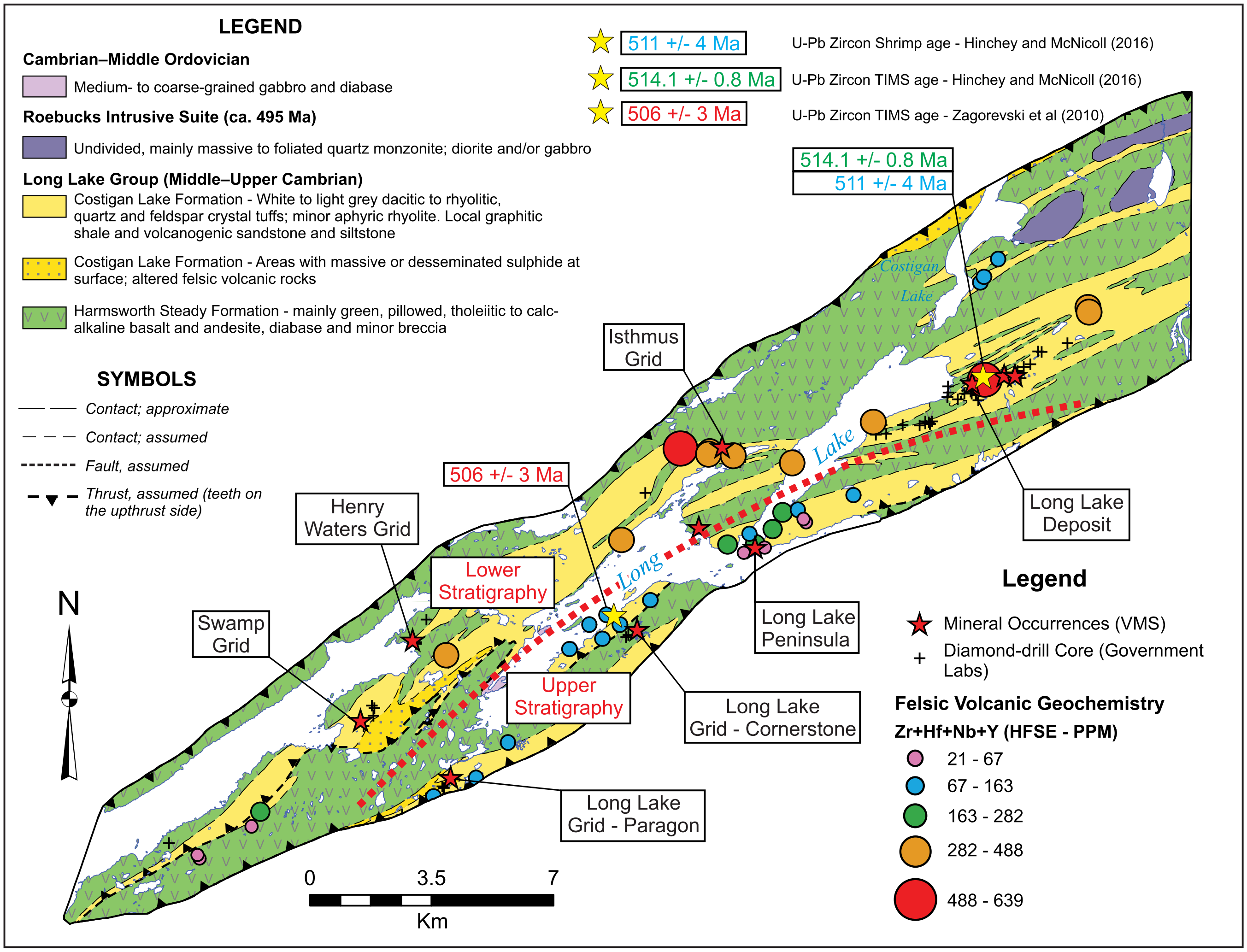

al. 2021). Underlying the massive sulfides are stringer sulfides dominated by pyrite with much lesser sphalerite, arsenopyrite, and chalcopyrite (Walker and Collins 1988; Stone et al. 2021).

The Lockport deposit is located proximal to Glover's Harbour in the northern part of the Wild Bight Group (Fig. S5). This deposit has seen past production in the 1880s and sporadic exploration to the present (Swinden 1984; Barbour and Churchill 2001). The deposit is hosted by variably deformed and altered pillowed to amygdaloidal basaltic flows, andesites, and hyaloclastite, in which mineralization occurs predominantly as stringers of pyrite–chalcopyrite associated with quartz–sericite–chlorite altered host rocks (Fig. 18; Swinden 1984; Swinden 1988*b*; Barbour and Churchill 2001). Felsic rocks are not immediate hosts to sulfide zones; they are found along strike within the mineralized package and regionally and are interpreted to be equivalent to felsic host rocks at Point Leamington (Swinden 1984, 1988*b*; Barbour and Churchill 2001). Swinden (1984) noted that there is no exhalative mineralization preserved in situ and on surface in the Lockport deposit; however, variably Zn-rich boulders occur within the waste pits in the region, suggesting that past mining may have mined Zn-rich massive sulfide. Numerous variably base metal-rich sections were also intersected in drilling in the late 1990s and early 2000s (Barbour and Churchill 2001).

Discussion

Tectonics, magmatism, and VMS formation

Volcanogenic massive sulfide deposits, including Appalachian VMS deposits, are associated with specific tectonic settings, tectonostratigraphy, and magmatic processes

Fig. 14. (A) Recrystallized barite-rich massive sulfide with pyrite and sphalerite from the Long Lake deposit. (B) Banded sphalerite–pyrite–chalcopyrite-rich massive sulfides from the Boomerang deposit. (C) Deformed sphalerite–chalcopyrite with chlorite-rich tuff inclusions from the Boomerang deposit. (D) Deformed sphalerite–pyrite–chalcopyrite with chlorite-altered inclusions (upper half) grading downwards into sericite-altered tuffs (lower half) from the Boomerang deposit. (E) Jigsaw fit rhyolite from the Bobby's Pond deposit with quartz–sericite alteration assemblage. (F) Minor sulfides from the Bobby's Pond native sulfur showing with pyrophyllite–dickite–topaz alteration assemblage. (G) Native sulfur- and alunite-altered rhyolite from the Bobby's Pond native sulfur showing. (H) Deformed felsic tuffs with montmorillonite and paragonite alteration assemblage from the Daniels Pond deposit.

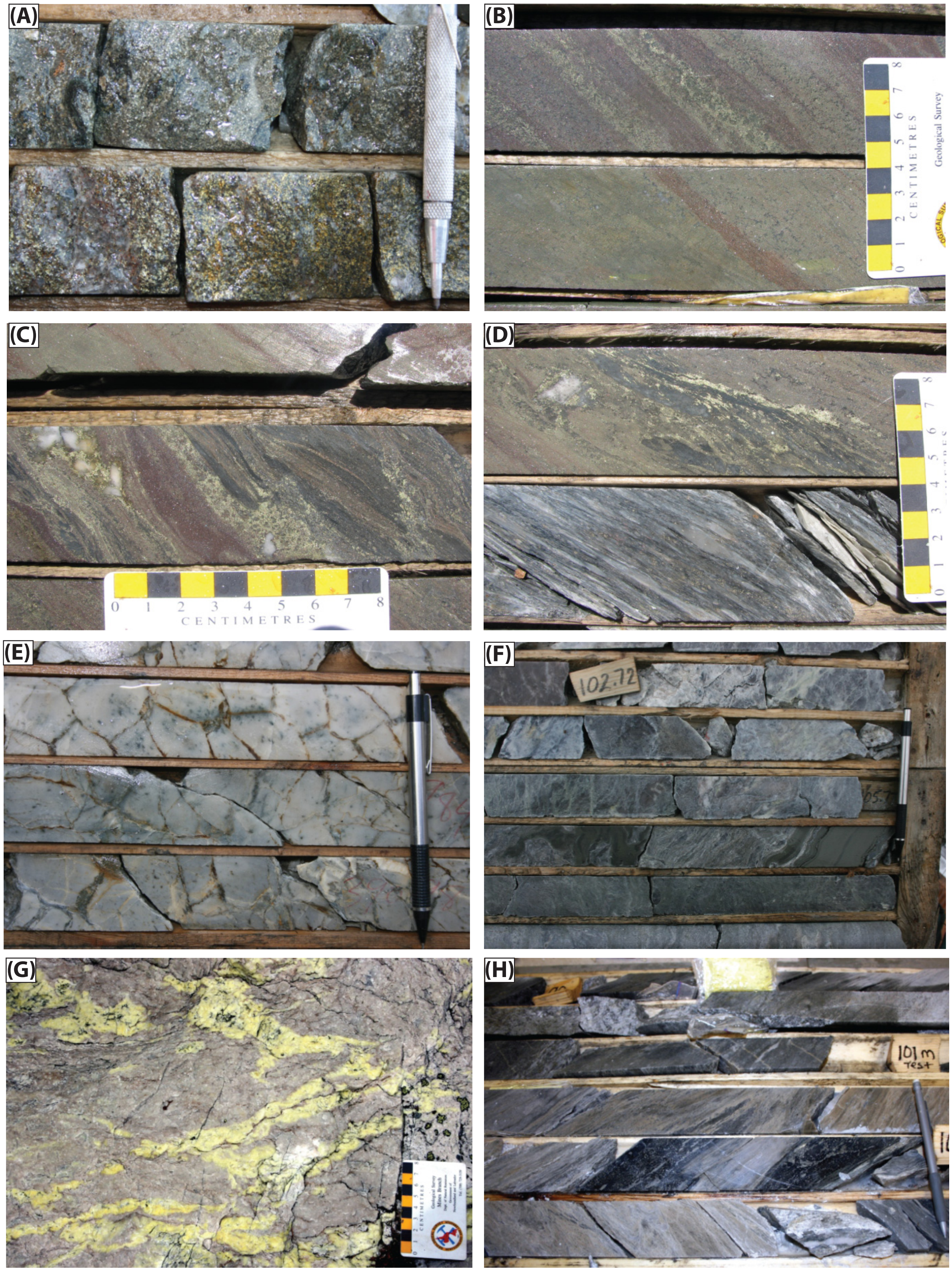

Fig. 15. (A) Geology map of the southern Tulks volcanic belt with VMS deposits and showings. (B) Geology map of the northern Tulks volcanic belt with VMS deposits and showings. Maps are lithological maps from both industry and government sources (modified after Hinchey 2011).

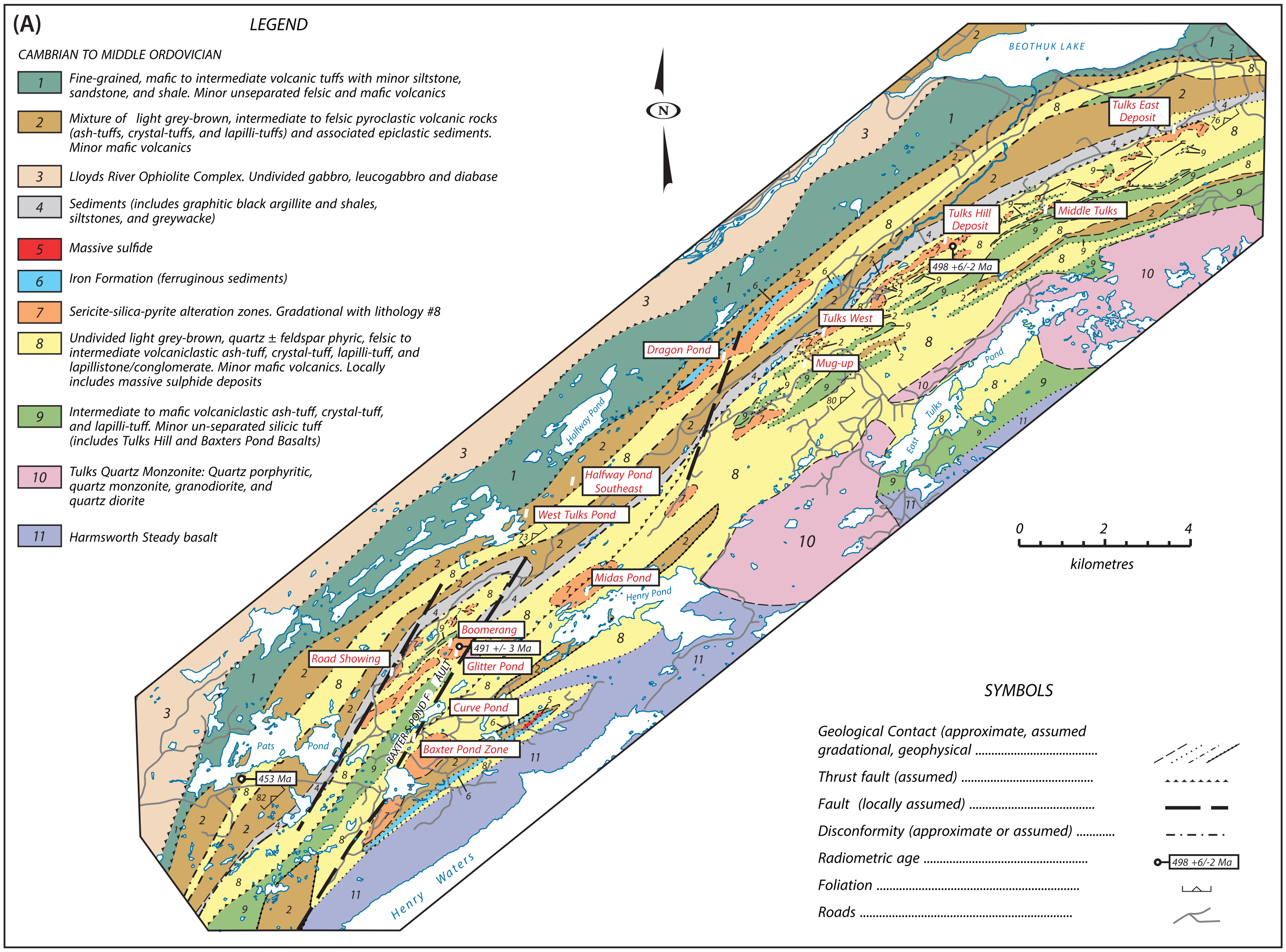

throughout geological time (e.g., Piercey 2011). For example, Swinden (1991) utilized trace element geochemistry of mafic rocks and noted that the most prospective sequences in Newfoundland are those associated with rifted arcs, be they intraoceanic (e.g., suprasubduction zone ophiolite environments) or continental (e.g., Buchans-Roberts Arm belt). Recent work has expanded on these original contributions and provided both regional and deposit-scale relationships that illustrate the complexity of magmatism and volcanism associated with VMS mineralization.

In the case of mafic-dominated deposits, available geochemical and isotopic data suggest that boninitic to arc tholeiitic rocks are important hosts and they are interpreted to have formed in forearc sequences, at least for those associated with the Lushs Bight Group and the Betts Cove ophiolite (van Staal 2007; Bedard et al. 1999). This boninite-low-Ti tholeiite association is also present in the bimodal mafic Point Leamington belt where mafic rocks are dominated by island arc tholeiites and lesser boninites (MacLachlan and Dunning 1998). Sulfide deposits in this district, however, are associated with tholeiitic felsic rocks that formed during arc rifting due to upwelling of basaltic magmas and remelting of hydrated mafic arc crust (MacLachlan and Dunning 1998), similar to models proposed for modern primitive arc rift environments (e.g., Schmitt and Vazquez 2006; Shukuno et al. 2006; Tamura et al. 2009). Remelting of crust during rifting was also an important process in the bimodal felsic environments of the Dunnage Zone. For example, in the Tally Pond, Tulks, and Buchans-Roberts Arm belts, arc rifting and remelting of variably evolved continental crust was important in generating the VMS-hosting felsic rocks in these belts (Rogers et al. 2006; Zagorevski et al. 2006; Piercey et al. 2014; McKinley 2013).

The relationships outlined above between VMS deposits and specific geochemical/petrological clans and their interpreted tectonic settings is not at all surprising. For example, the boninite-low Ti ± tholeiitic rhyolite association is common in many primitive arc VMS environments (e.g., Piercey 2011). These rocks are generally attributed to subduction initiation and forearc rifting, which result in extensive spreading and extension (e.g., Stern and Bloomer 1992) and creation of the crustal permeability needed for VMS hydrothermal fluid flow (e.g., Bedard et al. 1999). The forearc extension

Fig. 15. (*concluded*).

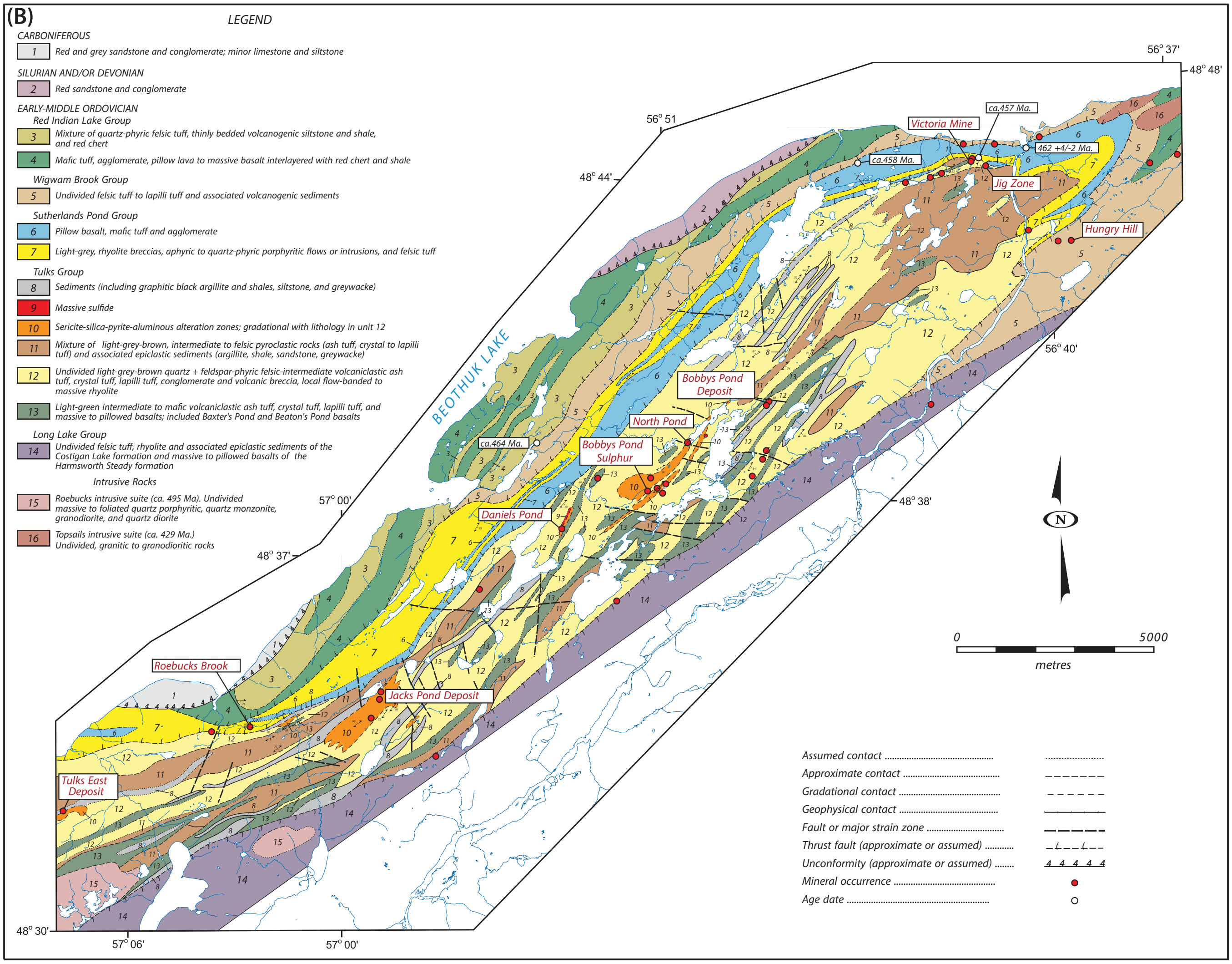

in these environments also likely resulted in upwelling of hot, asthenosphere-derived magmas that drove both crustal melting to form VMS-associated rhyolites and also fluid circulation for forming both mafic and bimodal mafic VMS deposits within these settings (e.g., Piercey 2011). Upwelling of basalt and underplating of continental crust were additionally important in the formation of VMS deposits in felsic-dominated belts. The upwelling of basalt during continental arc rifting and back-arc formation, and melting of continental crustal basement, is interpreted as the formation mechanism for VMS-associated felsic rocks in the Tally Pond, Long Lake, Tulks, and Buchans-Roberts Arm belts (Rogers et al. 2006; Zagorevski et al. 2006; Hinchey 2011, 2014; McKinley 2013; Piercey et al. 2014; Hinchey and McNicoll 2016). Rifting and upwelling of mafic magma were also likely critical for driving hydrothermal circulation and fluid focusing within these continental VMS environments (e.g., Piercey 2011).

In contrast to the models outlined above, the dacitic rocks that host the Au–(Cu)-rich deposits of the Rambler-Ming district in the Baie Verte belt have relatively unique geochemical and isotopic signatures and magmatic history. These rocks have extremely depleted Y and heavy rare earth element signatures, coupled with distinctly high La/Yb, Zr/Sm, εNd_t–εHf_t, and positive $\Delta\varepsilon Hf$ values, which have been attributed to these felsic rocks having been direct melts from the subducted oceanic slab (Pilote and Piercey 2018; Piercey and Pilote 2021). Previous work has suggested that gold enrichment, as well as other epithermal suite elements in the Rambler-Ming deposits were due to magmatic-hydrothermal contributions (Brueckner et al. 2014*b*, 2016).

Slab melting may provide a possible mechanism to explain this magmatic-hydrothermal association and gold enrichment. Numerous workers have shown that slab melting generates magmas that are siliceous, oxidized, sulfide-undersaturated, and SO_4-rich (Fig. 19; e.g., Mungall 2002). Further, the geochemical signatures of the Rambler felsic rocks suggest that garnet was a stable residual phase within the slab during magma genesis (e.g., Defant and Drummond 1990), which likely resulted in magmas that were rich in ferric iron, as garnet preferentially retains ferrous iron (Lee and Tang 2020). Such melts are sulfide-undersaturated and will not fractionate magmatic sulfide as they transit the crust,

Fig. 16. General geology of the area surrounding Great Burnt Lake VMS deposit (modified from Swinden 1988a).

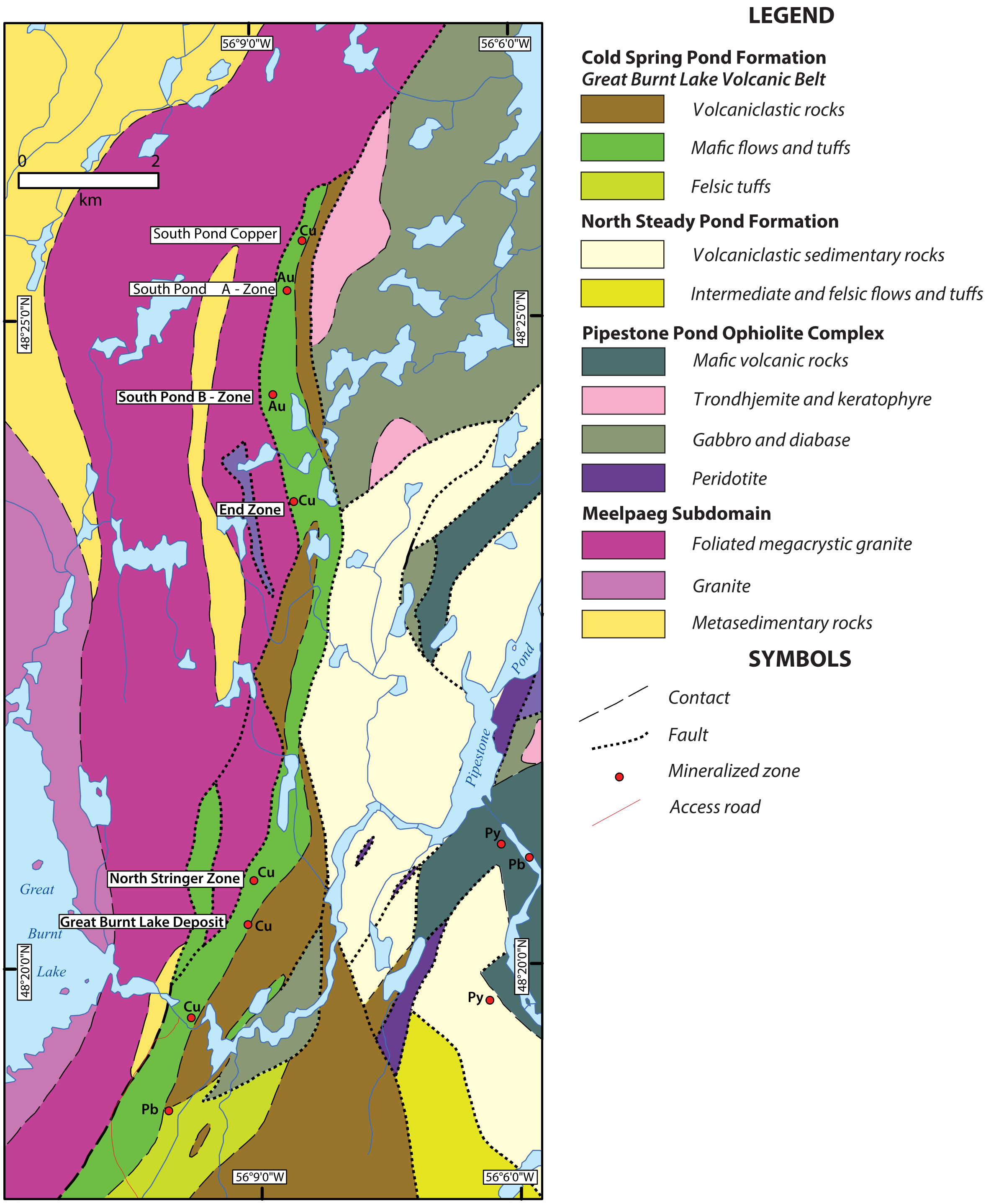

thus allowing for a build-up in both Au and Cu in the melt during magma fractionation and subsequent emplacement at higher crustal levels. Models for slab melts also suggest that they undergo melt-rock reaction with the mantle wedge en route to emplacement within the crust (Defant and Drummond 1990). Given the sulfur-undersaturated nature of slab melts, any potential interaction with sulfides in the mantle wedge, or with Au–Cu-rich boninitic rocks in the stratigraphy (e.g., Keays 1987), would have resulted in dissolution of sulfides from these rocks (Kerr and Leitch 2005; Yang 2012), potentially further increasing the metal abundance within the slab-derived melts (Fig. 19). If such a melt exsolved and contributed magmatic-hydrothermal fluids to the Rambler-Ming VMS system, this mechanism could explain the enrichment of Au and epithermal suite elements (Brueckner et al. 2014b, 2016) and alteration types (Pilote et al. 2020) found in this district (Fig. 19). The above processes may also explain the association of similar fractionated FI-type (Lesher et al. 1986; Hart et

Fig. 17. (A) Interlayered mafic volcaniclastic rocks and laminated sedimentary rocks from the Great Burnt Lake deposit. (B) Chlorite-altered mafic rocks with pyrrhotite and chalcopyrite stringers from the Great Burnt Lake deposit. (C–D) Variably deformed and sheared mafic volcanic rocks with pyrrhotite–chalcopyrite stringers from the South Pond Cu–Au occurrence.

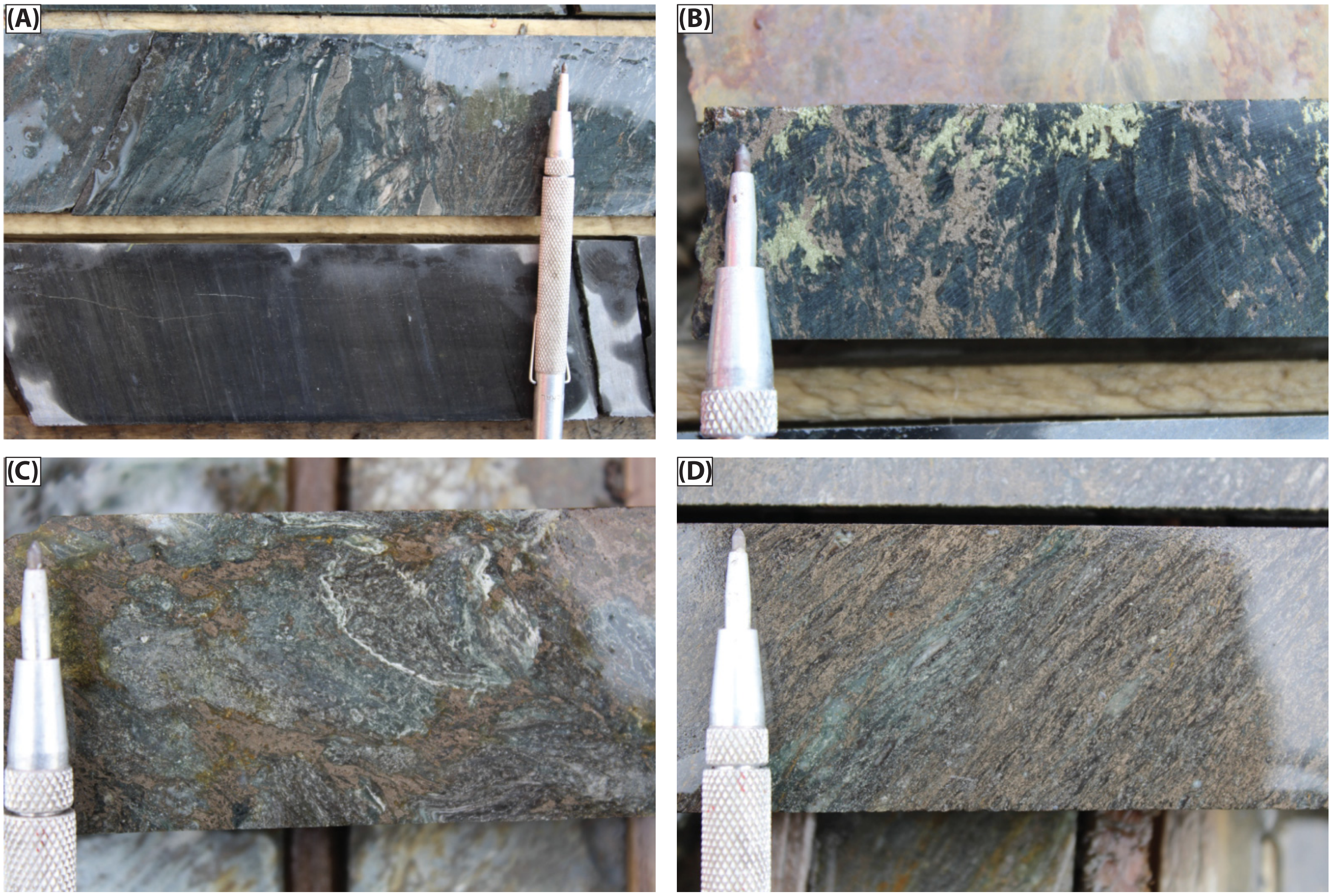

al. 2004) felsic rocks associated with Au-rich VMS deposits in Archean greenstone belts (e.g., Mercier-Langevin et al. 2007; Gaboury and Pearson 2008).

Although there are general understandings of the relationships between magmatism and VMS mineralization in the NL Appalachians, fundamental questions remain unanswered. For example, the general knowledge regarding tectonics and magmatic relationships to VMS is accepted, but there are very poor controls on the camp- and deposit-scale chemostratigraphy and petrochemical assemblages (e.g., Piercey 2011) associated with VMS deposits in many districts. Furthermore, how specific magmatic clans, their petrogenesis, and underlying basement and(or) footwall sequences in a given district control metal assemblages and abundances in each VMS belt is poorly understood. In the Buchans-Roberts Arm belt, for example, there are similarities in magmatic products and interpreted basement/footwall sequences, but in one part of the belt are some of the highest-grade VMS deposits in the world (e.g., Buchans), whereas in the other end of the belt there are large but generally pyrite-bearing deposits with low grades (e.g., Pilleys Island)—why this is the case is not well understood. A related problem involves minimal data and understanding of the bulk rock isotopic signatures (particularly Hf isotopes) and mineral-scale chemical and isotopic data for zircon or other resistate phases in VMS-related and barren rocks in Newfoundland and globally. These data can provide constraints on potential basement compositions, the role of juvenile basalt underplating (Manor et al. 2022), as well as the physicochemical conditions of magma formation (e.g., Ferry and Watson 2007; Dilles et al. 2015) and their potential role in sourcing and(or) concentrating metals in VMS environments. These topics are potentially fruitful avenues for future research, e.g., on the relationship of magmatism to VMS deposit genesis in the Dunnage Zone of the Newfoundland Appalachians.

Emplacement mechanisms

Genetic models for ancient VMS deposits are based on our understanding of their modern analogues, seafloor massive sulfide (SMS) deposits, which invoke fluids "exhaling" into the ocean forming sulfide/sulfate chimneys and accumulations of massive sulfide on the seafloor (e.g., Franklin et al. 2005; Hannington 2014). Although numerous VMS deposits are interpreted to have formed in this manner, there are also many deposits that show evidence for subseafloor replacement by either infilling permeable/porous material or via dissolution and replacement of existing rock units (e.g., Doyle and Allen 2003; Piercey 2015). In addition, some de-

Fig. 18. (A) Representative cross-section through the Point Leamington VMS deposit (modified after Barry et al. 2022). (B) Representative sulfide assemblages from Point Leamington deposit showing colloform pyrite, euhedral pyrite, and sphalerite with chalcopyrite disease and (C) colloform pyrite with atoll textures of partial replacement by chalcopyrite, surrounded by sphalerite and euhedral pyrite. (D) Representative cross-section through the Lockport deposit (modified after Swinden 1988*b*). Mineral and mineral textural abbreviations as in Fig. 11.

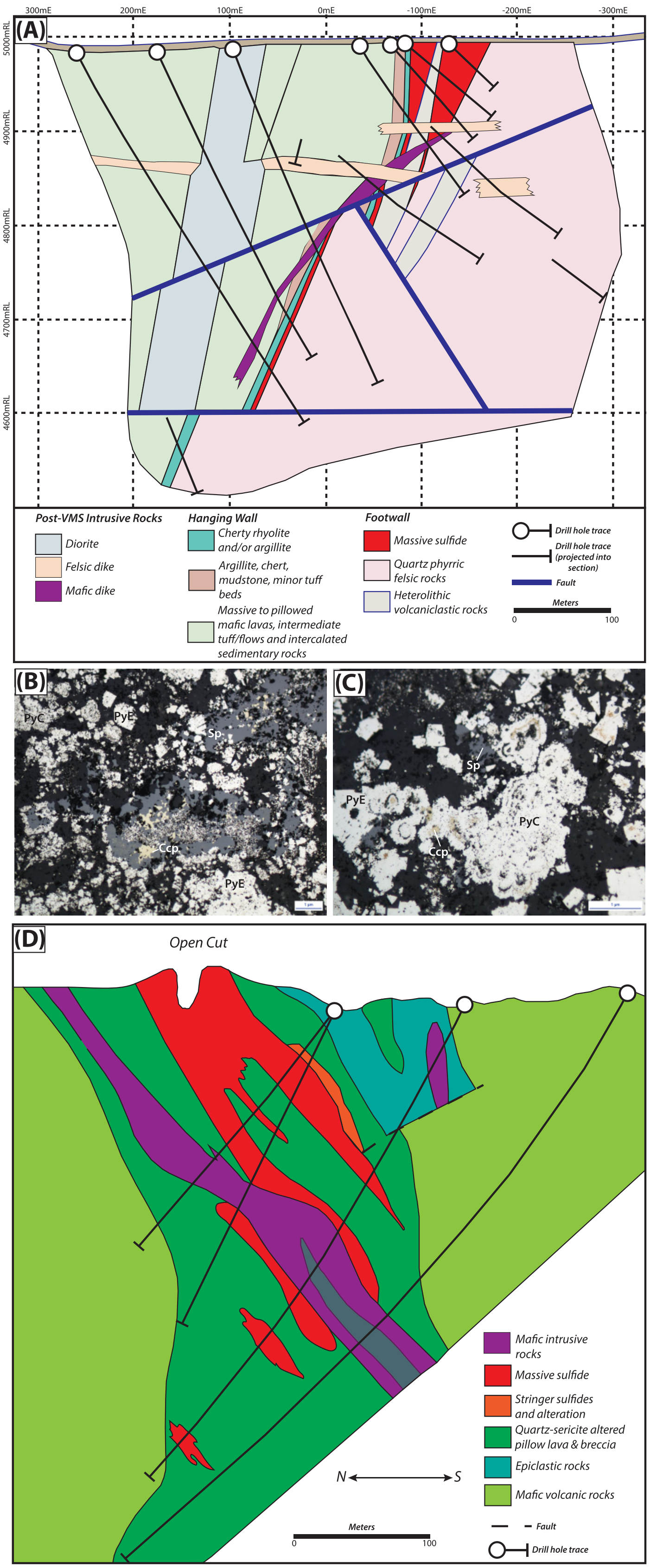

Fig. 19. Model for the genesis of incompatible element depleted rhyolites associated with Au-rich VMS deposits in the Rambler-Ming district (modified after Pilote and Piercey 2018). Slab melts would have had high fO_2 and been SO_4-rich and H_2S-undersaturated. During transition towards the upper crust, these melts would have been able to fractionate and in the absence of H_2S, Au, and Cu (+ other metals) would behave incompatibly and increase in concentration. Their sulfide-undersaturated nature would have allowed for dissolution of any sulfides present in the mantle, further increasing the Cu–Au–Zn content of the melts (inset (A)). These magmas could then through degassing give rise to magmatic hydrothermal Cu–Au-epithermal suite elements near the surface leading to the observed Au-enrichment found in the Rambler-Ming VMS deposits (inset (B)). Abbreviations: AC, Advocate Complex; PRC, Point Rousse Complex; PC, Pacquet Complex; BCC, Betts Cove Complex; LBOT, Lushs Bight oceanic tract; IAT, island arc tholeiite.

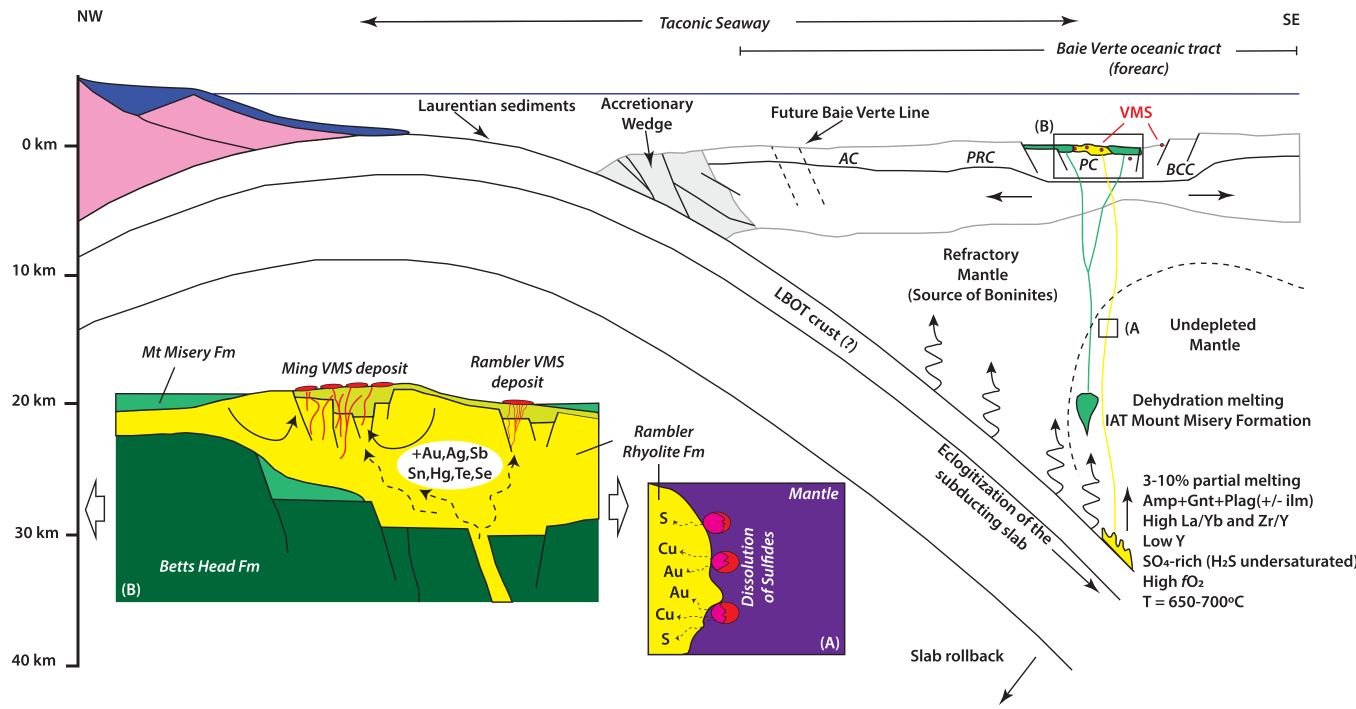

posits record deposition from debris flows via the collapse of chimneys and subsequent mass flow sedimentation (e.g., Thurlow and Swanson 1981; Binney 1987; Roth et al. 1999).

Numerous VMS deposits within the Dunnage Zone have features indicative of seafloor exhalative VMS activity, including mound-like barite chimneys (Thurlow 2010; Lajoie et al. 2020), and microscopic evidence, including colloform textures and micro-chimneys (Gill et al. 2016). These features are interpreted to record seawater and VMS vent fluid mixing and subsequent deposition of sulfates (Ohmoto 1996) and(or) sulfides (Lydon 1988) on the seafloor. Some of these exhalative deposits and occurrences are also spatially associated with laterally extensive hydrothermal mudstone and iron formations that have geological, mineralogical, geochemical, and isotopic signatures indicative of venting and deposition on the seafloor (Hinchey 2011; Lode et al. 2015; Piercey et al. 2018).

Transported sulfides also are interpreted to have formed on the seafloor, albeit due to gravity-induced redeposition of exhalative (±replacement) mineralization. In the Buchans district, transported ore bodies were attributed to the collapse of sulfide deposits and transportation as sediment-gravity flows (e.g., sulfide-rich turbidites; Thurlow and Swanson 1981; Binney 1987). In other cases, the transported deposits contain bedded to laminated sulfides, even in deposits interpreted to have formed primarily by subseafloor replacement (Piercey et al. 2014). In both cases, it is likely that basin extension played a role in the instability of sulfide chimneys/deposits and in their subsequent transport and deposition. Further, given the presence in many deposits of textures indicative of dissolution, reprecipitation, and zone refining (e.g., Eldridge et al. 1983), it is also likely that these exhalative deposits experienced chimney collapse due to retrograde solubility of anhydrite (Blounot and Dickson 1969), coupled with subsequent re-deposition of sulfide either proximal to the vent (e.g., Piercey et al. 2014) or distal within sediment-gravity flows (e.g., Thurlow and Swanson 1981; Binney 1987).

Recently, numerous workers have shown that subseafloor replacement is an important deposit-forming mechanism. Squires et al. (1991, 2001) suggested that many of the VMS ores in the Duck Pond deposit formed via replacement. Similarly, Thurlow (1996) proposed that ores in the Spencer's Dock area of the Pilley's Island district formed by partial replacement of perlitic cracks and glass in felsic flows. Hinchey (2011) illustrated that in the Tulks belt, some volcaniclastic- and sediment-rich VMS deposits (e.g., Boomerang, Tulks East) have lithofacies, alteration styles, and mineralized zones indicative of subseafloor replacement. Piercey et al. (2014) suggested that the Boundary deposit formed due to permeability contrasts between relatively impermeable, hanging wall flow banded rhyolites and unconsolidated and porous footwall lapilli tuff, resulting in the lateral replacement of pore spaces in volcaniclastic rocks by sulfide (Fig. 20). Observations and relationships from the Boundary and Duck Pond deposits were also critical for creating a revised global model for subseafloor replacement processes in VMS deposits (Piercey 2015).

Despite the recognition of variable emplacement mechanisms for VMS formation in the Newfoundland Dunnage Zone, it is still uncertain how such mechanisms control grades and tonnages and the metal assemblages preserved in these deposits. Further, in many VMS deposits and belts the nature of emplacement of sulfide deposits is not fully understood, but this is required for refinement and enhancement of predictive mineral exploration models for VMS deposits.

Sources of metals, fluids, and processes of metal enrichment

Insights into the origin of metals, fluids, and sulfur in VMS deposits have come from studies of ancient VMS deposits and from seafloor systems where the mineralizing fluids can be sampled directly. Research on modern seafloor vent fluids demonstrates significant diversity of compositions, but many of these fluids are dominated by modified seawater (e.g., Von Damm 1990; German and Seyfried 2014). Importantly, however, it has been demonstrated that some hydrothermal vent fields contain input from magmatic fluids/volatiles (e.g., de Ronde et al. 2011). This diversity of fluid compositions also results in contrasting metal and alteration assemblages (Hannington et al. 2005). In ancient VMS environments, fluid inclusion studies are very limited owing to preservation and resetting/overprinting by post-VMS orogenic events (e.g., Lajoie et al. 2020). Thus, a direct understanding of VMS fluid characteristics is poor in the Dunnage Zone; hence, it is inferred predominantly from metal assemblages and textures preserved in the sulfides and sulfates, from hydrothermal alteration assemblages, and to a lesser extent from S isotope systematics. For example, in many bimodal felsic deposits (e.g., Duck Pond and Boundary), there is well-developed metal zoning with low-temperature (<300 °C) Zn–Pb–sericite–(quartz) assemblages and higher temperature (>300 °C) Cu-chlorite assemblages (e.g., Piercey et al. 2014; Buschette and Piercey 2016), whereas some ophiolite-hosted mafic deposits display high-temperature, reduced chalcopyrite–pyrrhotite-stringer and chlorite-dominated assemblages (e.g., Cloutier et al. 2015), features typically found in zone-refined, seawater-dominated SMS on the modern seafloor (e.g., Haymon 1983; Graham et al. 1988). From this indirect evidence, it is reasonable to assume that hydrothermally modified seawater was a component of the hydrothermal fluids and sulfur in most VMS deposits in the Dunnage Zone.

The metals in VMS were in part derived from footwall rocks that underlie VMS deposits, be they crystalline basement and(or) footwall stratigraphic sequences (e.g., footwall volcanic and(or) sedimentary rocks). For example, empirical studies have shown that regional scale leaching of footwall rocks can provide sufficient Cu, Zn, Fe, and Pb to potentially explain the metals present in many VMS deposits (e.g., Gibson et al. 1983; Galley 1993; Skirrow and Franklin 1994; Jowitt et al. 2012). Furthermore, the metal assemblages of VMS deposits in Newfoundland are interpreted to be in part impacted by the footwall units that underlie these deposits. For example, ophiolite-hosted mafic VMS deposits are notable for being Cu–Zn-rich and Pb-poor, compared to more bimodal-felsic and felsic–siliciclastic deposits that are more Zn–Pb–(Cu)-rich and partially to fully underlain by continental crust and crustal-derived volcanic and sedimentary rocks (e.g., Swinden and Kean 1988). The sourcing of VMS metals from footwall sequences is also partly supported by Pb isotope data. For example, Swinden and Thorpe (1984) illustrated that there was distinct provincialism in Pb isotopic signatures of galena in VMS deposits in the Dunnage Zone that reflected their underlying footwall and(or) basement domains, an interpretation that has been replicated and supported by more recent studies (e.g., Gill et al. 2019).

Although there is evidence to suggest leaching of footwall rocks is important in generating the metals in some deposits, other deposits with exceptional metal endowment and(or) magmatic-hydrothermal metal and alteration assemblages cannot be explained solely by leaching. Mass-balance modelling of basement leaching for Pb by Sawkins and Kowalik (1981) in the Buchans district illustrated that basement leaching models cannot account for all the Pb in the Buchans VMS deposits, thereby requiring additional input, likely from magmatic-hydrothermal fluids. A similar case may be made for the exceptional Zn grades found in these deposits (e.g., Piercey et al. 2015). In other deposits, magmatic input has been used to explain the high concentrations in Au and Ag, as well as of other epithermal suite/magmatic-hydrothermal elements (Hg–As–Sb–Bi–Te–Se–Sn–W), present in some VMS deposits. For example, in the Ming deposit, Brueckner et al. (2014*b*, 2016) demonstrated that enrichments in Au–Ag and epithermal-suite elements were due to inputs from magmatic-hydrothermal fluids that also led to the formation of distinctive green mica (fuchsite) alteration and quartz alteration (Fig. 19; Pilote et al. 2020). In the Lemarchant deposit, features including the sulfosalt-rich, high fO_2–fS_2 ore mineral assemblages (with low-Fe sphalerite), Au–Ag-epithermal-suite element enrichments, illite–K–feldspar alteration zones, and textures like metal-rich bladed barite and carbonate have all been interpreted to record low- to intermediate-sulfidation magmatic-hydrothermal inputs into the VMS hydrothermal system (Gill et al. 2016, 2019; Cloutier et al. 2017; Lajoie et al. 2020; Fig. 21).

In other deposits, aluminous alteration assemblages have been invoked to reflect input from magmatic-hydrothermal fluids. For example, in the Tulks belt, aluminous alteration is present in the Bobby's Pond deposit and accompanied by precious metal enrichment at the Daniels Pond deposits, which collectively attribute the influence from acidic fluids derived from magmatic-hydrothermal activity (Hinchey 2011; Sparkes and Hinchey 2023). The nearby Bobby's Pond sulfur occurrence and the associated alunite–topaz–pyrophyllite–orpiment–stibnite alteration associated with the occurrence have features like those of high sulfida-

Fig. 20. Model for the subseafloor replacement origin of the Boundary VMS deposit (from Piercey et al. 2014). (A) Reconstructed environment of formation for the deposit. The deposit formed at the interface between coherent and likely impermeable hanging wall flow-banded rhyolites and a footwall of lapilli tuff. Mineralization formed in both the subsurface and on surface. Subsurface mineralization formed via replacement of space in between clasts in volcaniclastic rocks and in fractures in rhyolite flows and lapilli tuff (±dissolution and replacement of volcanic/volcaniclastic rocks). Surface mineralization is interpreted to have formed via sulfide-rich chimneys that locally collapsed and were transported to form bedded sulfides. (B) The textures observed in the Boundary deposit range from partial replacement of coherent rocks and volcaniclastic rocks to near massive sulfide with relict chlorite altered felsic clasts.

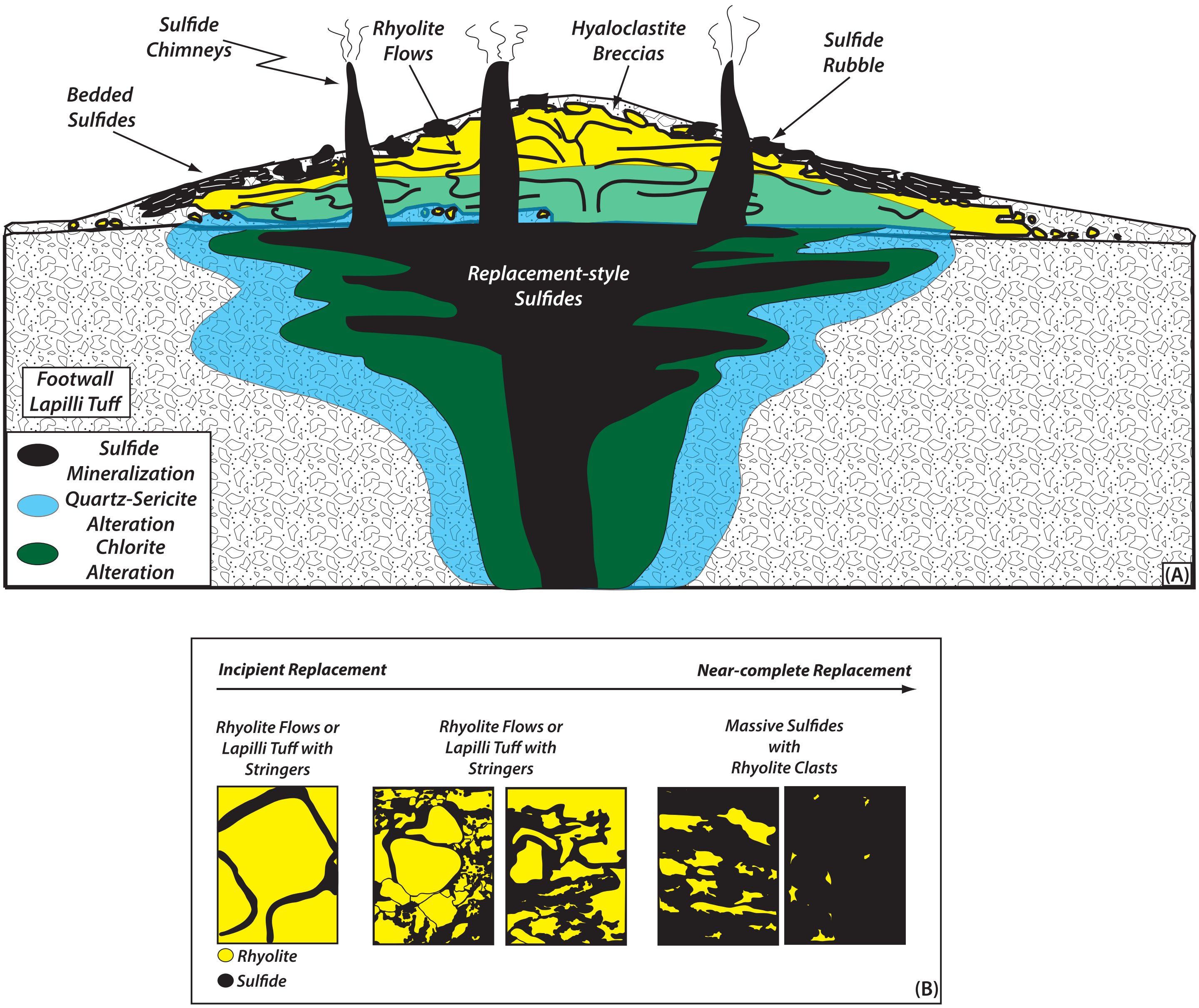

tion epithermal Au deposits interpreted to be derived from magmatic-hydrothermal fluids (e.g., Hedenquist and Arribas 2022), albeit in a subaqueous VMS setting (Hinchey 2011). Similarly, advanced argillic alteration zones recognized in the Buchans-Roberts Arm belt at the Mary March prospect are also suggestive of magmatic-hydrothermal input in a broadly VMS environment (Sparkes 2022; Sparkes and Hinchey 2023).

The increased recognition of magmatic-hydrothermal influences in some VMS deposits in the Dunnage Zone has been a major advancement in our understanding of VMS deposits in Newfoundland over the past decade. Despite this, there are still significant knowledge gaps, including what ultimately controls grade and tonnage in VMS deposits in Newfoundland—is it the source of metals, efficiency of deposition at the seafloor–vent interface, extent of zone refining, duration of magmatic activity and associated hydrothermal systems, permeability/porosity of hosting sequences, and(or) magmatic-hydrothermal fluid input? Moreover, although there is a reasonable understanding of the causes of enrichment of some critical metals (e.g., Cu and Zn), the dis-

Fig. 21. Potential hydrothermal environment and S isotope model for the Lemarchant VMS deposit (modified after Lode et al. 2017). Most of the sulfides found in the Lemarchant deposit are interpreted to be from black smoker deposition and dominated by sulfur derived from TSR and igneous sulfur with or without S derivation from magmatic-hydrothermal SO_2 disproportionation (e.g., Gill et al. 2019). Hydrothermal muds proximal to mineralization are interpreted to represent microbial mats that had input from TSR/igneous sulfur proximal to the vent; however, with distance, complex sulfur cycling occurred involving BSR of seawater sulfate, microbial sulfide oxidation, and microbial disproportionation of intermediate sulfur compounds. Large purple–pink lines represent deep hydrothermal fluid recharge (downwelling), large black lines represent focused hydrothermal fluid discharge (upwelling), black squiggly lines represent diffuse hydrothermal fluid (upwelling), and pink squiggly lines represent potential magmatic-hydrothermal fluid discharge (upwelling).

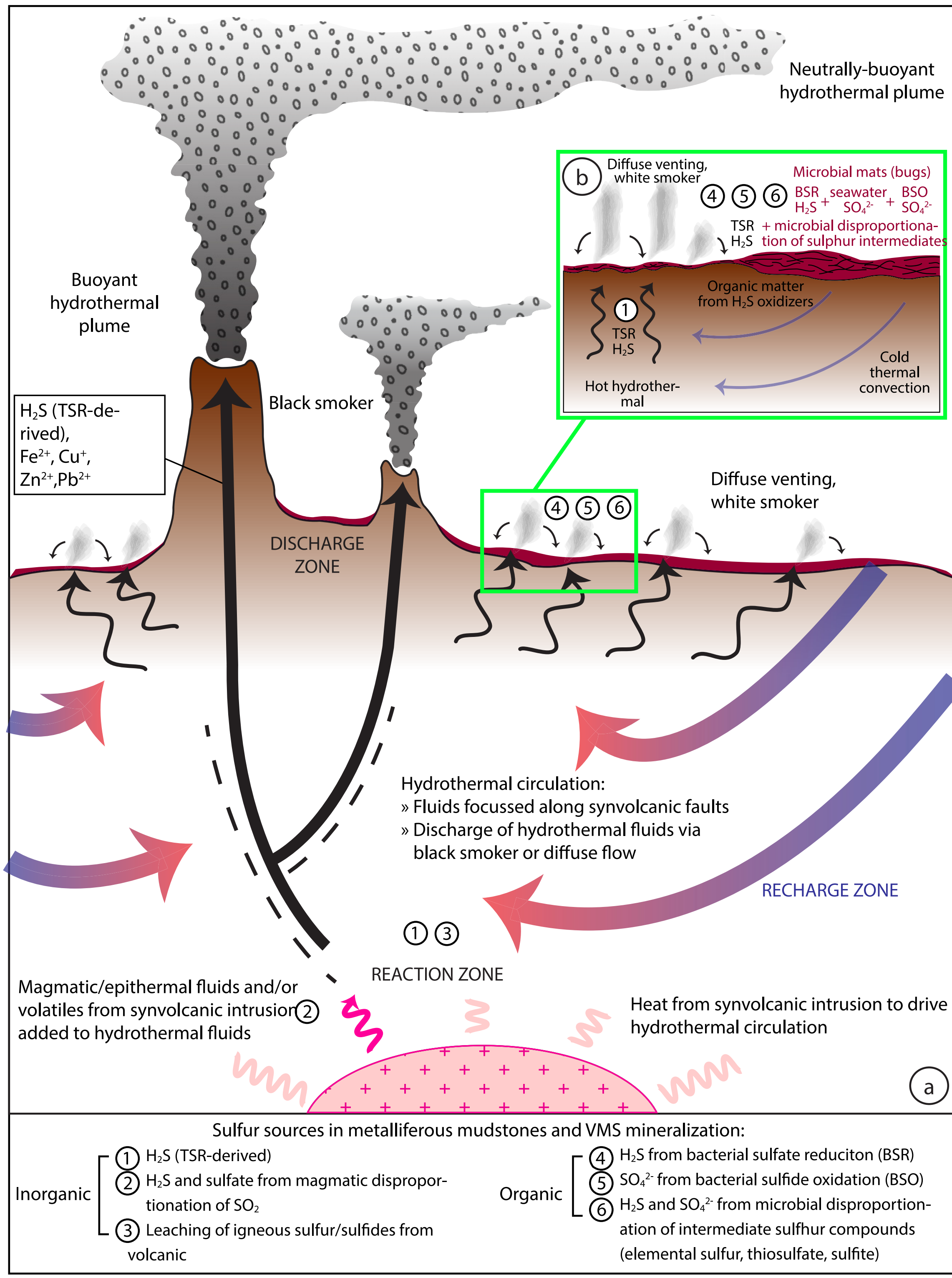

tributions and causes of enrichments in critical metals, like Co, Ni, Te, As, and Sb in VMS deposits in Newfoundland (e.g., Papezik 1964; Toman 2013) and globally (Monecke et al. 2016; Grant et al. 2018), is incompletely understood. Given the predicted increased need for such elements for electrification of the economy, having a better understanding of critical metal siting and enrichment processes in Newfoundland VMS deposits (and others globally) is essential and a potentially fruitful area for future research.

Diverse sources of sulfur

Most sulfur in VMS deposits comes from leaching of igneous sulfur from the underlying footwall rocks and subsequently TSR of seawater sulfate (e.g., Huston 1999). Less commonly, sulfur is derived from the bacteriogenic reduction of seawater sulfate (e.g., Lode et al. 2017) or rarely from magmatic-hydrothermal fluids by disproportionation of magmatic SO_2 (e.g., Herzig et al. 1998). There have been remarkably few studies of sulfur isotopes in VMS deposits of the Dunnage Zone until recently. Classic work by Bachinski (1977) and Kowalik et al. (1981) demonstrated that sulfur in mafic and bimodal felsic deposits in the Betts Cove ($\delta^{34}S = +5.5‰$ to $+23‰$) and Lushs Bight ($\delta^{34}S = +3.5‰$ to $+7.4‰$) complexes and Buchans district ($\delta^{34}S = +2.9$ to $+8.7$), respectively, had $\delta^{34}S$ values consistent with sulfur derivation by TSR of (Cambrian)-Ordovician seawater sulfate. In other VMS showings in the Buchans-Roberts Arm belt, there are indicators of TSR-derived S but also potentially S leached from footwall igneous rocks ($\delta^{34}S = +2.5‰$ to $+6.5‰$; Waldie et al. 1991; Santaguida et al. 1992).

All the S isotope studies cited above employed conventional methods using mineral separates, which generally consist of impure mineral mixtures, particularly for fine-grained materials. Most recent S isotope work on VMS deposits in the Dunnage Zone has utilized in situ methods (e.g., secondary ion mass spectrometry), which allows for greater absolute numbers of isotope determinations and importantly microscale paragenetic and textural control on S-isotope signatures of the sulfide minerals. Brueckner et al. (2015) illustrated that there was both igneous sulfur and TSR-derived sulfur in the Ming VMS deposit and that the sulfides there with higher temperature origins have greater igneous sulfur contributions. These authors also indicated some of the lower $\delta^{34}S$ values may be from magmatic volatiles; however, it was not possible to delineate this source from leached igneous sulfur on the basis of S isotopes alone. Cloutier et al. (2015) demonstrated similar TSR-igneous sulfur sourcing in the mafic Whalesback deposit and that the S-isotope signatures in sulfides were unchanged during metamorphism and reflected original syngenetic VMS values, corroborating the classic work of Bachinski (1977). In the Lemarchant deposit, Gill et al. (2019) illustrated shifts in S-isotope signatures with paragenesis, by which early low-temperature (150–250 °C) Zn–Pb–sulfosalt-rich mineralization produced relatively low $\delta^{34}S$ signatures and was dominated by igneous sulfur, whereas higher-temperature (>300 °C) Cu-rich assemblages had higher $\delta^{34}S$ values and were dominated by TSR-derived S. They also argued that some of the lower $\delta^{34}S$ values ($\delta^{34}S < 0‰$) in the Zn–Pb–sulfosalt-rich assemblages at Lemarchant may be due to input from disproportionated magmatic SO_2. Lode et al. (2017) also report extreme diversity in sulfur sources in hydrothermal exhalites/mudstones metres from massive sulfide in the Lemarchant deposit. Sulfide assemblages within these mudstones have extreme $\delta^{34}S$ variability ($-38.8‰$ to $+14.4‰$), which involved sulfur derived from bacterial reduction of seawater sulfate, microbial sulfide oxidation, and microbial disproportionation of intermediate sulfur compounds, as well as sulfur derivation from TSR and igneous sulfur; contributions from the latter sources increase in proximity to the deposit (e.g., within metres; Fig. 21).

The S-isotope studies of the VMS deposits of the Dunnage Zone illustrate the complex and diverse origins of sulfur in these deposits; however, detailed paragenetically and texturally controlled samples are restricted to only a few deposits and more research is needed to evaluate deposits with different metal assemblages, alteration types, and emplacement mechanisms (e.g., biogenic S is likely to be important in some replacement systems; Piercey 2015). Nevertheless, these recent studies demonstrate that the complexity of S-isotope signatures observed in ancient VMS in the Newfoundland Dunnage Zone is like that documented in other VMS belts globally and in modern SMS environments (Shanks and Seyfried 1987; Herzig et al. 1998; Nozaki et al. 2021).

Summary

The Dunnage Zone of the Newfoundland Appalachians hosts diverse styles of Cambrian-Ordovician VMS deposits in both the peri-Laurentian Notre Dame Subzone and the peri-Gondwanan Exploits Subzone. In the Notre Dame Subzone, ophiolitic rocks of the ∼510–501 Ma Lushs Bight oceanic tract and ∼488–485 Ma Baie Verte oceanic tract host Cu–(Zn)-rich mafic-type deposits within mafic rocks in ophiolite sequences. Bimodal mafic, Au-rich VMS deposits are hosted by ∼488–485 Ma dacitic rocks in the Baie Verte oceanic tract, whereas bimodal felsic deposits are within felsic-dominated sequences in the Buchans-Roberts Arm belt, including some of the highest-grade Zn–Pb–Cu–(Au–Ag) ore bodies ever mined on Earth. In the Exploits Subzone, Cambrian (∼513–509 Ma) bimodal felsic deposits are hosted in the Tally Pond and Long Lake belts, which are stratigraphically overlain by felsic-dominated VMS deposits in the ∼498–491 Ma Tulks belt. The Tulks belt has remarkable metallogenic diversity, with the southern end of the belt having polymetallic felsic siliciclastic deposits, whereas the northern part of the belt contains hybrid bimodal felsic deposits with some attributes typical of VMS deposits (e.g., massive Zn-rich sulfides and felsic host rocks) and other attributes that are hallmarks of epithermal Au deposits (e.g., precious metal- and epithermal-suite element enrichment and aluminous alteration). In the northern extremity of the Exploits Subzone, the Wild Bight Group hosts the ∼486 Ma Point Leamington belt that contains Cu–Zn-bearing bimodal felsic to bimodal mafic deposits. The youngest VMS mineralization in the Ex-

 Can. J. Earth Sci. 00: 1–39 (2023) | dx.doi.org/10.1139/cjes-2022-0148

ploits Subzone consists of the Cu–Au mafic-siliciclastic deposits in the Great Burnt Lake/South Pond belt.

The VMS deposits of the Dunnage Zone in Newfoundland are associated with rift episodes and mineralization in extensional tectonic regimes (e.g., forearc rift, arc rift, and back-arc basins) with coeval magmatism that is interpreted to have driven hydrothermal circulation. Some Au-enriched deposits of the Rambler-Ming district are also associated with slab-melt-related felsic rocks. Slab melting, subsequent melt-rock interaction and magmatic-hydrothermal fluid/volatile exsolution, was likely important in causing Au enrichment in this district and possibly in other Au-rich VMS deposits globally.

Many of the VMS deposits formed by exhalative processes and deposition on the seafloor (e.g., Lemarchant and some in situ deposits in Buchans). Parts of some deposits formed via re-sedimentation and transportation of sulfide as sediment gravity flows (e.g., transported deposits in Buchans) or by subseafloor replacement of volcanic (e.g., some Jane's Cove deposit in Pilley's Island), volcaniclastic (e.g., Duck Pond and Boundary deposits), and(or) sedimentary rocks (e.g., Boomerang deposit) beneath the seafloor.

Metals within the VMS deposits were likely derived mainly by the leaching of underlying footwall rocks, but some have features indicative of derivation from magmatic–hydrothermal fluids, particularly deposits enriched in precious metals (e.g., Au–Ag) and epithermal-suite elements (e.g., Hg–As–Sb–Bi–Te–Se–Sn–W).

Sulfur in most of VMS deposits was sourced from either leached igneous sulfur in footwall rocks followed by TSR of seawater sulfate. A subset of deposits show evidence of influence from bacterial sulfur-derived BSR of seawater sulfate with the sulfur in some deposits potentially derived by disproportionation of magmatic SO_2.

Despite a long history of mining, exploration, and research on VMS deposits in the Newfoundland Appalachians, numerous questions remain unresolved, thus providing important opportunities for future research and resource exploration and development.

Acknowledgements

There have been numerous graduate students and postdoctoral fellows in the Piercey research group who have contributed significantly to our understanding of VMS in the central Newfoundland Appalachians, including Alicia Escribano, Stefanie Bruckner, Mike Buschette, Jonathan Cloutier, Michelle English, Shannon Gill, Regan Jacobson, Kyra Kennedy, Marie-Eve Lajoie, Stefanie Lode, Conor McKinley, Taylor Mugford, Jean-Luc Pilote, and Helena Toman. We also build on the work of numerous geologists who have contributed immensely to our understanding of VMS deposits in Newfoundland and would like to recognize their contributions, including Terry Brace, Peter Dimmell, Greg Dunning, David Evans, George Jenner, Baxter Kean, Paul Moore, Brian O'Brien, Larry Pilgrim, Frank Santaguida, Tom Skulski, Kerry Sparkes, Gerry Squires, Peter Tallman, Scott Swinden, Geoff Thurlow, and Lawrence Winter. Frank Santaguida is especially thanked for donating Piercey his extensive collection of samples from VMS deposits in the Notre Dame Bay area, which have become a valuable resource for research (and teaching!) and have contributed significantly to this manuscript. Piercey's VMS research has been supported by numerous partners in industry (Altius Minerals, Aur Resources, Canadian Zinc, Champion Iron, Cornerstone Resources, Messina Minerals, Paragon, Rambler Metals, and Teck) and government (Geological Survey of Canada, Geological Survey of Newfoundland and Labrador), and by the Natural Sciences and Engineering Research Council of Canada (NSERC) through both the Discovery Grant and Collaborative Research and Development grant programs. We thank John Slack and Jan Peter for formal reviews and Associate Editor Michelle DeWolfe for editorial comments—their suggestions have greatly improved this manuscript. Brendan Murphy and Sally Pehrsson are thanked for the invitation to contribute this manuscript (and gentle nudges to get it finished!).

Article information

History dates

Received: 26 December 2022
Accepted: 11 May 2023
Accepted manuscript online: 30 May 2023
Version of record online: 5 July 2023

Notes

This invited article is part of a collection that celebrates the Canadian Journal of Earth Sciences' 60th anniversary.

Copyright

Data availability

All data presented in the paper are available in the original manuscripts cited or can be obtained from the authors upon request. The data used for constructing Figs. 4 and 5 can be found in Table S1 and are also available from publicly available sources cited in the table.

Author information

Author ORCIDs

Stephen J. Piercey https://orcid.org/0000-0002-1931-5745

Author contributions

Conceptualization: SJP, JGH, GWS
Data curation: SJP, JGH, GWS
Formal analysis: SJP, JGH, GWS
Funding acquisition: SJP, JGH, GWS
Investigation: SJP, JGH, GWS
Methodology: SJP, JGH, GWS
Project administration: SJP, JGH, GWS
Resources: SJP, JGH, GWS

Validation: SJP, JGH, GWS
Visualization: SJP, JGH, GWS
Writing – original draft: SJP, JGH, GWS
Writing – review & editing: SJP, JGH, GWS

Competing interests

The authors declare there are no competing interests.

Funding information

During construction of this manuscript, SJP was supported by an NSERC Discovery Grant. Previous research conducted by the authors and reviewed in this article was funded by various sources as outlined in the Acknowledgements.

Supplementary material

Supplementary data are available with the article at https://doi.org/10.1139/cjes-2022-0148.

References

Alt, J.C. 1995. Subseafloor processes in mid-ocean ridge hydrothermal systems. Geophysical Monograph, **91**: 85–114.
Bachinski, D.J. 1977. Sulfur isotopic composition of ophiolitic cupriferous iron sulfide deposits, Notre Dame Bay, Newfoundland. Economic Geology, **72**: 243–257. doi:10.2113/gsecongeo.72.2.243.
Barbour, D.M., and Churchill, R. 2001. First and sixth year assessment report on geological mapping, lithogeochemistry, diamond drilling, and borehole TDEM surveys, mineral licenses 7629 M, 7726 M and 7771 M, Glover's Harbour area, Notre Dame Bay, Newfoundland, NTS Sheets 2E/05 and 2E/06. Assessment File 002E/1203. Newfoundland and Labrador Geological Survey. p. 35(+appendicies).
Barr, S.M., White, C.E., and Miller, B.V. 2003. Age and geochemistry of late Neoproterozoic and early Cambrian igneous rocks in southern New Brunswick: similarities and contrasts. Atlantic Geoscience, **39**: 55–73. doi:10.4138/1050.
Barrie, C.T., and Hannington, M.D. 1999. Classification of volcanic-associated massive sulfide deposits based on host-rock composition. Reviews in Economic Geology, **8**: 1–11.
Barry, J., Feasby, D.G., Froude, T., Putrich, E., and Stone, W. 2022. Updated mineral resource estimate and preliminary economic assessment of the Great Burnt copper–gold property, central Newfoundland. NI-43-101 Technical Report for Spruce Ridge Resources Ltd. p. 249.
,Barton, P.B., Jr., and Bethke, P.M. 1987. Chalcopyrite disease in sphalerite: pathology and epidemiology. American Mineralogist, **72**: 451–467.
Bedard, J.H. 1999. Petrogenesis of boninites from the Betts Cove ophiolite, Newfoundland, Canada: identification of subducted source components. Journal of Petrology, **40**: 1853–1889. doi:10.1093/petroj/40.12.1853.
Bedard, J.H., Lauziere, K., Tremblay, A., and Sangster, A. 1999. Evidence for forearc seafloor-spreading from the Betts Cove Ophiolite, Newfoundland: oceanic crust of boninitic affinity. Tectonophysics, **284**: 223–245.
Bedard, J.H., Lauziere, K., Tremblay, A., Sangster, A., Douma, S.L., and Dec, T. 2000. Betts Cove ophiolite and its cover rocks, Newfoundland. Geological Survey of Canada Bulletin, **550**: 76.
Binney, W.P. 1987. A sedimentological investigation of MacLean channel transported sulfide ores. Geological Survey of Canada Paper 86-24. pp. 107–147.
Binns, R.A., and Scott, S.D. 1993. Activity-forming poylmetallic sulfide deposits associated with felsic volcanic rocks in the eastern Manus Basin, Papua—New Guinea. Economic Geology, **88**: 2226–2236. doi:10.2113/gsecongeo.88.8.2226.
Blounot, C.W., and Dickson, F.W. 1969. The solubility of anhydrite ($CaSO_4$) in NaCl-H_2O from 100 to 450° C and 1 to 1000 bars. Geochimica et Cosmochimica Acta, **33**: 227–245. doi:10.1016/0016-7037(69)90140-9.
Bradley, D.C., Tucker, R.D., Lux, D.R., Harris, A.G., and McGregor, D.C. 2000. Migration of the Acadian orogen and foreland basin across the northern Appalachians of Maine and adjacent areas. US Geological Survey Professional Paper 1624. p. 55.
Brueckner, S.M., Piercey, S.J., Sylvester, P.J., Maloney, S., and Pilgrim, L. 2014b. Evidence for syngenetic precious metal enrichment in an Appalachian volcanogenic massive sulfide system: The 1806 zone, Ming mine, Newfoundland, Canada. Economic Geology, **109**: 1611–1642. doi:10.2113/econgeo.109.6.1611.
Brueckner, S.M., Piercey, S.J., Layne, G.D., Piercey, G., and Sylvester, P.J. 2015. Variations of sulfur isotope signatures in sulfides from the metamorphosed Ming Cu(–Au) volcanogenic massive sulfide deposit, Newfoundland Appalachians, Canada. Mineralium Deposita, **50**: 619. doi:10.1007/s00126-014-0567-7.
Brueckner, S.M., Piercey, S.J., Pilote, J.-L., Layne, G.D., and Sylvester, P.J. 2016. Mineralogy and mineral chemistry of the metamorphosed and precious metal-bearing Ming deposit, Canada. Ore Geology Reviews, **72**: 914–939.
Buschette, M.J., and Piercey, S.J. 2016. Hydrothermal alteration and lithogeochemistry of the Boundary volcanogenic massive sulfide deposit, central Newfoundland, Canada. Canadian Journal of Earth Sciences, **53**: 506–527. doi:10.1139/cjes-2015-0237.
Castonguay, S., and Tremblay, A. 2003. Tectonic evolution and significance of Silurian-early Devonian hinterland-directed deformation in the internal Humber zone of the southern Quebec Appalachians. Canadian Journal of Earth Sciences, **40**: 255–268. doi:10.1139/e02-045.
Castonguay, S., van Staal, C.R., Joyce, N., Skulski, T., and Hibbard, J.P. 2014. Taconic metamorphism preserved in the Baie Verte Peninsula, Newfoundland Appalachians: geochronological evidence for ophiolite obduction and subduction and exhumation of the leading edge of the Laurentian (Humber) margin during closure of the Taconic seaway. Geoscience Canada, **41**: 459–482.
Cloutier, J., Piercey, S.J., Layne, G., Heslop, J., Hussey, A., and Piercey, G. 2015. Styles, textural evolution, and sulfur isotope systematics of Cu-rich sulfides from the Cambrian Whalesback volcanogenic massive sulfide deposit, central Newfoundland. Economic Geology, **110**: 1215–1234. doi:10.2113/econgeo.110.5.1215.
Cloutier, J., Piercey, S.J., Lode, S., Vande Guchte, M., and Copeland, D.A. 2017. Lithostratigraphic and structural reconstruction of the Zn–Pb–Cu–Ag–Au lemarchant volcanogenic massive sulfide (VMS) deposit, Tally Pond group, central Newfoundland, Canada. Ore Geology Reviews, **84**: 154–173. doi:10.1016/j.oregeorev.2017.01.010.
Coates, H. 1990. Geology and mineral deposits of the Rambler property in metallogenic framework of base and precious metal deposits, central and western Newfoundland (Field Trip 1). *In* Proceedings of the Field Trip Guidebook for 8th IAGOD Symposium. Open File 2156. Geological Survey of Canada. pp. 184–193.
Colman-Sadd, S.P., Dunning, G.R., and Dec, T. 1992. Dunnage–Gander relationships and Ordovician orogeny in central Newfoundland: a sediment provenance and U/Pb age study. American Journal of Science, **292**: 317–355. doi:10.2475/ajs.292.5.317.
de Ronde, C.E.J., Hannington, M.D., Stoffers, P., Wright, I.C., Ditchburn, R.G., Reyes, A.G., et al. 2005. Evolution of a submarine magmatic-hydrothermal system: Brothers Volcano, southern Kermadec arc, New Zealand. Economic Geology, **100**: 1097–1133. doi:10.2113/gsecongeo.100.6.1097.
de Ronde, C., Massoth, G.J., Butterfield, D.A., Christenson, B.W., Ishibashi, J., Ditchburn, R.G., et al. 2011. Submarine hydrothermal activity and gold-rich mineralization at Brothers Volcano, Kermadec Arc, New Zealand. Mineralium Deposita, **46**: 541–584. doi:10.1007/s00126-011-0345-8.
Defant, M.J., and Drummond, M.S. 1990. Derivation of some modern arc magmas of young subducted lithosphere. Nature, **347**: 662–665.
Denoyers, D.W. 1991. The South Pond copper/gold prospect, central Newfoundland *In* Ore horizons. Geological Survey Branch, Department of Mines and Energy, Government of Newfoundland and Labrador. **1**: 22–31.
Dilles, J.H., Kent, A.J.R., Wooden, J.L., Tosdal, R.M., Koleszar, A., Lee, R.G., and Farmer, L.P. 2015. Zircon compositional evidence for sulfur-degassing from ore-forming arc magmas. Economic Geology, **110**: 241–251. doi:10.2113/econgeo.110.1.241.

Doyle, M.G., and Allen, R.L. 2003. Subsea-floor replacement in volcanic-hosted massive sulfide deposits. Ore Geology Reviews, **23**: 183–222. doi:10.1016/S0169-1368(03)00035-0.

Dubé, B., Gosselin, P., Mercier-Langevin, P., Hannington, M., and Galley, A. 2007. Gold-rich volcanogenic massive sulfide deposits. *In* Mineral deposits of Canada: a synthesis of major deposit-types, district metallogeny, the evolution of geological provinces, and exploration methods. Special Publication 5. *Edited by* W.D. Goodfellow. Mineral Deposits Division, Geological Association of Canada. pp. 75–94.

Dunning, G.R., and Krogh, T.E. 1985. Geochronology of ophiolites of the Newfoundland Appalachians. Canadian Journal of Earth Sciences, **22**: 1659–1670.

Dunning, G.R., O'Brien, S.J., Colman-Sadd, S.P., Blackwood, R.F., Dickson, W.L., O'Neill, P.P., and Krogh, T.E. 1990. Silurian orogeny in the Newfoundland Appalachians. Journal of Geology, **98**: 895–913.

Dunning, G.R., Swinden, H.S., Kean, B.F., Evans, D.T.W., and Jenner, G.A. 1991. A Cambrian island arc in Iapetus: geochronology and geochemistry of the Lake Ambrose volcanic belt. Geological Magazine, **128**: 1–17. doi:10.1017/S0016756800018008.

Eldridge, C.W., Barton, P.B., and Ohmoto, H. 1983. Mineral textures and their bearing on formation of the Kuroko orebodies. Economic Geology Monograph, **5**: 241–281.

English, M.L.R. 2019. Lithofacies and alteration of the Hurricaine Zone of the Boomerang volcanogenic massive sulfide deposit, Tulks Belt, Central Newfoundland, Canada. Unpublished M.Sc. thesis, Memorial University of Newfoundland. p. 226.

Evans, D.T.W., and Kean, B.F. 2002. The Victoria Lake supergroup, central Newfoundland—its definition, setting and volcanogenic massive sulfide mineralization. Open File NFLD/2790. Geological Survey, Newfoundland and Labrador Department of Mines and Energy. p. 68.

Ferry, J.M., and Watson, E.B. 2007. New thermodynamic models and revised calibrations for the Ti-in-zircon and Zr-in-rutile thermometers. Contributions to Mineralogy and Petrology, **154**: 429–437. doi:10.1007/s00410-007-0201-0.

Franklin, J.M., Sangster, D.M., and Lydon, J.W. 1981. Volcanic-associated massive sulfide deposits. *In* Proceedings of the Economic Geology Seventy-Fifth Anniversary. *Edited by* B.J. Skinner. The Economic Geology Publishing Company, Lancaster, PA. pp. 485–627.

Franklin, J.M., Gibson, H.L., Galley, A.G., and Jonasson, I.R. 2005. Volcanogenic massive sulfide deposits. *In* Proceedings of the Economic Geology 100th Anniversary. *Edited by* J.W. Hedenquist, J.F.H. Thompson, R.J. Goldfarb and J.P. Richards. Society of Economic Geologists Inc., Littleton, CO. pp. 523–560.

Fyffe, L.R., Johnson, S.C., and van Staal, C.R. 2012. A review of Proterozoic to early Paleozoic lithotectonic terranes in New Brunswick, Canada and their tectonic evolution during penobscot, taconic, salinic and Acadian orogenesis. Atlantic Geoscience, **47**: 211–248. doi:10.4138/atlgeol.2011.010.

Gaboury, D., and Pearson, V. 2008. Rhyolite geochemical signatures and association with volcanogenic massive sulfide deposits: examples from the Abitibi Belt. Economic Geology, **103**: 1531–1562. doi:10.2113/gsecongeo.103.7.1531.

Galley, A.G. 1993. Characteristics of semi-conformable alteration zones associated with volcanogenic massive sulfide districts. Journal of Geochemical Exploration, **48**: 175–200. doi:10.1016/0375-6742(93)90004-6.

Galley, A.G., Hannington, M., and Jonasson, I. 2007. Volcanogenic massive sulfide deposits. *In* Mineral deposits of Canada: a synthesis of major deposit-types, district metallogeny, the evolution of geological provinces, and exploration methods. Special Publication 5. *Edited by* W.D. Goodfellow. Mineral Deposits Division, Geological Association of Canada. pp. 141–161.

German, C.R., and Seyfried, W.E. 2014. Hydrothermal processes. *In* The oceans and marine geochemistry. Treatise on geochemistry. 2nd ed. M.J. Mottle and H. Elderfield. Elsevier-Pergamon Oxford. pp. 191–233.

Gibson, H.L., Watkinson, D.H., and Comba, C.D.A. 1983. Silicification: hydrothermal alteration in an Archean geothermal system within the Amulet Rhyolite Formation, Noranda, Quebec. Economic Geology, **78**: 954–971.

Gibson, H.L., Morton, R.L., and Hudak, G.J. 1999. Submarine volcanic processes, deposits, and environments favorable for the location of volcanic-associated massive sulfide deposits. Reviews in Economic Geology, **8**: 13–51.

Gill, S.B., Piercey, S.J., and Layton-Matthews, D. 2016. Mineralogy and metal zoning of the cambrian Zn–Pb–Cu–Ag–Au lemarchant volcanogenic massive sulfide (VMS) deposit, Newfoundland. Canadian Mineralogist, **54**: 1307–1344. doi:10.3749/canmin.1500069.

Gill, S.B., Piercey, S.J., Layne, G.D., and Piercey, G. 2019. Sulfur and lead isotope geochemistry of sulfide minerals from the Zn–Pb–Cu–Ag–Au Lemarchant volcanogenic massive sulfide (VMS) deposit, Newfoundland, Canada. Ore Geology Reviews, **104**: 422–435. doi:10.1016/j.oregeorev.2018.11.008.

Goodfellow, W.D. 2007. Metallogeny of the Bathurst Mining Camp, Northern New Brunswick. *In* Mineral deposits of Canada: a synthesis of major deposit-types, district metallogeny, the evolution of geological provinces, and exploration methods. Special Publication 5. *Edited by* W.D. Goodfellow. Mineral Deposits Division, Geological Association of Canada. pp. 449–469.

Graham, U.M., Bluth, G.J., and Ohmoto, H. 1988. Sulfide–sulfate chimneys on the East Pacific Rise, 11 degrees and 13 degrees N latitudes; part I, mineralogy and paragenesis. The Canadian Mineralogist, **26**: 487–504.

Grant, H.L.J., Hannington, M.D., Petersen, S., Frische, M., and Fuchs, S.H. 2018. Constraints on the behavior of trace elements in the actively-forming TAG deposit, Mid-Atlantic Ridge, based on LA-ICP-MS analyses of pyrite. Chemical Geology, **498**: 45–71. doi:10.1016/j.chemgeo.2018.08.019.

Hannington, M. 2014. Volcanogenic massive sulfide deposits. *In* Geochemistry of mineral deposits. Treatise on geochemistry. 2nd ed. *Edited by* S.D. Scott. Elsevier-Pergamon Oxford. pp. 463–488.

Hannington, M.D., Poulsen, K.H., Thompson, J.F.H., and Sillitoe, R.H. 1999. Volcanogenic gold in the massive sulfide environment. Reviews in Economic Geology, **8**: 325–356.

Hannington, M.D., de Ronde, C.E.J., and Petersen, S. 2005. Sea floor tectonics and submarine hydrothermal systems. *In* Proceedings of Economic geology: One Hundredth Anniversary. *Edited by* J. W. Hedenquist, J.F.H. Thompson, R.J. Goldfarb and J.P. Richards. Society of Economic Geologists. pp. 111–142.

Hart, T.R., Gibson, H.L., and Lesher, C.M. 2004. Trace element geochemistry and petrogenesis of felsic volcanic rocks associated with volcanogenic massive Cu–Zn–Pb sulfide deposits. Economic Geology, **99**: 1003–1013. doi:10.2113/gsecongeo.99.5.1003.

Haymon, R.M. 1983. Growth history of hydrothermal black smoker chimneys. Nature, **301**: 695–698. doi:10.1038/301695a0.

Hedenquist, J.W., and Arribas, A. 2022. Exploration implications of multiple formation environments of advanced argillic minerals. Economic Geology, **117**: 609–643. doi:10.5382/econgeo.4880.

Herzig, P.M., Hannington, M.D., and Arribas Jr., A. 1998. Sulfur isotopic composition of hydrothermal precipitates from the Lau back-arc: implications for magmatic contributions to seafloor hydrothermal systems. Mineralium Deposita, **33**: 226–237. doi:10.1007/s001260050143.

Hibbard, J. 1983. Geology of the Baie Verte Peninsula, Newfoundland. Government of Newfoundland and Labrador, Department of Mines and Energy, Mineral Development Division, Memoir 2. p. 279.

Hinchey, J.G. 2011. The Tulks volcanic belt, Victoria Lake supergroup, central Newfoundland—geology, tectonic setting, and volcanogenic massive sulfide mineralization. Report 2011-02. Geological Survey, Newfoundland and Labrador Department of Natural Resources. p. 167.

Hinchey, J.G. 2014. The Long Lake Group: preliminary U–Pb geochronology and lithogeochemistry, and implications for tectonostratigraphic architecture and VMS mineralization. Geological Survey Report 14-1. Current Research, Newfoundland and Labrador Department of Natural Resources. pp. 15–44.

Hinchey, J.G., and McNicoll, V. 2016. The Long Lake Group: an update on U–Pb geochronological studies. Geological Survey Report 16-1. Current Research, Newfoundland and Labrador Department of Natural Resources. pp. 27–38.

Huston, D.L. 1999. Stable isotopes and their significance for understanding the genesis of volcanic-hosted massive sulfide deposits: a review. Reviews in Economic Geology, **8**: 157–179.

Huston, D.L., and Kamprad, J. 2001. Zonation of alteration facies at western Tharsis: implications for the genesis of Cu–Au deposits, Mount Lyell field, western Tasmania. Economic Geology, **96**: 1123–1132.

Huston, D.L., Eglington, B.M., Pehrsson, S., and Piercey, S.J. 2015. The metallogeny of zinc through time: links to secular changes in the atmosphere, hydrosphere, and the supercontinent cycle. *In* Current perspectives on zinc deposits. *Edited by* S.M. Archibald and S.J. Piercey. Irish Association for Economic Geology, Dublin. pp. 1–16.

Johnson, S.C., Fyffe, L.R., McLeod, M.J., and Dunning, G.R. 2012. U–Pb ages, geochemistry, and tectonomagmatic history of the Cambro-Ordovician Annidale Group: a Remnant of the Penobscot arc system in southern New Brunswick? Canadian Journal of Earth Sciences, **49**: 166–188. doi:10.1139/e11-031.

Jowitt, S.M., Jenkin, G.R.T., Coogan, L.A., and Naden, J. 2012. Quantifying the release of base metals from source rocks for volcanogenic massive sulfide deposits: effects of protolith composition and alteration mineralogy. Journal of Geochemical Exploration, **118**: 47–59. doi:10.1016/j.gexplo.2012.04.005.

Kanehira, K., and Bachinski, D. 1968. Mineralogy and textural relationships of ores from the Whalesback mine, northeastern Newfoundland. Canadian Journal of Earth Sciences, **5**: 1387–1395. doi:10.1139/e68-137.

Kean, B.F., and Evans, D.T.W. 1986. Metallogeny of the Tulks Hill Volcanics, Victoria Lake Group, central Newfoundland. Mineral Development Division Report 86-1. Department of Mines and Energy, Government of Newfoundland and Labrador. pp. 51–57.

Kean, B.F., Evans, D.T.W., and Jenner, G.A. 1995. Geology and mineralization of the Lushs Bight Group. Report 95-02. Geological Survey of Newfoundland and Labrador, Newfoundland Department of Natural Resources. p. 204.

Keays, R.R. 1987. Principles of mobilization (dissolution) of metals in mafic and ultramafic rocks—the role of immiscible magmatic sulfides in the generation of hydrothermal gold and volcanogenic massive sulfide deposits. Ore Geology Reviews, **2**: 47–63.

Kerr, A., and Leitch, A.M. 2005. Self-destructive sulfide segregation systems and the formation of high-grade magmatic ore deposits. Economic Geology, **100**: 311–332.

Kirkham, R.V. 1987. Buchans Geology, Newfoundland. Paper 86-24. Geological Survey of Canada. 288p.

Kowalik, J., Rye, R.O., and Sawkins, F.J. 1981. Stable-isotope study of the Buchans, Newfoundland, polymetallic sulfide deposits. *In* The Buchans orebodies: fifty years of geology and mining. Special Paper 22. *Edited by* E.A. Swanson, D.F. Strong and J.G. Thurlow. Geological Association of Canada. pp. 229–254.

Lafrance, B., Gibson, H.L., and Stewart, M.S. 2020. Internal and external deformation and modification of volcanogenic massive sulfide deposits. Reviews in Economic Geology, **21**: 147–171.

Lajoie, M.-È., Piercey, S.J., Conliffe, J., and Layton-Matthews, D. 2020. Geology, mineralogy, S and Sr isotope geochemistry, and fluid inclusion analysis of barite associated with the Lemarchant Zn–Pb–Cu–Ag–Au-rich volcanogenic massive sulfide deposit, Newfoundland, Canada. Canadian Journal of Earth Sciences, **57**: 133–166. doi:10.1139/cjes-2018-0161.

Large, R.R. 1992. Australian volcanic-hosted massive sulfide deposits: features, styles, and genetic models. Economic Geology, **87**: 471–510. doi:10.2113/gsecongeo.87.3.471.

Lee, C.-T.A., and Tang, M. 2020. How to make porphyry copper deposits. Earth and Planetary Science Letters, **529**: 115868. doi:10.1016/j.epsl.2019.115868.

Lesher, C.M., Goodwin, A.M., Campbell, I.H., and Gorton, M.P. 1986. Trace element geochemistry of ore-associated and barren felsic metavolcanic rocks in the Superior Province, Canada. Canadian Journal of Earth Sciences, **23**: 222–237. doi:10.1139/e86-025.

Lissenberg, C.J., Zagorevski, A., Rogers, N., van Staal, C.R., and Whalen, J.B. 2005. Geology, Star Lake, Newfoundland and Labrador. Open File 1669, 1:50,000 scale map. Geological Survey of Canada.

Lode, S., Piercey, S.J., and Devine, C.A. 2015. Geology, mineralogy, and lithogeochemistry of metalliferous mudstones associated with the Lemarchant volcanogenic massive sulfide deposit, Tally Pond belt, central Newfoundland. Economic Geology, **110**: 1835–1859.

Lode, S., Piercey, S.J., Layne, G.D., Piercey, G., and Cloutier, J. 2017. Multiple sulfur and lead sources recorded in hydrothermal exhalites associated with the Lemarchant volcanogenic massive sulfide deposit, central Newfoundland, Canada. Mineralium Deposita, **52**: 105–128. doi:10.1007/s00126-016-0652-1.

Lydon, J.W. 1988. Volcanogenic massive sulfide deposits: Part 2, genetic models. Geoscience Canada, **15**: 43–65.

MacLachlan, K., and Dunning, G.R. 1998. U–Pb ages and tectonomagmatic relationships to early Ordovician low-Ti tholeiites, boninites, and related plutonic rocks in central Newfoundland, Canada. Contributions to Mineralogy and Petrology, **133**: 235–258.

MacLachlan, K., O'Brien, B.H., and Dunning, G.R. 2001. Redefinition of the Wild Bight Group, Newfoundland: implications for models of island-arc evolution in the Exploits Subzone. Canadian Journal of Earth Sciences, **38**: 889–907. doi:10.1139/e01-006.

McKinley, C.P. 2013. Volcanic and hydrothermal reconstruction of the Pilley's Island volcanogenic massive sulfide district, central Newfoundland. Unpublished M.Sc. thesis, Memorial University of Newfoundland, St. John's. p. 261.

McNicoll, V., Squires, G., Kerr, A., and Moore, P. 2010. The Duck Pond and Boundary Cu–Zn deposits, Newfoundland: new insights into the ages of host rocks and the timing of VHMS mineralization. Canadian Journal of Earth Sciences, **47**: 1481–1506. doi:10.1139/E10-075.

Manor, M.J., Piercey, S.J., Wall, C.J., and Denisová, N. 2022. High-precision CA-ID-TIMS U–Pb zircon geochronology of felsic rocks in the Finlayson Lake VMS district, Yukon: linking Paleozoic Basin-scale accumulation rates to the occurrence of subseafloor replacement-style mineralization. Economic Geology, **117**: 1173–1201. doi:10.5382/econgeo.4910.

Martin, W. 1983. Once upon a mine: story of pre-Confederation mines on the island of Newfoundland. Canadian Institute of Mining and Metallurgy, Montreal, QC, Canada. pp. 26–98.

Mercier-Langevin, P., Dube, B., Hannington, M.D., Richer-Lafleche, M., and Gosselin, G. 2007. The LaRonde Penna Au-rich volcanogenic massive sulfide deposit, Abitibi greenstone belt, Quebec. Part II. lithogeochemistry and paleotectonic setting. Economic Geology, **102**: 611–631. doi:10.2113/gsecongeo.102.4.611.

Mercier-Langevin, P., Hannington, M., Dubé, B., and Bécu, V. 2011. The gold content of volcanogenic massive sulfide deposits. Mineralium Deposita, **46**: 509–539. doi:10.1007/s00126-010-0300-0.

Monecke, T., Petersen, S., Hannington, M.D., Grant, H.L.J., and Samson, I.M. 2016. The minor element endowment of modern sea-floor massive sulfides and comparisons with deposits hosted in ancient volcanic succesions. Reviews in Economic Geology, **18**: 245–306.

Mueller, C., Piercey, S.J., Babechuk, M.G., and Copeland, D. 2021a. Stratigraphy and lithogeochemistry of rocks from the Goldenville horizon and associated rocks. Grant Program Full Results (2018–2020). Open File 8755. Targeted Geoscience Initiative 5. Geological Survey of Canada, Baie Verte Peninsula, Newfoundland. pp. 235–249.

Mueller, C., Piercey, S.J., Babechuk, M.G., and Copeland, D. 2021b. Stratigraphy and lithogeochemistry of rocks from the Nugget Pond deposit area, Grant Program Full Results (2018–2020). Open File 8755. Targeted Geoscience Initiative 5. Geological Survey of Canada, Baie Verte Peninsula, Newfoundland. pp. 217–234.

Mungall, J.E. 2002. Roasting the mantle: slab melting and the genesis of major Au and Au-rich Cu deposits. Geology, **30**: 915–918. doi:10.1130/0091-7613(2002)030%3c0915:RTMSMA%3e2.0.CO;2.

Murphy, J.B., van Staal, C.R., and Keppie, J.D. 1999. Middle to late paleozoic acadian orogeny in the northern Appalachians: A Laramide-style plume-modified orogeny? Geol, **27**: 653–656. doi:10.1130/0091-7613(1999)027%3c0653:MTLPAO%3e2.3.CO;2.

Nozaki, T., Nagase, T., Ushikubo, T., Shimizu, K., and Ishibashi, J.-I. 2021. Microbial sulfate reduction plays an important role at the initial stage of subseafloor sulfide mineralization. Geology, **49**: 222–227. doi:10.1130/G47943.1.

O'Brien, B.H. 2007. Geology of the Buchans-Roberts Arm volcanic belt, near Great Gull Lake. Geological Survey Report 07-01. Current Research. Newfoundland and Labrador Department of Natural Resources. pp. 85–102.

Ohmoto, H. 1996. Formation of volcanogenic massive sulfide deposits: the Kuroko perspective. Ore Geology Reviews, **10**: 135–177. doi:10.1016/0169-1368(95)00021-6.

Papezik, V.S. 1964. Nickel minerals at Tilt Cove, Notre Dame Bay, Newfoundland. Proceedings of the Geological Association of Canada. pp. 27–32.

Patten, C.G.C., Coltat, R., Junge, M., Peillod, A., Ulrich, M., Manatschal, G., and Kolb, J. 2022. Ultramafic-hosted volcanogenic massive sulfide deposits: an overlooked sub-class of VMS deposit forming in complex tectonic environments. Earth-Science Reviews, **224**: 103891. doi:10.1016/j.earscirev.2021.103891.

Piercey, S.J. 2011. The setting, style, and role of magmatism in the formation of volcanogenic massive sulfide deposits. Mineralium Deposita, **46**: 449–471. doi:10.1007/s00126-011-0341-z.

Piercey, S.J. 2015. A semipermeable interface model for the genesis of subseafloor replacement-type volcanogenic massive sulfide (VMS) deposits. Economic Geology, **110**: 1655–1660. doi:10.2113/econgeo.110.7.1655.

Piercey, S.J., and Pilote, J.-L. 2021. Nd-Hf isotope geochemistry and lithogeochemistry of the Rambler rhyolite, Ming VMS deposit, Baie Verte Peninsula, Newfoundland: evidence for slab melting and implications for VMS localization, Geological Survey of Canada. pp. 201–215.

Piercey, S.J., Squires, G.C., and Brace, T.D. 2014. Lithostratigraphic, hydrothermal, and tectonic setting of the Boundary volcanogenic massive sulfide deposit, Newfoundland Appalachians, Canada: formation by subseafloor replacement in a Cambrian rifted arc. Economic Geology, **109**: 661–687.

Piercey, S.J., Peter, J.M., and Herrington, R. 2015. Zn-rich volcanogenic massive sulfide (VMS) deposits. *In* Current perspectives on zinc deposits. *Edited by* S.M. Archibald and S.J. Piercey. Irish Association for Economic Geology, Dublin. pp. 37–58.

Piercey, S.J., Squires, G., and Brace, T. 2018. Geology and lithogeochemistry of hydrothermal mudstones from the upper block near the Duck Pond volcanogenic massive sulfide (VMS) deposit, Newfoundland, Canada: evidence for low-temperature venting into oxygenated mid-Cambrian seawater. Mineralium Deposita, **53**: 1167–1191. doi:10.1007/s00126-018-0795-3.

Pilote, J.-L., and Piercey, S.J. 2018. Petrogenesis of the Rambler rhyolite formation: controls on the Ming VMS deposit and geodynamic implications for the Taconic seaway, Newfoundland Appalachians, Canada. American Journal of Science, **318**: 640–683. doi:10.2475/06.2018.02.

Pilote, J.-L., Piercey, S.J., Brueckner, S.M., and Grant, D. 2016. Resolving the relative timing of Au enrichment in volcanogenic massive sulfide deposits using scanning electron microscopy-mineral liberation analyzer: empirical evidence from the Ming deposit, Newfoundland, Canada. Economic Geology, **111**: 1495–1508. doi:10.2113/econgeo.111.6.1495.

Pilote, J.-L., Piercey, S.J., and Mercier-Langevin, P. 2017. Volcanic and structural reconstruction of the deformed and metamorphosed Ming volcanogenic massive sulfide deposit, Canada: implications for ore zone geometry and metal distribution. Economic Geology, **112**: 1305–1332. doi:10.5382/econgeo.2017.4511.

Pilote, J.-L., Piercey, S.J., and Mercier-Langevin, P. 2020. Evolution of the subseafloor hydrothermal system associated with the Ming VMS deposit, Newfoundland Appalachians, and its controls on base and precious metal distribution. Mineralium Deposita, 913. doi:10.1007/s00126-019-00899-z.

Putrich, E., and Barry, J. 2015. Technical report and resource estimate of the Great Burnt copper property, central Newfoundland. NI-43-101 Technical Report for Spruce Ridge Resources Ltd. p. 116.

Robinson, P., Tucker, R.D., Bradley, D., ,Berry, H.N., IV, and Osberg, P.H. 1998. Paleozoic orogens in New England, USA. Geologiska Foereningens I Stockholm Foerhandlingar, **120**: 119–148. doi:10.1080/11035899801202119.

Rogers, N., van Staal, C.R., McNicoll, V., Pollock, J., Zagorevski, A., and Whalen, J. 2006. Neoproterozoic and Cambrian arc magmatism along the eastern margin of the Victoria Lake Supergroup: a remnant of Ganderian basement in central Newfoundland? Precambrian Research, **147**: 320–341.

Ross, P.-S., and Mercier-Langevin, P. 2014. Igneous rock associations 14. The volcanic setting of VMS and SMS deposits: a review. Geoscience Canada, **41**: 365–377. doi:10.12789/geocanj.2014.41.045.

Roth, T., Thompson, J.F.H., and Barrett, T.J. 1999. The precious metal-rich Eskay Creek deposit, northwestern British Columbia. Reviews in Economic Geology, **8**: 357–373.

Sangster, A.L., Douma, S.L., and Lavigne, J. 2007. Base metal and gold deposits of the Betts Cove Complex, Baie Verte Peninsula, Newfoundland. *In* Mineral deposits of Canada: a synthesis of major deposit-types, district metallogeny, the evolution of geological provinces, and exploration methods. Speical Publication 5. *Edited by* W.D. Goodfellow. Mineral Deposits Division, Geological Association of Canada. pp. 703–721.

Santaguida, F., and Hannington, M.D. 1996. Characteristics of gold mineralization in volcanogenic massive sulphide deposits of the Notre Dame Bay area, central Newfoundland. Canadian Journal of Earth Sciences, **33**: 316–334. doi:10.1139/e96-024.

Santaguida, F., Hannington, M., and Jowett, C. 1992. An alteration and sulfur isotope study of the Pilley's Island massive sulfides, central Newfoundland. Geological Survey of Canada Report 92-01D. pp. 265–274.

Sawkins, F., and Kowalik, J. 1981. The source of ore metals at Buchans: Magmatic Versus leaching models. *In* The Buchans orebodies: fifty years of geology and mining. Special Paper 22. *Edited by* E.A. Swanson, D.F. Strong and J.G. Thurlow. Geological Association of Canada. pp. 255–267.

Schmitt, A.K., and Vazquez, J.A. 2006. Alteration and remelting of nascent oceanic crust during continental rupture: evidence from zircon geochemistry of rhyolites and xenoliths from the Salton trough, California. Earth and Planetary Science Letters, **252**: 260–274. doi:10.1016/j.epsl.2006.09.041.

Shanks, W.C., III, and ,Seyfried, W.E., Jr. 1987. Stable isotope studies of vent fluids and chimney minerals, southern Juan de Fuca Ridge: sodium metasomatism and seawater sulfate reduction. Journal of Geophysical Research, **92**: (B11): 11387–11399. doi:10.1029/JB092iB11p11387.

Shanks, W.C., III, Bischoff, J.L., and Rosenbauer, R.J. 1981. Seawater sulfate reduction and sulfur isotope fractionation in basaltic systems: interaction of seawater with fayalite and magnetite at 200-350° C. Geochimica et Cosmochimica Acta, **45**: 1977–1995. doi:10.1016/0016-7037(81)90054-5.

Shukuno, H., Tamura, Y., Tani, K., Chang, Q., Suzuki, T., and Fiske, R.S. 2006. Origin of silicic magmas and the compositional gap at Sumisu submarine caldera, Izu-Bonin arc, Japan. Journal of Volcanology and Geothermal Research, **156**: 187–216. doi:10.1016/j.jvolgeores.2006.03.018.

Sillitoe, R.H., Hannington, M.D., and Thompson, J.F.H. 1996. High sulfidation deposits in the volcanogenic massive sulfide environment. Economic Geology, **91**: 204–212. doi:10.2113/gsecongeo.91.1.204.

Skirrow, R.G., and Franklin, J.M. 1994. Silicification and metal leaching in semiconformable alteration beneath the Chisel Lake massive sulfide deposit, Snow Lake, Manitoba. Economic Geology, **89**: 31–50. doi:10.2113/gsecongeo.89.1.31.

Skulski, T., Castonguay, S., van Staal, C., Rogers, N., McNicoll, V., Kerr, A., and Escayloa, M. 2009. Baie Verte Peninsula: an evolving geological story. Field Trip Guidebook. Geological Association of Canada Newfoundland and Labrador Section, St. John's. p. 60.

Skulski, T., Castonguay, S., McNicoll, V., van Staal, C., Kidd, W., Rogers, N., et al. 2010. Tectonostratigraphy of the Baie Verte oceanic tract and its ophiolite cover sequence on the Baie Verte Peninsula. Current Research. Geological Survey Report 10-1. Newfoundland and Labrador Department of Natural Resources. pp. 315–225.

Sparkes, G.W. 2020. The style and setting of select VMS occurrences, central Buchans-Roberts Arm belt, Newfoundland. Current Research. Geological Survey Report 2020-1. Newfoundland and Labrador Department of Natural Resources. pp. 207–233.

Sparkes, G.W. 2022. Short wavelength infrared spectrometry studies of sericitic alteration zones, southern Buchans-Roberts Arm Belt, Newfoundland. Current Research. Geological Survey Report 22-1. Newfoundland and Labrador Department of Industry, Energy, and Technology. pp. 85–118.

Sparkes, G.W., and Hinchey, J.G. 2023. White mica zonation patterns associated with hybrid bimodal-felsic VMS systems: examples from the Tulks Volcanic and Buchans-Roberts Arm belts, Central Newfoundland. Current Research. Geological Survey Report 23-1. Department of Industry, Energy and Technology. pp. 1–27.

Sparkes, G.W., Hamilton, M.A., and Dunning, G.R. 2021. Age constraints on VMS mineralization, central Buchans-Roberts Arm belt, Newfoundland. Current Research. Geological Survey Report 21-1. Newfoundland and Labrador Department of Industry, Energy, and Technology. pp. 49–64.

Squires, G.C., and Moore, P.J. 2004. Volcanogenic massive sulfide environments of the Tally Pond Volcanics and adjacent area: geological, lithogeochemical and geochronological results. Current Research. Report 04-1. Geological Survey of Newfoundland and Labrador. pp. 63–91.

Squires, G.C., MacKenzie, A.C., and MacInnis, D. 1991. Geology and genesis of the Duck Pond volcanogenic massive sulfide deposit. *In* Metallogenic framework of base and precious metal deposits, central and western newfoundland. Open File 2156. *Edited by* H.S. Swinden, D.T.W. Evans and B.F. Kean. Geological Survey of Canada. pp. 56–64.

Squires, G.C., Brace, T.D., and Hussey, A.M. 2001. Newfoundland's polymetallic Duck Pond deposit: earliest Iapetan VMS mineralization formed within a sub-seafloor, carbonate-rich alteration system. *In* Geology and mineral deposits of the Northern Dunnage Zone, Newfoundland Appalachians. Field Trip Guide A2. *Edited by* D.T.W. Evans and A. Kerr. Geological Association of Canada/Mineralogical Association of Canada. pp. 167–187.

Stern, R.J., and Bloomer, S.H. 1992. Subduction zone infancy: examples from the Eocene Izu–Bonin–Mariana and Jurassic California arcs. Geological Society of America Bulletin, **104**: 1621–1636. doi:10.1130/0016-7606(1992)104%3c1621:SZIEFT%3e2.3.CO;2.

Stone, W., Putrich, E., Feasby, D.G., Froude, T., and Bartsch, C. 2021. NI-43-101 Technical Report for Callinex Mines Inc. 145p.

Strong, D.F., and Saunders, C.M. 1988. Ophiolitic sulfide mineralization at Tilt Cove, Newfoundland: controls By upper mantle and crustal processes. Economic Geology, **83**: 239–255. doi:10.2113/gsecongeo.83.2.239.

Swanson, E.A., Strong, D.F., and Thurlow, J.G. 1981. The Buchans orebodies: fifty years of geology and mining. Special Paper 22. Geological Association of Canada, St. John's. p. 350(+maps).

Swinden, H.S. 1984. Geological setting of volcanogenic sulfide mineralization of the eastern Wild Bight Group, north-central Newfoundland. Current Research. Geological Survey Report 84-1. Newfoundland Department of Mines and Energy. pp. 157–165.

Swinden, H.S. 1988a. Geology and economic potential of the Pipestone Pond area (12A/1 NE 12A/8 E), central Newfoundland. Geological Survey Report 88-2. Department of Mines, Government of Newfoundland and Labrador. p. 88.

Swinden, H.S. 1988b. Volcanogenic sulfide deposits of the Wild Bight Group, Notre Dame Bay. *In* The volcanogenic sulfide districts of Newfoundland. Special Publication. *Edited by* H.S. Swinden and B.F. Kean. Mineral Deposits Division, Geological Association of Canada. pp. 179–192.

Swinden, H.S. 1991. Paleotectonic settings of volcanogenic massive sulfide deposits in the Dunnage zone, Newfoundland Appalachians. Canadian Institute of Mining and Metallurgy Bulletin, **84**: 59–89.

Swinden, H.S., and Kean, B.F. 1988. Volcanogenic sulfide districts of central Newfoundland. Special Publication. Mineral Deposits Division, Geological Association of Canada. p. 250.

Swinden, H.S., and Thorpe, R.I. 1984. Variations in style of volcanism and massive sulfide deposition in early to middle Ordovician Island-arc sequences of the Newfoundland Central Mobile Belt. Economic Geology, **79**: 1596–1619.

Swinden, H.S., Jenner, G.A., and Szybinski, Z.A. 1997. Magmatic and tectonic evolution of the Cambrian-Ordovician Laurentian margin of Iapetus: geochemical and isotopic constraints from the Notre Dame Subzone, Newfoundland. The nature of magmatism in the Appalachian Orogen. *Edited by* A.K. Sinha, J.B. Whalen and J.P. Hogan. Geological Society of America. pp. 337–365.

Tamura, Y., Gill, J.B., Tollstrup, D., Kawabata, H., Shukuno, H., Chang, Q., et al. 2009. Silicic magmas in the Izu–Bonin Oceanic Arc and implications for crustal evolution. Journal of Petrology, **50**: 685–723. doi:10.1093/petrology/egp017.

Thurlow, J.G. 1996. Geology of a newly discovered cluster of blind massive-sulfide deposits, Pilley's Island, central Newfoundland. Current Research. Geological Survey Report 96-1. Newfoundland Department of Mines and Energy. pp. 181–189.

Thurlow, J.G. 2010. Great mining camps of Canada 3. *In* The history and geology of the Buchans mine. Geoscience Canada, NL. pp. 145–173.

Thurlow, J.G., and Swanson, E.A. 1981. Geology and ore deposits of the Buchans area, central Newfoundland. *In* The Buchans orebodies: fifty years of geology and mining. Special Paper 22. *Edited by* E.A. Swanson, D.F. Strong and J.G. Thurlow. Geological Association of Canada. pp. 113–142.

Thurlow, J.G., and Swanson, E.A. 1987. Stratigraphy and structure of the Buchans Group. Geological Survey of Canada Paper 86-24. pp. 35–46.

Thurlow, J.G., Spencer, C.P., Boerner, D.E., Reed, L.E., and Wright, J.A. 1992. Geological interpretation of a high resolution reflection seismic survey at the Buchans mine, Newfoundland. Canadian Journal of Earth Sciences, **29**: 2022–2037. doi:10.1139/e92-159.

Toman, H. 2013. Geology and metallogeny of north-central Newfoundland and the Little Deer VMS deposit. Unpublished M.Sc. thesis, Memorial University of Newfoundland, St. John's, 184p.

Tuach, J. 1988. Geology and sulfide mineralization in the Robert's Arm Group on Pilley's Island, central Newfoundland. *In* The volcanogenic sulfide districts of Central Newfoundland. Special Publication. *Edited by* H.S. Swinden and B.F. Kean. Mineral Deposits Division, Geological Association of Canada. pp. 117–122.

Tuach, J. 1990. The Pilley's Island volcanogenic massive sulfide deposits, central Newfoundland. *In* Metallogenic framework of base and precious metals deposits, Central and Western Newfoundland: Proceedings of the 8th IAGOD Symposium Field Trip 1 Guidebook. Open File Report 2156. *Edited by* H.S. Swinden, D.T.W. Evans and B.F. Kean. Geological Survey of Canada. pp. 109–115.

Upadhyay, H.D., and Smitheringale, W.G. 1972. Geology of the Gullbridge copper deposit, Newfoundland: volcanogenic sulfides in cordierite–anthophyllite rocks. Canadian Journal of Earth Sciences, **9**: 1061–1073. doi:10.1139/e72-092.

Upadhyay, H.D., and Strong, D.F. 1973. Geological setting of the Betts Cove copper deposits, Newfoundland: an example of ophiolite sulfide mineralization. Economic Geology, **68**: 161–167. doi:10.2113/gsecongeo.68.2.161.

van Hees, G.W.H., Zagorevski, A., and Hannington, M.D. 2012. Volcanology and stratigraphy of the Lundberg zone, Buchans, Newfoundland. Current Research. Geological Survey Report 12-1. Newfoundland and Labrador Department of Natural Resources. pp. 147–166.

van Staal, C.R. 1994. Brunswick subduction complex in the Canadian Appalachians: record of the Late Ordovician to Late Silurian collision between Laurentia and the Gander margin of Avalon. Tectonics, **13**: 946–962. doi:10.1029/93TC03604.

van Staal, C.R. 2007. Pre-carboniferous tectonic evolution and metallogeny of the Canadian Appalachians. *In* Mineral deposits of Canada: a synthesis of major deposit-types, district metallogeny, the evolution of geological provinces, and exploration methods. Special Publication 5. *Edited by* W.D. Goodfellow. Mineral Deposits Division, Geological Association of Canada. pp. 793–818.

van Staal, C., and Barr, S.M. 2012. Lithospheric architecture and tectonic evolution of the Canadian Appalachians and associated Atlantic margin. *In* Tectonic styles in Canada: the LITHOPROBE perspective. Special Paper 49. *Edited by* J.A. Percival, F.A. Cook and R.M. Clowes. Geological Association of Canada, St. John's. 41–96pp.

van Staal, C.R., Dewey, J.F., Niocaill, C.M., and McKerrow, W.S. 1998. The Cambrian–Silurian tectonic evolution of the northern Appalachians and British Caledonides: history of a complex, west and southwest Pacific-type segment of Iapetus. Special Publications 143. Geological Society, London. pp. 197–242.

van Staal, C.R., Wilson, R.A., Rogers, N., Fyfee, L.R., Langton, J.P., McCutcheon, S.R., et al. 2003. Geology and tectonic history of the Bathurst Supergroup, Bathurst mining camp, and its relationships to coeval rocks in southwestern New Brunswick and adjacent mine: a synthesis. *In* Massive sulfide deposits of the Bathurst Mining Camp, New Brunswick, and Northern Maine. Monograph 11. *Edited by* W.D. Goodfellow, S.R. McCutcheon and J.M. Peter. Society of Economic Geologists. pp. 37–60.

van Staal, C.R., Valverde-Varuero, P., Zagorevski, A., Rogers, N., Lissenberg, C.J., and McNicoll, V.J. 2005. Geology, Victoria Lake, Newfoundland and Labrador. Open File 1667, scale 1:50,000. Geological Survey of Canada.

van Staal, C.R., Whalen, J.B., McNicoll, V.J., Pehrsson, S., Lissenberg, C.J., Zagorevski, A., et al. 2007. The Notre Dame arc and the Taconic orogeny in Newfoundland. Geological Society of America Memoir 200. Geological Society of America. pp. 511–552.

van Staal, C.R., Whalen, J.B., Valverde-Vaquero, P., Zagorevski, A., and Rogers, N. 2009. Pre-Carboniferous, episodic accretion-related, orogenesis along the Laurentian margin of the northern Appalachians. Special Publications 327. Geological Society, London. pp. 271–316.

van Staal, C.R., Zagorevski, A., McNicoll, V.J., and Rogers, N. 2014. Time-transgressive Salinic and Acadian orogenesis, magmatism and Old Red Sandstone sedimentation in Newfoundland. Geoscience Canada, **41**: 138–164. doi:10.12789/geocanj.2014.41.031.

Von Damm, K.L. 1990. Seafloor hydrothermal activity: black smoker chemistry and chimneys. Annual Review of Earth and Planetary Sciences, **18**: 173–204. doi:10.1146/annurev.ea.18.050190.001133.

Waldie, C., Jowett, E., and Swinden, H. 1991. The Crescent Lake copper deposit, central Newfoundland: deep levels of a volcanogenic hydrothermal system? Atlantic Geology, **27**: 1–13. doi:10.4138/1716.

Waldron, J.W.F., and van Staal, C.R. 2001. Taconian orogeny and the accretion of the Dashwoods block: a peri-Laurentian microcontinent in the Iapetus Ocean. Geology, **29**: 811–814. doi:10.1130/0091-7613(2001)029%3c0811:TOATAO%3e2.0.CO;2.

Walker, S.D., and Collins, C. 1988. The Point Leamington massive sulfide deposit. *In* The volcanogenic sulfide districts of central Newfoundland. *Edited by* H.S. Swinden and B.F. Kean. Mineral Deposits Division, Geological Association of Canada. pp. 193–198.

Weick, R.J. 1993. Petrography and stable isotope geochemistry of alteration and mineralization in the Rambler volcanogenic massive sulfide deposit. Unpublished MSc thesis, Memorial University of Newfoundland St. John's, Baie Verte, Newfoundland. 171p.

Whalen, J.B., Jenner, G.A., Longstaffe, F.J., Gariepy, C., and Fryer, B.J. 1997. Implications of granitoid geochemical and isotopic (Nd, O, Pb) data from the Cambrian–Ordovician Notre Dame Arc for the evolution of the central mobile belt, Newfoundland Appalachians. Geological Society of America Memoir 191. Geological Society of America. pp. 367–395.

Williams, H. 1979. Appalachian orogen in Canada. Canadian Journal of Earth Sciences, **16**: 792–807. doi:10.1139/e79-070.

Williams, H., Colman-Sadd, S.P., and Swinden, H.S. 1988. Tectonostratigraphic subdivisions of central Newfoundland. Current Research Part B. Paper 88-1B. Geological Survey of Canada. pp. 91–98.

Yang, X.-M. 2012. Sulfur solubility in felsic magmas: implications for genesis of intrusion-related gold mineralization. Geoscience Canada, **39**: 17–32.

Zagorevski, A., Rogers, N., van Staal, C.R., McNicoll, V., Lissenberg, C.J., and Valverde-Vaquero, P. 2006. Lower to middle Ordovician evolution of peri-Laurentian arc and backarc complexes in Iapetus: constraints from the Annieopsquotch accretionary tract, central Newfoundland. Geological Society of America Bulletin, **118**: 324–342.

Zagorevski, A., van Staal, C.R., McNicoll, V.J., and Rogers, N. 2007. Upper Cambrian to upper Ordovician peri-Gondwanan Island arc activity in the Victoria Lake Supergroup, central Newfoundland: tectonic development of the northern Ganderian margin. American Journal of Science, **307**: 339–370. doi:10.2475/02.2007.02.

Zagorevski, A., Lissenberg, C.J., and van Staal, C.R. 2009. Dynamics of accretion of arc and backarc crust to continental margins: inferences from the Annieopsquotch accretionary tract. Tectonophysics, **479**: 150–164. doi:10.1016/j.tecto.2008.12.002.

Zagorevski, A., van Staal, C.R., Rogers, N., McNicoll, V.J., and Pollock, J. 2010. Middle Cambrian to Ordovician arc–backarc development on the leading edge of Ganderia, Newfoundland Appalachians. Geological Society of America Memoir 206. Geological Society of America. pp. 367–396.